The Pliocene-Pleistocene development, uplift and emergence history of the Manawatu Strait, New Zealand

By

Aidan Gordon Milner

A thesis submitted to the Victoria University of Wellington as partial fulfilment of the requirements for the degree of Masters of Science in Geology

School of Geography, Environment and Earth Sciences

Victoria University of Wellington

July 2017

Frontispiece:

View from Wharite Peak looking south over the Manawatu Saddle with the Manawatu Gorge and Tararua Range in the distance

Abstract:

The Manawatu Saddle is located within the structural and topographical low separating the Ruahine and Tararua axial ranges of the lower North Island. Pliocene-Pleistocene sedimentary rocks unconformably drape over Cretaceous aged basement rock in the structural low and record the existence of a paleo seaway known as the Manawatu Strait, which connected the West Coast (Whanganui Basin) to the East Coast (Ruataniwha Strait). The sedimentary sequence shows a succession of alternating marine and terrestrial units recoding the development of the Manawatu Strait. These sedimentary rock formations range in age from Opoitian to Castlecliffian.

This study investigates the stratigraphy, lithofacies and resulting geological history of the Manawatu Strait spanning the development, uplift and final emergence history of the strait. Five key measured sections were constructed to take advantage of new outcrop exposure allowed detailed descriptions of the Manawatu Saddle geology to be presented. Four formations are identified and the formation boundary overlaps between past authors is constrained based on field observations. The age range for each formation is also constrained. Based on these results for the first time a detailed lithofacies scheme is applied to the sedimentary rocks within the Manawatu Saddle to understand the changing depositional environments within the Manawatu Strait throughout its development and uplift. A series of 3D schematic paleogeographic figures are presented showing the depositional environments within the Manawatu Strait, at key time intervals.

Results highlighted by this thesis show four major formations within the Manawatu Saddle. The oldest formation, the Mangatoro Formation (Opoitian), records the initial formation of the Manawatu Strait attributed to a regional subsidence event known as the Tangahoe pull down event. The Mangatoro Formation also shows sedimentary deposited during peak marine transgression within the Manawatu Strait. The Te Aute Formation (Waipipian-Mangapanian) provides an insight into the uplift timing of the axial ranges and the resulting effect on the Manawatu Strait. The Kumeroa Formation (Nukumaruan) shows the influence of eustatic sea level change in the Manawatu Saddle. The youngest formation within the Manawatu Saddle is the Mangatarata Formation (Castlecliffian), and marks the final uplift and emergence of the Manawatu Strait, indicated by the presence of marginal marine lithofacies this also marks the final separation of the West Coast (Rauataniwha Strait) and West Coast (Whanganui Basin).

Acknowledgements

Firstly I would like to acknowledge my supervisors, Cliff Atkins, Mike Hannah and Kyle Bland (GNS Science) for their assistance. Also a special thank-you to Katie Collins for her assistance in the field, help with macro fossil identification, and proof reading. Thank-you to Jane Chewings for support in the sedimentology lab. Also thank-you to Aline Homes for her proof reading, sample identification help and in depth discussions.

Thank-you to Merijn Thornton, Joanna Elliott and Dominic Strogen for their assistance in the field. A special thanks to Hugh Morgans for the use of his house in Dannevirke as accommodation, and Victoria University of Wellington and GNS Science for field work funding. Also thank-you to the land owners Hugh and Judy Akers of the Broadlands station, Ballantrae Farm (John Napier: Ag Research and Angus Brown: Taratahi) and Mark, owner of Ferry Reserve quarry on the eastern entrance to the Manawatu Gorge, for access to their land. Everyone involved in this project would like to extend a thank-you to Kiwirails on-track program for site accesses.

I would like to thank the team at VUW student learning and disability services, especially Deborah Laurs (proof reading), Laila Faisal (formatting) and Matt Truman (disability advisor) for going above and beyond to provide invaluable sport, and for truly understanding dyslexia.

Thank-you to my office mates in the John Bradly library for their support and friendship, Andrea, Hannah, Lauren, Tom, Ben, Karsten, Gracie and Alex. Thank-you to Ben Hines for his assistance and to Sandra Koenigseder for her support. A very special thank-you to my partner Gracie Miles, who joined the roller coaster ride that is a thesis midway through but has been my rock and biggest supporter ever since. Thank-you to my sister Heather for her support, also a very special thank-you to my Mum, Ruth Gordon, and Dad, Ian Milner. As without their support help and guidance, university would be nothing more an imaginary dream and I owe them a very big thank-you.

Dyslexia is not a barrier to life or academic achievements, but a tool to see the world form a different perspective and to appreciate and cherish successes and victories more, as you truly appreciate how nothing in life comes without hard work.

Contents Page

Table of Figures

Table of Tables

Chapter 1 Introduction

1.1 Introduction:

The Pliocene-Pleistocene sedimentary rocks which drape over the Torlesse basement between the Ruahine and Tararua Axial Ranges, mark the topographic and structural low known as the Manawatu Saddle. The sedimentary rocks record the emergence of the relatively short lived paleo-seaway between the East Coast and West Coast, (Lillie, 1953; Beu *et al*., 1980, 1995). The Manawatu Strait also allows an insight into the uplift history of the southern Ruahine Range and northern Tararua Range, as the facies present are influenced by uplift events. Despite the strait's unique location straddling the uplifting ranges, relatively little work has been carried out to understand the development, geological history and implications of the Manawatu Strait within a local and regional context. Work carried out by Lillie (1953) and Piyasin (1966) is the most comprehensive to date and focused on defining the formations and their boundaries within the Manawatu Saddle. This study clarifies the formation boundaries by taking advantage of fresh outcrop exposure to improve the stratigraphic resolution, and defines lithofacies and their interpreted depositional settings. This allows the broad paleogeography and uplift history of the Manawatu Strait to be constrained.

1.1 Aims and Objectives:

1.1.1 Aim:

This study aims to investigate the Pliocene-Pleistocene sedimentary rocks within the Manawatu Saddle in order to understand the formation, uplift and emergence history of the Manawatu Strait, and how this feature fits within the wider context of the development of the East Coast and West Coast basins. A stratigraphic approach and framework is applied in order to achieve the following objectives.

1.1.2 Objectives:

- Produce a composite geological map, to clarify the mapped formation boundaries between past authors.

- Produce detailed measured sections in key locations to take advantage of fresh outcrop exposure. To clarify the formation boundaries at a stratigraphic level.

- Provide an up to date biostratigraphic framework for the formations within the Manawatu Saddle in order to provide improved age constraints for each formation.

- Develop a lithofacies scheme and model, to provide interpretations of depositional environments for each lithofacies.

- Use the above results to provide a geological history of the formation, uplift and emergence of the Manawatu Strait.

1.2 Study location:

The Manawatu Saddle is located between the Tararua and Ruahine Ranges, in the lower North Island of New Zealand. The field area is marked as a structural and topographic low between these two ranges, and contains soft sedimentary rocks unconformably overlying basement rock. The field area is approximately 64 km squared, and contains moderate topography. The Manawatu Saddle is accessed by the Saddle Road and is a 28 km drive from Palmerston North, the nearest major city.

Five sections were logged in key locations in the Manawatu Saddle; their locations can be seen in Fig 1-1. Section locations were chosen to provide maximum exposure of geology and to include sections freshly exposed due to recent earthworks.

This page has been deliberately left blank for formatting purposes

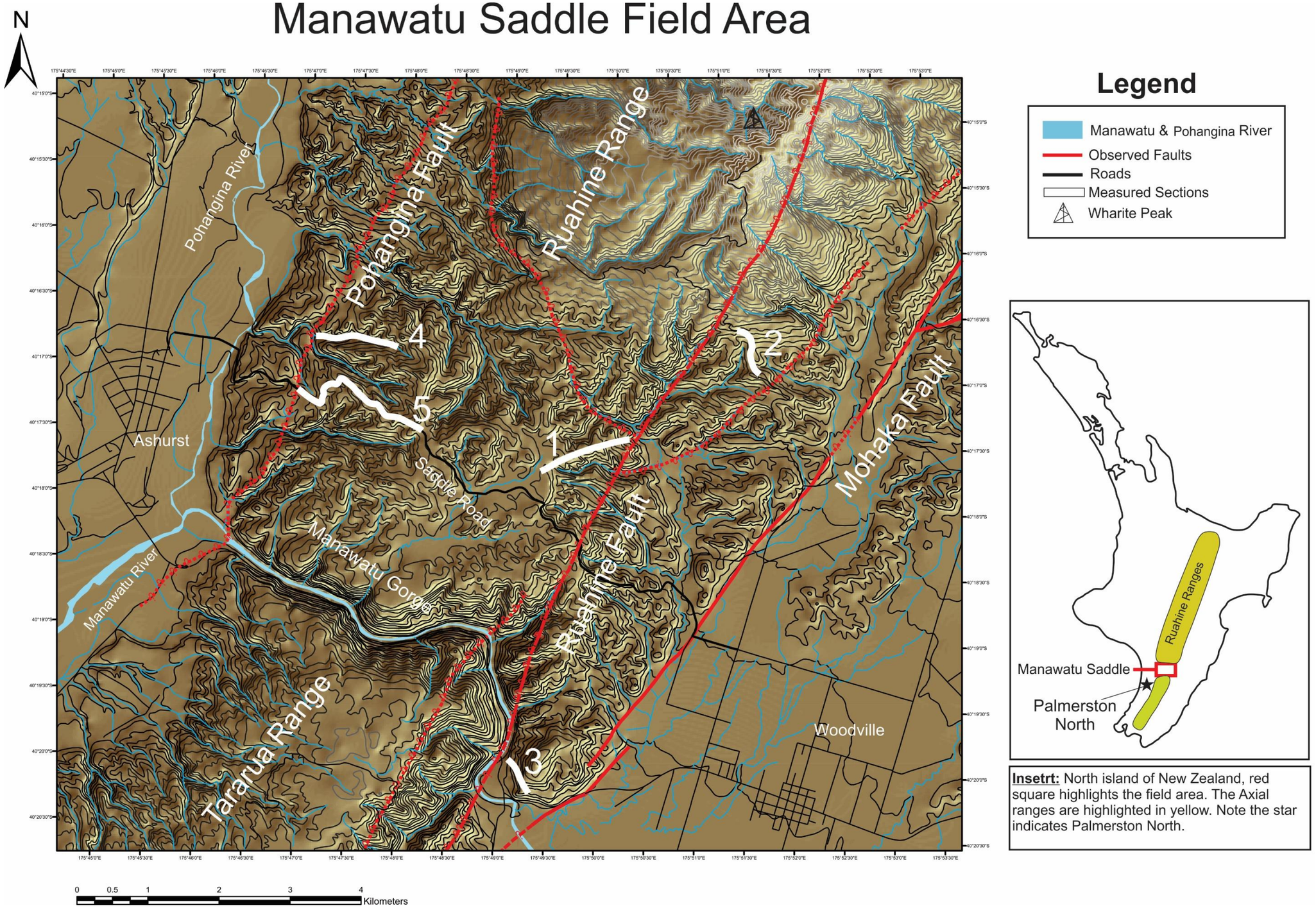

Figure 1-1: Location map of the Manawatu Saddle.
1: Ballantrae Farm measured section, 2: Wharite Road measured section, 3: Eastern Manawatu Gorge Entrance measured section, 4: Broadlands Stream measured section, 5: Western Saddle Road measured section.

1.3 Geological Background:

The Manawatu Saddle is located within the structural and topographical low which separates the Ruahine and Tararua axial ranges, in the lower North Island of New Zealand. The northeast southwest trending axial ranges are comprised of Jurassic to earliest Cretaceous greywacke and argillite (Mortimer, 1994). The axial ranges are a result of uplift that is a product of the rotation and resulting subduction of the Pacific Plate associated Hikurangi Margin (King, 2000), as the axial ranges mark the frontal ridge between the East Coast forearc basin and the Wanganui Basin backarc basin (Fig 1-2). The Manawatu Saddle straddles these two features and offers a unique insight to the development of the axial ranges and their effects on the developing East Coast and Wanganui Basin.

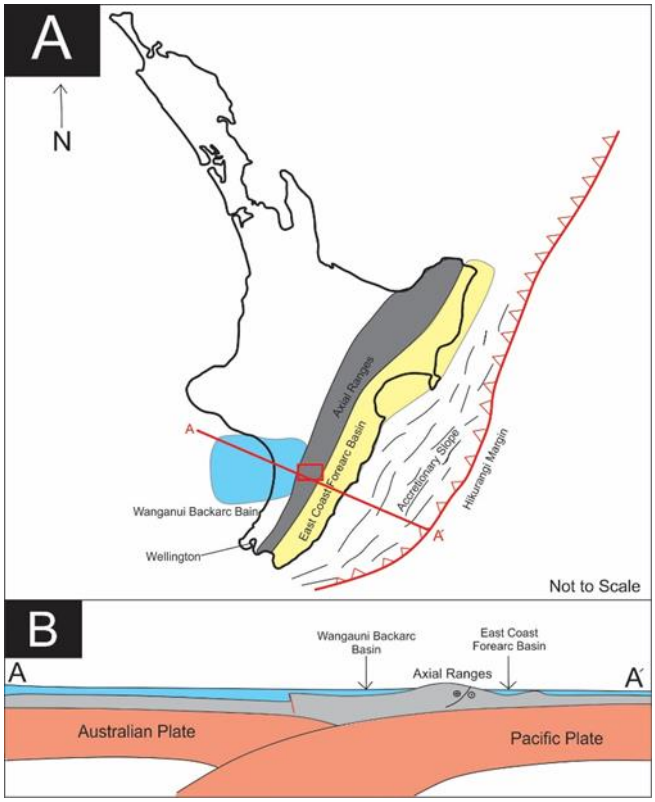

Figure 1-2: The position of the Hikurangi Margin in relation to the East Coast forearc basin and Wanganui Basin backarc basin.
A) Schematic diagram of the East Coast and Wanganui Basin relationship to the Hikurangi Margin, the red square highlights the location of the Manawatu Saddle. Figure adapted from Cole and Lewis (1981). B) Shows a schematic East-West cross section through the lower central North Island. Figure adapted from Naish and Wilson (2009).

During the Pliocene-Pleistocene there were a number of active seaways throughout the uplifting North Island of proto-New Zealand. To the east of the Manawatu Saddle, was the north-south orientated Ruataniwha Strait, (Beu *et al*., 1980; Beu, 1995). The strait dominated

the east coast forearc basin from the Tongaporutuan (11.04 Ma) to late Nukumaruan (1.36 Ma), (Fig 1-3) (Trewick & Bland, 2011; Beu, 1995). As can also be seen in fig 1-3, another seaway named the Kuripapango Strait, was active in the northern uplifting Ruahine Ranges providing a passage way between the two basins. According to Browne (2004) the Kuripapango Strait connected the western basins and eastern Ruataniwha Strait, and ranged in age from the Tongaporutuan (11.40 Ma) to Late Nukumaruan (~2.40 Ma). This range makes the Kuripapango Strait older than the Manawatu Strait and it also closed earlier. The demise of the Kuripapango Strait is attributed to progressive uplift of the Ruahine Range and changing eustatic sea level (Browne, 2004). The emergence of the Ruataniwha Strait occurred after the uplift of the Kuripapango Strait. The Ruataniwha Strait began draining and uplifting in the Late Nukumaruan (1.36 Ma) as the Mt Bruce fault block uplifted, (Lee *et al.*, 2002).

To the west of the active Manawatu Strait was the developing Wanganui and King Country basins. The Wanganui Basin is a result of the locked zone between the subducting Australian and Pacific tectonic plates, the resulting gradual pull down effect caused the flooding and development of the basin (Naish et al, 1998). The pull down and flooding of the basin is thought to have begun in the Pliocene (5.33-2.58 Ma) (Anderton, 1981). As a result, the Wanganui Basin contains a very high resolution and world renowned record of global eustatic sea level change from this time interval, (Naish *et al*., 1998). Within the same time window the 'Tangahoe pulldown' event occurred approximately five million years ago in the Opoitian, due to mantle instabilities (Kamp *et al*., 2004; Pulford *et al.*, 2004; Nicol, 2011). The resulting pull down event flooded the King Country Basin and likely had an effect on the Wanganui Basin, causing faulting within the basement rock as rapid subsidence occurred, (Kamp *et al.*, 2004).

The Manawatu Strait is thought to have played an important role in connecting the East Coast basin with the Wanganui basin, (Anderton, 1981; Beu, 1995). This connection likely allowed the supply of sediment, a migration pathway for important marine fauna such as Zygochlamys delicatula and provided a pathway for the movement of paleo-ocean currents between the basins, (Beu *et al*., 1980, 1995; Nelson et al, 2003; Trewick & Bland *et al.*, 2011). This highlights the important role that the Manawatu Strait played in the development of each basin and why it is important to understand the record of changing geometry and water depths in the Manawatu Saddle, as these changes likely had a large impact on the adjacent basins, and the paleogeography of the region.

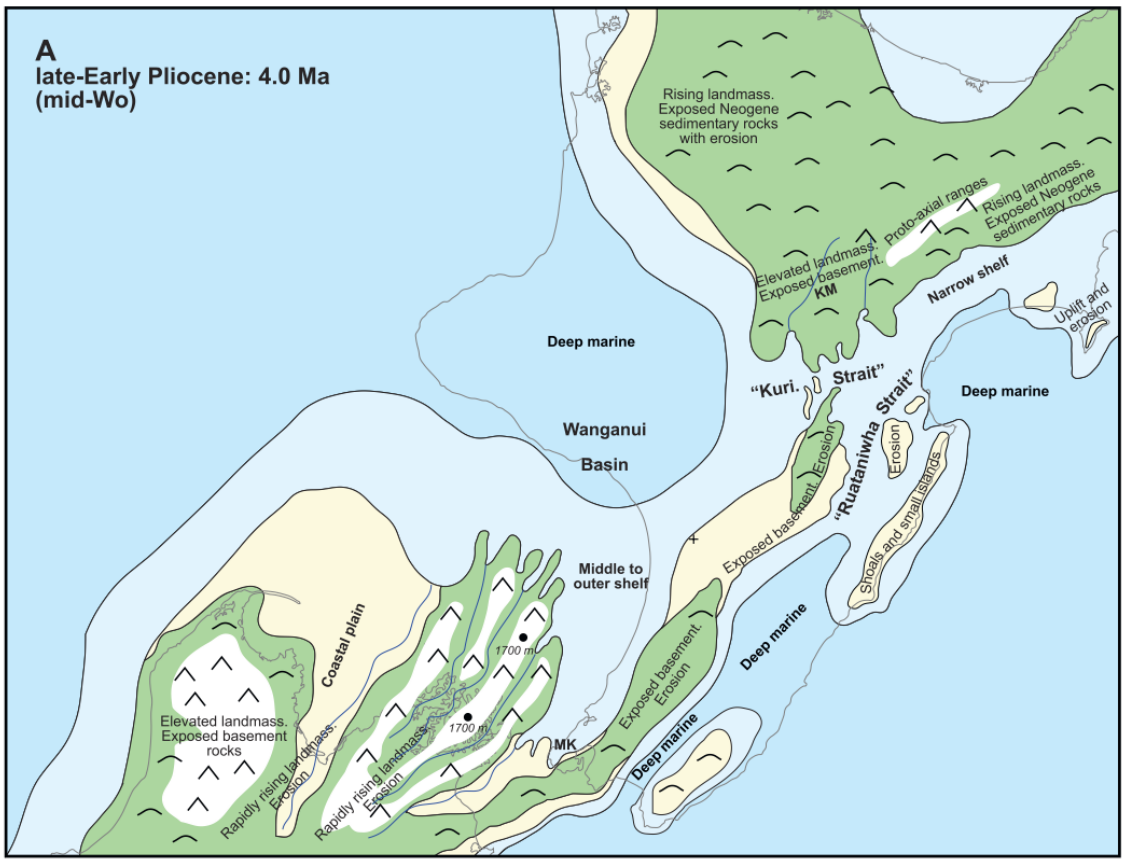
A
late-Early Pliocene: 4.0 Ma
(mid-Wo)
Rising landmass.
Exposed Neogene
sedimentary rocks
with erosion
Proto-axial ranges
Rising landmass.
Exposed Neogene
sedimentary rocks
Elevated landmass.
Exposed basement.
KM
Narrow shelf
Uplift and
erosion
Deep marine
"Kuri. Strait"
"Ruataniwha Strait"
Deep marine
Wanganui
Basin
Erosion
Erosion
Shoals and small islands
Exposed basement. Erosion
Middle to
outer shelf
Coastal plain
1700 m
1700 m
Elevated landmass.
Exposed basement
rocks
Rapidly rising landmass.
Erosion
Rapidly rising landmass.
Erosion
MK
Exposed basement.
Erosion
Deep marine
Deep marine

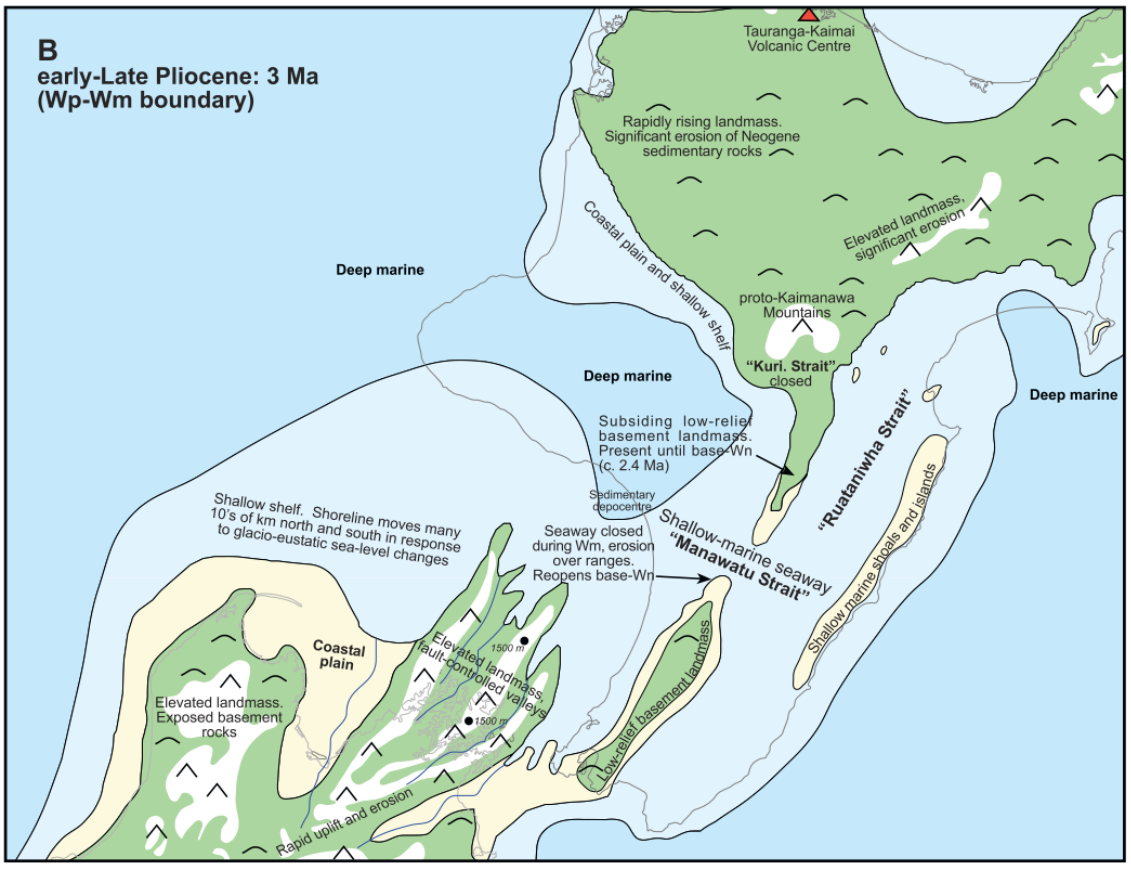
B
early-Late Pliocene: 3 Ma
(Wp-Wm boundary)
Tauranga-Kaimai
Volcanic Centre
Rapidly rising landmass.
Significant erosion of Neogene
sedimentary rocks
Coastal plain and shallow shelf
Elevated landmass,
significant erosion
Deep marine
proto-Kaimanawa
Mountains
"Kuri. Strait"
closed
Deep marine
Deep marine
Subsiding low-relief
basement landmass.
Present until base-Wn
(c. 2.4 Ma)
Sedimentary
depocentre
"Ruataniwha Strait"
Shallow shelf. Shoreline moves many
10's of km north and south in response
to glacio-eustatic sea-level changes
Seaway closed
during Wm, erosion
over ranges.
Reopens base-Wn
Shallow-marine seaway
"Manawatu Strait"
Shallow marine shoals and islands
Coastal
plain
Elevated landmass,
fault-controlled valleys
1500 m
1500 m
Elevated landmass.
Exposed basement
rocks
Low-relief basement landmass
Rapid uplift and erosion

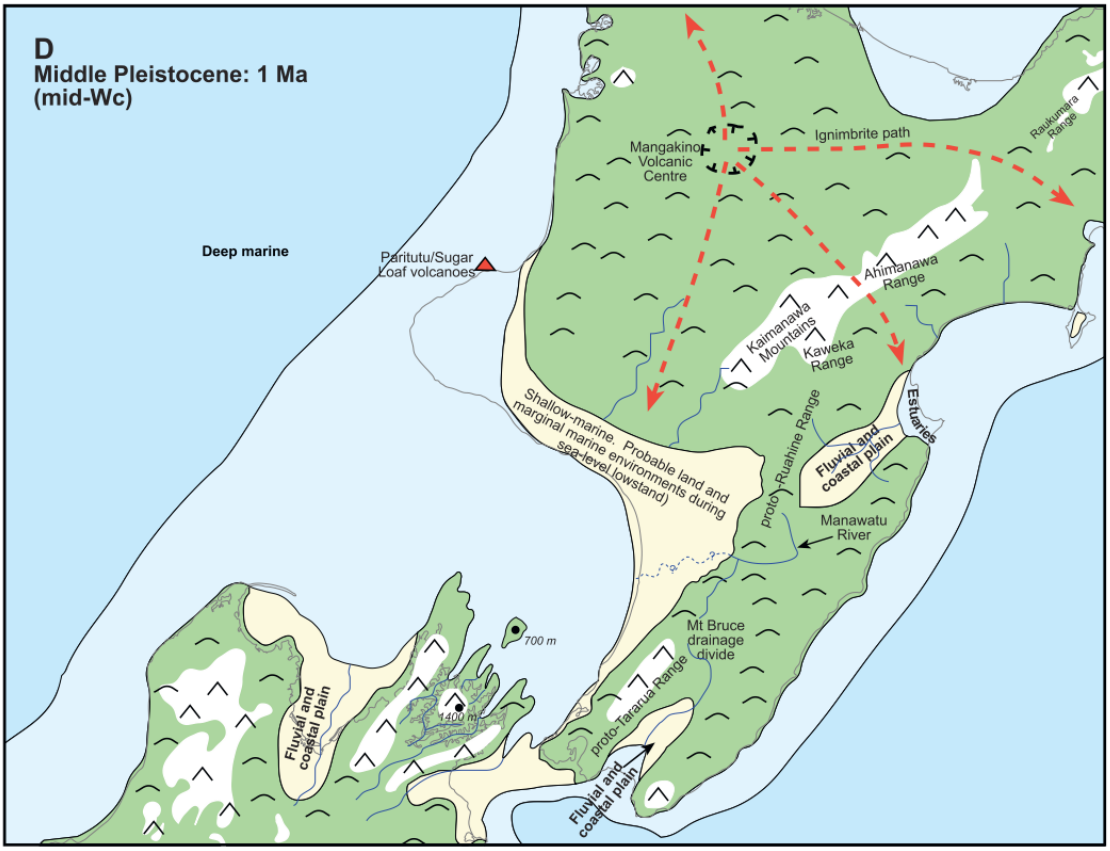

Figure 1-3: Broad scale paleogeographic maps showing the timing, development and emergence of major seaways throughout the developing North Island.
A) Shows the mid-Opoitian, where the Ruataniwha Strait and Kuripapango Strait were active. This figure however shows the Manawatu Strait closed at this time, but work presented in this thesis suggests the Manawatu Strait was active at this time. B) Shows the developing North Island at the Waipipian Mangapanian boundary, and shows the Kuripapango Strait is no longer active. The figure shows both the Ruataniwha Strait and Manawatu Strait active. D) Shows the developing North Island in the mid Castlecliffian, at this stage no seaways are active due to the up lift and emergence of the North Island. Above figures selected from Trewick and Bland (2011).

The modern day Manawatu Saddle contains four major sedimentary rock formations deposited in the Manawatu Strait. These formations are as follows, the Mangatoro, Te Aute, Kumeroa and Mangatarata formations. Each formation consists broadly of the following lithologies: the Mangatoro Formation consists of sandstone and sandy mudstone, the Te Aute Formation contains mainly conglomerates, the Kumeroa Formation consists of shell hash limestone and sandstone and the Mangatarata Formation consists of decimetre scale sandstones siltstones.

Based on structural data collected during field work and data from previous studies' the sedimentary rocks that make up the Manawatu Saddle form an anticline structure, (Fig 1-4). This anticline structure shows the sedimentary rocks draping over the basement rock in the

structural low of the field area. The basement rock within the Manawatu Saddle shows an undulating topography, with a basement out crop observed on the eastern Manawatu Saddle. Fig 1-5 shows a schematic cross section of the basement; small out crops of basement are exposed in the base of streams throughout the eastern Manawatu Saddle. The basement rock also marks the edge of the field area, making up the axial ranges on either side of the Manawatu Saddle.

Three major faults are present within the Manawatu Saddle; the Mohaka and Ruahine Faults on the eastern side of the Manawatu Saddle, (Beanland, 1995; Langridge *et al.*, 2005). The Pohangina Fault is located on the western margin of the Manawatu Saddle (Rich, 1959; Jackson *et al*., 1998). The exact amount of vertical and horizontal offset for the Mohaka and Ruahine Faults within the Manawatu Saddle is unclear. These two faults are thought to have a significantly larger strike-slip offset opposed to vertical offset (Beanland, 1995; Langridge *et al.*, 2005). An important note to make is that both the Mohaka and Ruahine Faults bifurcate from the Wellington Fault, only a few kilometres south of the Manawatu Saddle (Langridge *et al.*, 2005). The amount of offset on the Pohangina Fault is also uncertain, but it is thought that the Pohangina Fault shows mostly vertical offset as opposed to strike-slip offset.

Clarifying and refining the stratigraphy using a stratigraphic approach, will allow this study to investigate the formation, uplift and emergence history of the Manawatu Strait. Using detailed measured sections and a lithofacies scheme and up to date bio-stratigraphy, changes in water depth and depositional environments can be identified. Understanding the timing and magnitude of changes occurring within the Manawatu Strait will allow this study to explore how the paleogeography of the region has changed over time, and the impact these changes likely had on the surrounding basins.

This page has been deliberately left blank for formatting purposes

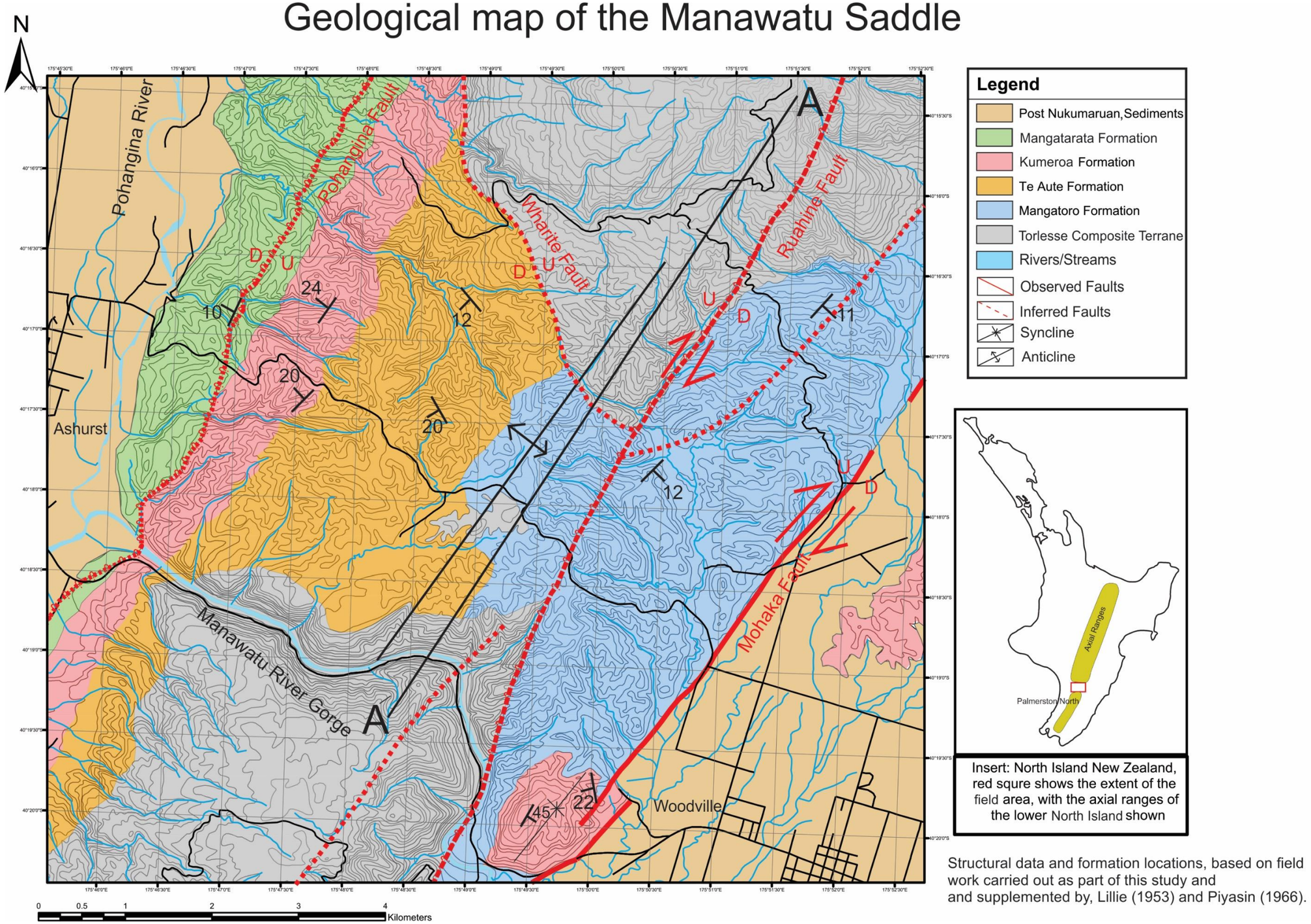

Figure 1-4: Geological map of the Manawatu Saddle.

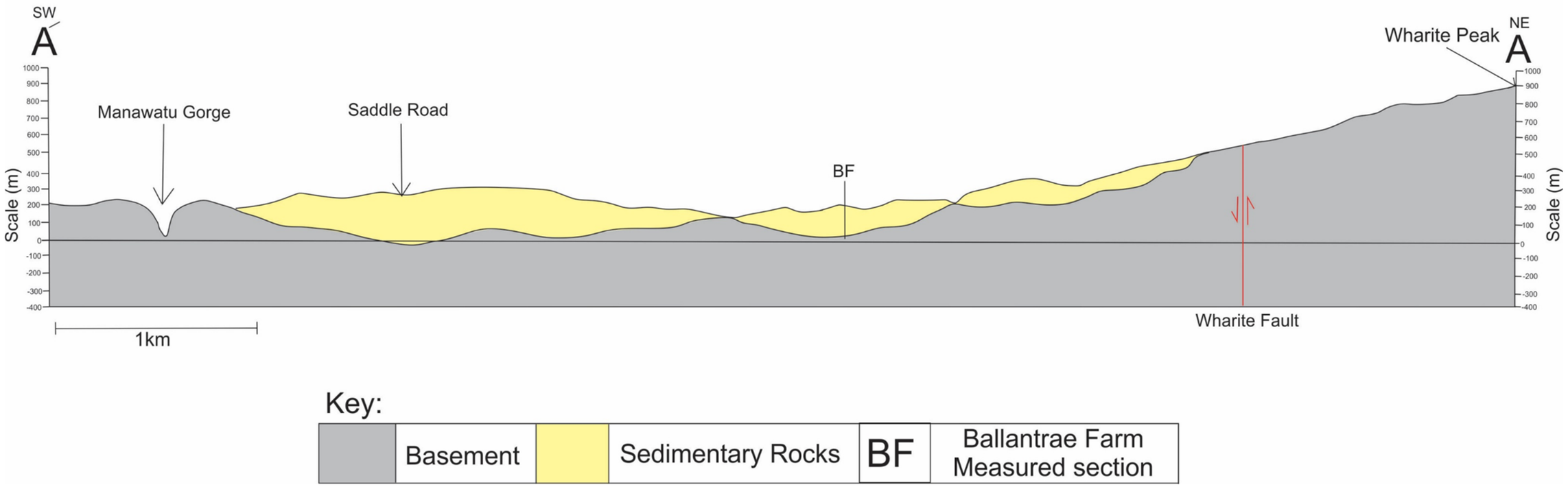

Figure 1-5: Schematic cross section of the Manawatu Saddle basement.

Chapter 2 Methods

2.1 Mapping:

Several geological maps of the Manawatu Saddle have been produced by previous authors, such as Lillie (1953), Piyasin (1966) and Grammer (1971). This project presents a composite geological map in Figure 1.4. As field mapping was not the primary focus of this project, maps from past studies and data from measured sections were combined to create a geological map. The map was produced in ARC GIS 10.1. The base map was constructed using NZMS 260 topographic map series contour data.

2.2 Section Measuring and Sample Collection:

Five sections were logged at key locations throughout the Manawatu Saddle, on both the western and eastern sides. Most sections made use of the recent earth works exposing fresh outcrop. Sections were constructed using a combination of methods: Jacob's staff and Abney level, pace and compass techniques. Where outcrop exposure was not ideal, thickness estimates were made by using GPS locations projected onto cross sections and thickness estimated based on structural field data.

The following information was recorded in the field when measuring the sections, and is presented in the detailed lithological descriptions found in Chapter three: stratigraphy.
1) The lithology of the units; 2) concentration of macrofossils present, their conditions and the species present; 3) the nature of contacts between units; 4) presence and nature of sedimentary structures; 5) the nature of clasts, grain size and sorting were also noted. Strike and dip data were recorded when possible along with the stratigraphic height of samples taken.

2.3 Grain size Analysis:

The oldest and thickest sandstone was sampled, to provide another proxy for water depth from the grain size distribution due to the highly bioturbated nature of the outcrop. Grain size was also carried out to confirm that visual field observations are correct in terms of the grain size approximation, a summary figure representative of the results is presented in appendix two along with the raw data for this figure. The first step in this processes involved taking a bulk sample in the field. The bulk sample was dried in an oven at Victoria University of Wellington (VUW), at 40 degrees Celsius for 24 hours. Once the bulk sample was fully dried and disaggregated, three sub-samples weighing one gram each were weighed out.

The sub samples were chemically treated to remove the organic components. The first stage in this chemical treatment required the use of 27% concentration hydrogen peroxide (H_2O_2). The samples were placed in a cold-water bath and H_2O_2 was added. After the initial reaction between the organic matter and the H_2O_2 had appeared to near completion, the water bath was heated to 60 degrees Celsius, for 4-6 hours. The samples were then rinsed in a centrifuge.

The rinsed samples were tested with 10% hydrogen chloride acid (HCl), to asses if any carbonate material was present. The samples in this study showed minimal fizzing when HCl was added, therefore indicating a low percentage of carbonate material was present. As a result no HCl treatment was required.

The chemically treated samples were then analysed using the Beackman Coulter LS 13320 multi-wavelength laser diffraction particle size analyser at VUW. The processes was carried out by the sedimentology lab technician. The samples were placed in an aqueous liquid model assembly. The optical module used in this study was Quartz natural.rf 780d. The samples were ran at a slightly higher obscuration value than usual (usual values are between 8-12%), and this study used values ~14-17%. Despite the higher than usual values, the sample data are deemed robust. Before the samples were passed through the machine, they were placed in a solution of 0.5g per 1 L of Calgon solution. These samples were ultra-sonicated for ~15 minutes prior to analysis, to ensure the particles were fully disaggregated and dissolved.

2.4 Micro and Macrofossil Identification:

Both microfossils and macrofossils were collected and identified for use in this study. Most macrofossils were identified in the field, in situ. Macrofossils which could be collected were washed to remove any sediment, in order to show the key features required for identification purposes. The fossils were identified using Beu *et al.* (1990); samples that were not able to be confidently identified were checked with Dr Katie Collins at VUW and Dr Alan Beu at GNS. Once the macrofossils were confidently identified, the age range and preferred depositional settings for each fossil were noted using references such as Beu *et al.* (1990). The age ranges of the macrofossils are presented in chapter four.

Samples to be inspected for microfossils (foraminifera) were collected from siltstone beds throughout the Manawatu Saddle. The bulk field samples were first dried in an oven at 40 degrees Celsius for 24 hours, then 200g of each sample was weighed and sieved. The samples were first wet sieved using a 4-phi sieve. The dried samples were then split 8-9 times using a

riffle splitter. The split samples were dry sieved through a 2 and 3-phi sieve, and each fraction was picked. Three hundred microfossils were picked wherever possible. The microfossil age ranges can be found in Chapter four.

Chapter 3 Stratigraphy

3.1 Introduction:

This chapter outlines the stratigraphy observed in the Manawatu Saddle at both regional and measured section scales. The formation boundaries proposed by past authors and the overlap and disparities are reviewed. Lillie (1953) was the first author to propose formation boundaries in this region. This study largely adopts formation boundaries similar to those used by Lillie (1953). Four formations are recognised in this study: the Mangatoro, Te Aute, Kumeroa and Mangatarata formations.

3.2 Previous work:

3.2.1 Lillie (1953):

Lillie (1953) conducted the first in-depth geological study into the Dannevirke region, which includes the Manawatu Saddle. The formations identified and mapped by Lillie in the Manawatu Saddle can be found in Table 1. A total of four formations were mapped by Lillie, the oldest being the Mangatoro Formation deposited during the Opoitian. This is overlain by the Te Aute Formation ranging from Waipipian-Mangapanian in age. The Te Aute Formation is overlain by the Kumeroa Formation, which Lillie states spans the Nukumaruan. The youngest formation recognised in the Manawatu Saddle is the Mangatarata Formation, spanning the Castlecliffian.

3.2.2 Piyasin (1966):

Piyasin (1966) carried out a master's thesis focusing on the stratigraphy in the Manawatu Saddle and the geological history of the region. Piyasin's formations are presented in Table 1, and are broadly similar to those identified by Lillie (1953). The oldest formation is the Mangatoro Formation, within the same age range as Lillie (1953) i.e. deposited during the Opoitian. Piyasin also mapped the Te Aute Formation and found a similar age range to Lillie (1953): Waipipian-Mangapanian. A point of difference to Lillie's work is that Piyasin split the Kumeroa Formation in two separate formations, creating the Saddle Road Formation occupying the early Nukumaruan and the Kumeroa Formation spanning the late Nukumaruan. Piyasin also recognised the Mangatarata Formation spanning the Castlecliffian, similar to Lillie (1953).

3.2.3 Grammer (1971):

Grammer adopted formation names and ages vastly different to those used by Lillie (1953) and Piyasin (1966), Table 1. Grammer is the only author to identify a formation older that Opoitian. Grammer has identified the Te Apiti Sandstone, ranging in age from the Tongaporutuan to Kapitean. Grammer also identified the Morgan Grit Formation spanning the Opoitian, this formation also appears to be a Mangatoro Formation equivalent. Instead of recognising one formation spanning the Waipipian-Mangapanian like pervious workers Grammer identified a formation spanning each time zone. The Wharite Siltstone Formation spans the Waipipian and the Hope Sandstone Formation spans the Mangapanian. Grammer states that the Gorge Limestone Formation spans the Nukumaruan, which is once again different to past authors. No formations younger than the Nukumaruan were either mapped or recognised in Grammer's study.

3.2.4 Rees (2015):

Rees (2015) carried out a recent study on the Pohangina region, which includes the western Manawatu Saddle. The formations and ages can be found in Table 1. It is clear that the formation names and ages are significantly different from all past authors. As Rees focused on the younger Pohangina sedimentary rocks, the formations used in Rees study will not be adopted in this study.

3.2.5 This Study:

As can be seen in Table 1, this study has adopted similar formations to those proposed by Lillie (1953). Lillie's formation descriptions and formation boundaries best match the observations made during this study. So it is proposed that Lillie's (1953) formation boundaries should be quoted when working in the Manawatu Saddle

Table 1: Past authors' formation and time ranges
For more information on the time ranges of formations determined by this study, refer to chapter four, biostratigraphy.

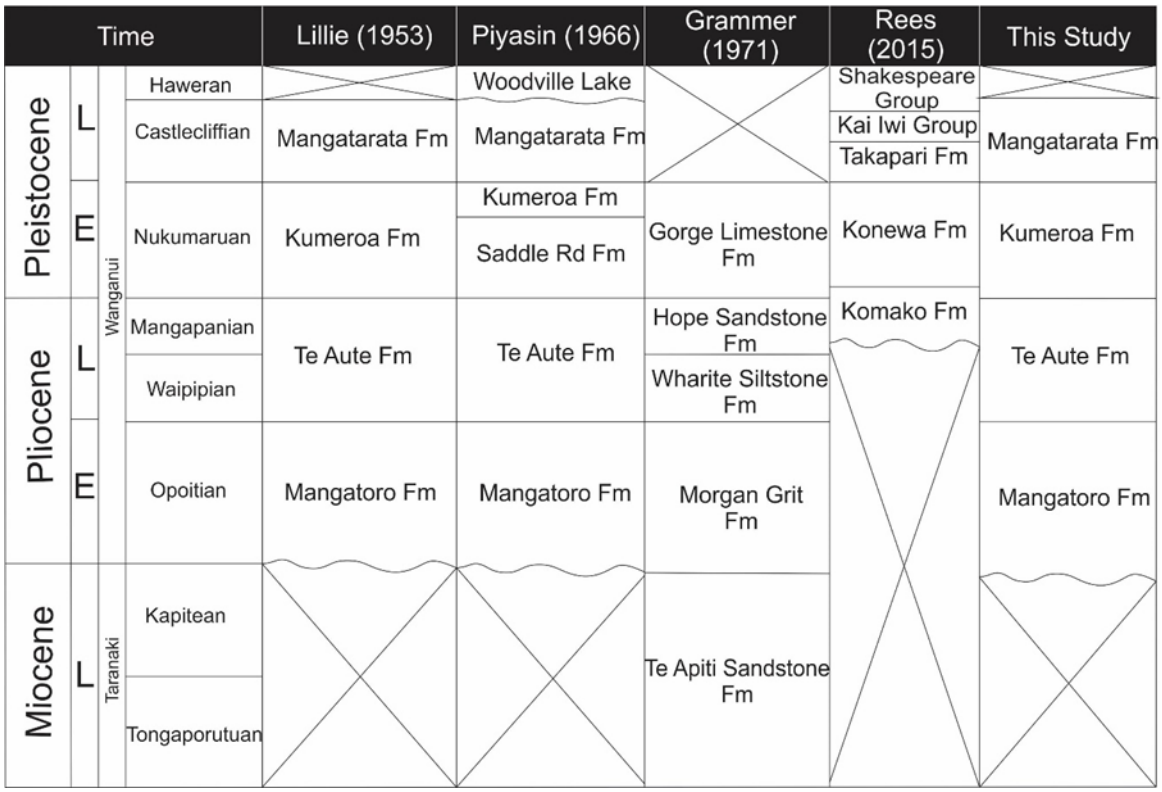

3.3 Regional Formation Descriptions

3.3.1 Basement:

The basement rock of the Manawatu Saddle consists of jointed greywacke and argillite collectively referred to as the Torlesse composite terrane or more specifically the Pahau terrane (Lee & Begg, 2002; Mortimer *et al*., 2014). The age of the basement ranges from Jurassic to earliest Cretaceous.

Formation Boundaries:

The upper unconformable contact is marked by a change in lithology, from the Torlesse Group to a coarse-grained pebble to bolder conglomerate. There is no dispute among past authors that this boundary marks the contact between the basement rock and the oldest Pliocene-Pleistocene formation in the Manawatu Saddle.

Location and Distribution:

The basement rock crops out extensively on the North Eastern and South Western margins of the Saddle. The low laying farm land on the eastern side of the Manawatu Saddle contains streams, which cut through the Mangatoro Formation to expose the basement rock.

3.3.2 Mangatoro Formation:

The Mangatoro Formation consists of an estimated 400-metre-thick sequence, marked at the base by a thin boulder to pebble conglomerate, overlain by a coarse-grained poorly-sorted sandstone. An upwards sequence fining to a sandy mudstone is observed. The upper section of the Mangatoro Formation consists of interbedded fine to medium-grained sandstone with interbedded coarse-grained sandstone, and scattered concretions.

Formation Boundaries:

The formation boundaries for the Mangatoro Formation recognised in this study are consistent with those proposed by Lillie (1953). The lower boundary between the Mangatoro Formation and basement rock is marked by an irregular unconformity and a coarse-grained conglomerate with clast sizes ranging from pebble to boulder. The upper contact is also thought to be unconformable, and marked by a lithology change from a medium-grained sandstone with interbedded coarse-grained sandstone, to a coarse-grained, moderately to poorly-sorted, conglomerate of the Te Aute Formation.

Location and Distribution:

The Mangatoro Formation dominates the eastern side of the Manawatu Saddle as seen in the geological map (Fig 1-4). Both Lillie (1953) and Piyasin (1966) have suggested the Mangatoro Formation is present on the western side of the Manawatu Saddle, but does not crop out and is instead covered by the overlying Te Aute Formation. This study was unable to confirm this assumption, and, as there is little evidence for or against this idea, we will assume that the Mangatoro Formation is present, albeit covered on the western side.

3.3.3 Te Aute Formation:

The Te Aute Formation consists of a 70-80 metre thick sequence of conglomerates. The lower section of the Te Aute Formation is marked by a sub-rounded, moderately to poorly sorted, conglomerate with blocky clasts, with interbedded coarse-grained sandstone lenses. The bulk of the formation consists of sub from well-rounded, blocky to oblate-shaped pebbles

to cobble sized clasts. A distinctive feature of this formation is beds dominated by the presence of clasts with whole attached barnacles.

Formation Boundaries:

The lower boundary of the Te Aute Formation was not observed in this study due to poor exposure. However past authors state that it is marked by an unconformity indicated by a sharp planar lithological change from the sandstones of the Mangatoro Formation, to the coarse-grained moderately to poorly sorted conglomerates of the Te Aute Formation (Lillie, 1953).

Location and distribution:

The Te Aute Formation is located on the western side of the Manawatu Saddle, as seen on the geological map (Fig 1-4). This formation is not observed to outcrop on the eastern Manawatu Saddle, and is thought to be covered by younger rocks.

3.3.4 Kumeroa Formation:

The Kumeroa Formation is an estimated 80 metres thick, and outcrops on the western and eastern margins of the Manawatu Saddle. The western formation outcrops consist of thin, vaguely bedded siltstone and sandy limestones. The eastern exposure of the Kumeroa Formation consists dominantly of a pebbly, coarse-grained shell-hash limestone, with interbedded thin conglomerate beds and siltstones.

Formation Boundaries:

The lithological boundaries of the Kumeroa Formation exposed on the western side of the Manawatu Saddle are similar to those used by Lillie (1953), where the lower boundary is marked on the western Manawatu Saddle by a sharp contact between the conglomerates of the underlying Te Aute Formation and the lower-most siltstone of the Kumeroa Formation. The upper contact is much less obvious in the field and Lillie (1953) stated that there was a gradational change from the Kumeroa Formation to the Mangatarata Formation. The Kumeroa Formation on the eastern side of the Manawatu Saddle shows an unconformable lower contact. The transition from the underlying Mangatoro Formation is identified by a sharp and wavy change in lithology from the muddy sandstone of the Mangatoro Formation, to thin sandy conglomerate of the Kumeroa Formation.

Location and Distribution:

The Kumeroa Formation is located on the western margin of the Manawatu Saddle and has good exposure in fresh road work outcrops along the Saddle Road and nearby streams. The eastern exposure of the Kumeroa Formation, at the eastern entrance to the Manawatu Saddle, is much less extensive. This exposure is bound by the Ruahine and Mohaka Faults.

3.3.5 Mangatarata Formation:

The total Mangatarata Formation thickness is unknown, as it was not fully measured in this study, due to only a small proportion outcropping on the western Manawatu Saddle margin. The formation broadly consists of a fine to medium-grained sandstone, with decimetre scale interbedded sandstone and siltstone. The formation also contains scattered coarse-grained sandstone lenses, tephra layers and reworked pumice. This regional description is based on work carried out by this study and by Lillie (1953), Piyasin (1966) and Rees (2015).

Formation Boundaries:

The lower boundary of the Mangatarata Formation is marked by a gradational change from the underlying Kumeroa Formation. The change between formations is marked by a gradational change from coarse-grained sandstone to decimetre scale sandstone and siltstone interbeds.

Location and Distribution:

The Mangatarata Formation is found only on the western margin of the Manawatu Saddle and extends into the Pohangina Valley as shown by this study. However, it has also been noted by Lee and Begg (2002) to be present throughout the eastern Woodville region.

3.4 Measured sections:

3.4.1 Introduction:

Five sections were logged at key locations throughout the Manawatu Saddle. Three sections were measured on the eastern side of the Manawatu Saddle, these are the Ballantrae Farm, Wharite Road and Eastern Manawatu Gorge Entrance measured sections. The Eastern Manawatu Gorge Entrance measured section made use of unprecedented exposure due to large sale earth works related to the removal of railway tunnels. Two sections were measured on the western side of the Manawatu Saddle; these are the Western Saddle Road and Broadlands Stream measured sections. The Western Saddle Road measured section was constructed to take advantage of the fresh outcrop exposure due to recent road works. Outcrop photos and detailed lithological descriptions are shown in this chapter for each section.

3.4.2 Ballantrae Farm Measured Section:

Location: Lat: -40.296385, Long: 175.786142, Coordinate system NZTM

The Ballantrae Farm measured section (Fig 3-3) was measured on the eastern side of the Manawatu Saddle (Location as per Fig 1-1). Fig 3-1 shows a field photo of the section. This section shows the unconformable contact between the basement rock and Mangatoro Formation. The thickness of this section was estimated by using a combination of GPS points throughout the section, and projecting these points onto a cross section. The section was too steep for conventional Jacob's staff and Abney level measuring but shows a patchy outcrop exposure. In addition, the Ruahine Fault cuts through the Ballantrae Farm creating some uncertainty regarding the true thickness.

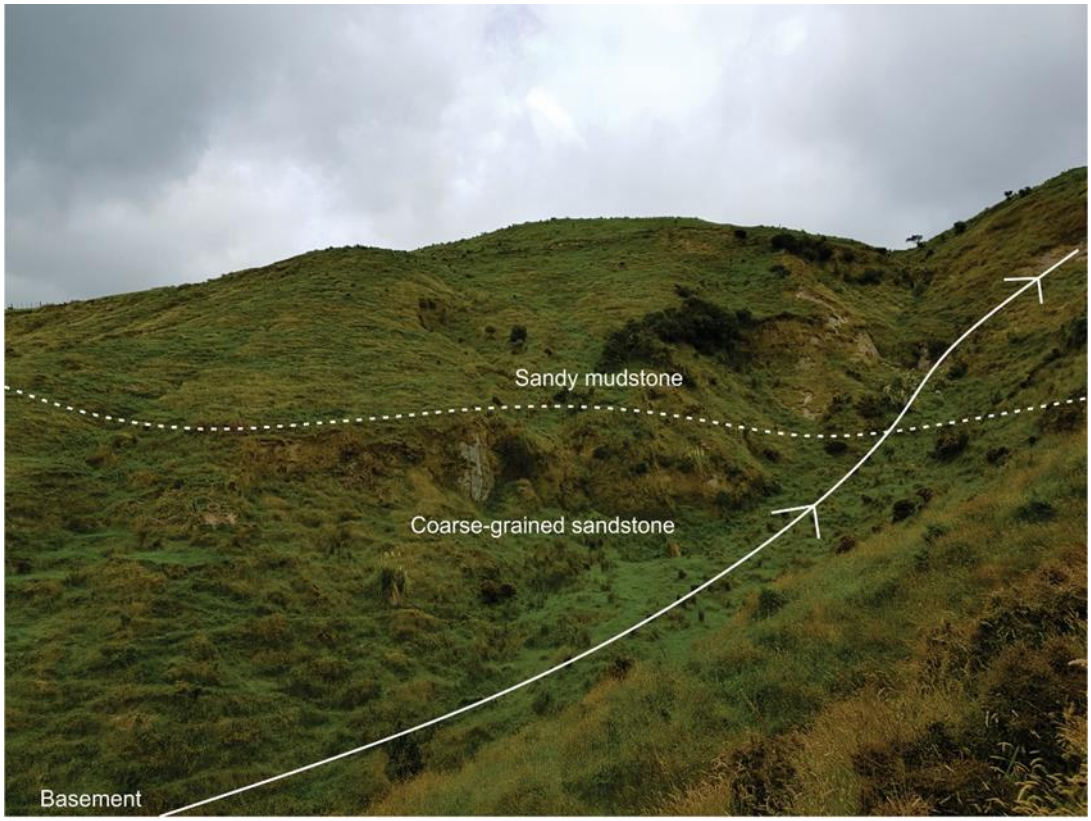

Figure 3-1: Field photo showing the location of the Ballantrae Farm measured Section. Note the white line indicates the broad location of the section. This image also highlights the patchy exposure of the section.

Four distinctive units based on lithological characteristics are observed. The base of the section is marked by a thin three metre thick conglomerate, unconformably overlaying the basement. Overlaying the thin conglomerate is a 27 metre thick coarse-grained sandstone, overlying which is a sandy mudstone an estimated 150 metres thick. The contact between the sandstone and sandy siltstone was not observed due to poor exposure. Overlying the sandy mudstone is a 170 metre thick medium-grained sandstone with interbedded coarse-grained sandstone.

The conglomerate (0-3m on the log) consists of gravel to boulder sized blocky-shaped clasts. The conglomerate is clast supported and contains whole thick walled macro fossils. The lower contact is marked by an irregular wavy surface with up to two to three metres of refile (Fig 3-2A). Overlying the conglomerate is a coarse-grained sandstone (3-30m on the log). The sandstone is poorly sorted and contains scattered shell hash and from pebble to cobble sub-round blocky shaped Torlesse clasts.

Overlying the coarse-grained sandstone is a sandy mudstone (30-230 m on the log), vaguely bedded on a one to three metre scale. Scattered shell hash and Torlesse pebbles form irregularly spaced lenses less than one metre thick and, scattered decimetre-scale coarse-grained sandstone lenses (Fig 3-2B). Overlying the sandy mudstone is a medium-grained sandstone with interbedded coarse-grained sandstone beds (Fig 3-2C: 230-400m on the log) well bedded on a five metre scale, highly bioturbated, with scattered whole and fragmented shell hash and concretions.

Figure 3-2: Mangatoro Formation Ballantrae Farm.
Wavy unconformable nature of the lower contact of the Mangatoro Formation, hammer for scale ~30cm (Lat: -40.307153, Long: 175.840688) B) Coarse-grained sandstone lenses present in the middle interval of the Mangatoro Formation (Lat:-40.299527, Long:175.832748). C) Coarse-grained sandstone interbed of the Mangatoro Formation (Lat: -40.29884, Long: 175.829744)

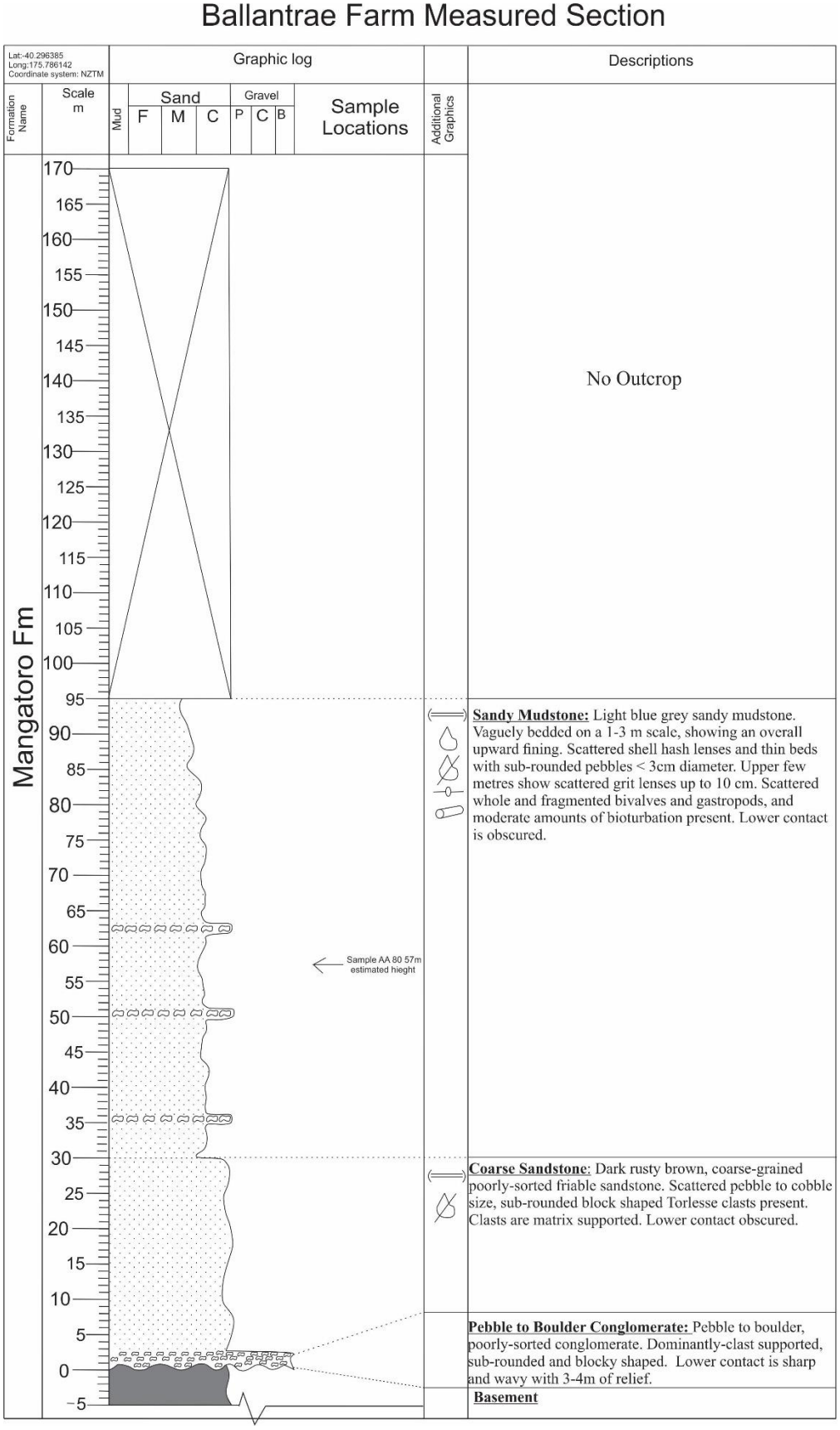

Figure 3-3: Ballantrae Farm measured section.

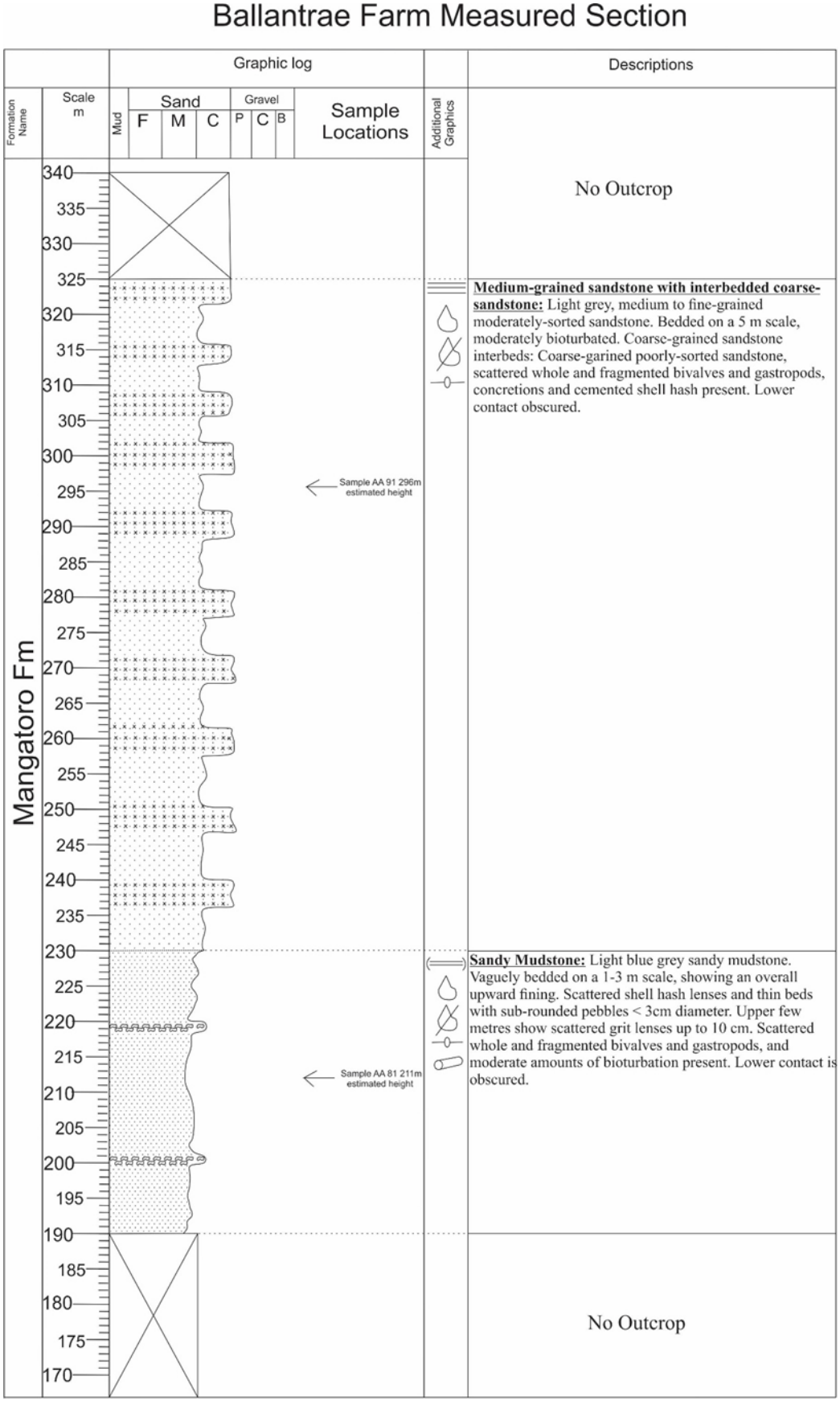

Figure 3-3 Continued

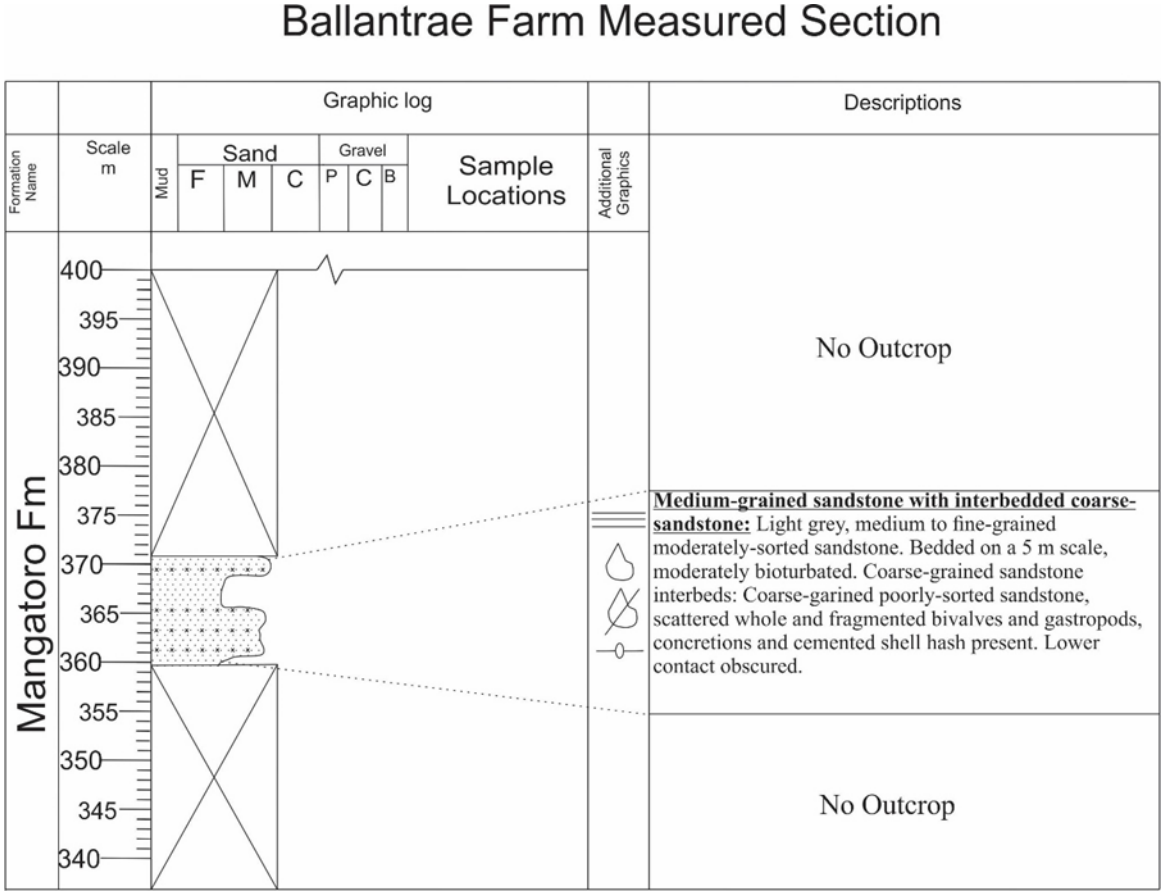

Figure 3-3 Continued

3.5 Wharite Road Measured Section

Location: Lat: -40.277136, Long: 175.853219, Coordinate system: NZTM.

This section is located on the eastern side of the Manawatu Saddle on Wharite Road (Fig 3-6). The measured section was constructed using a combination of GPS points, and outcrop thickness measurements where available. The middle of the measured section was not exposed, so GPS locations were placed on a cross section. The dip was projected on the cross section and the thickness estimated this way. The exposed section was measured using a tape measure (Fig 3-4).

Figure 3-4: Outcrop exposure of the upper sandstone of the Wharite Road measured section. (Lat: -40.285779, Long 175.863647:).

The Mangatoro Formation was the only formation observed in this section, and 90 metres of the formation was measured. The base is marked by a 10 metre thick, well-bedded, clast supported conglomerate (Fig 3-5 A, B, C). Clasts that make up the conglomerate range in shape from blocky to disk, and range in roundness from sub to well-rounded. The upper three metres are marked by a coarse-grained, poorly-sorted sandstone (Fig 3-5 D), scattered pebble to cobble size clasts are present along with cross bed structures.

Overlying the conglomerate is a poorly-sorted, coarse-grained sandstone. The sandstone is well bedded on a 2-4 metre scale indicated by concretionary bands (Fig 3-5 E). It is highly bioturbated with scattered whole and fragmented bivalves and gastropods present.

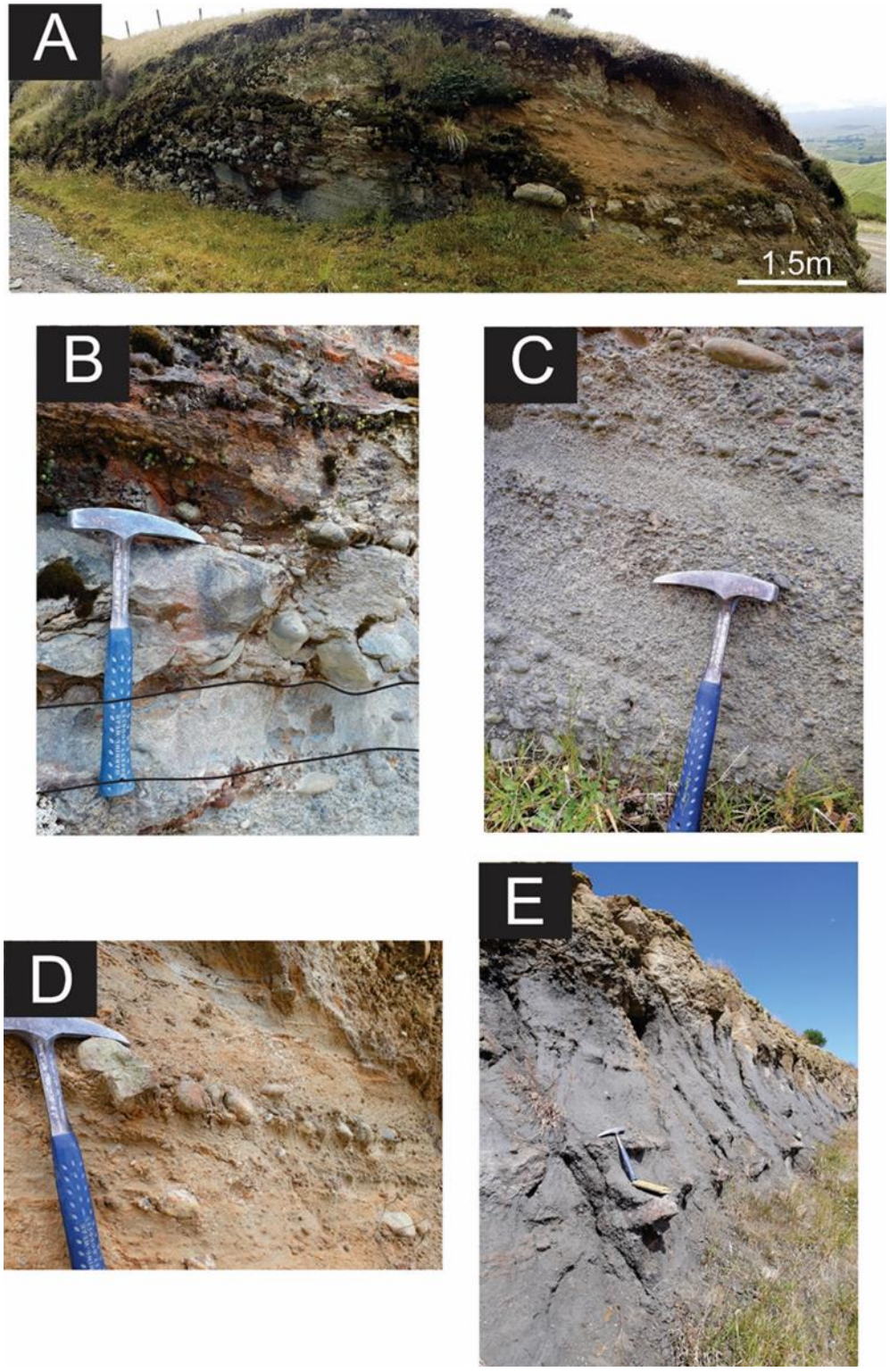

Figure 3-5: Outcrop photos of the Wharite Road measured section.
A) An outcrop of the conglomerate exposed on Wharite Road (Lat: -40.277136, Long: 175.853219) B and C) Bedding in the conglomerate indicated by grain size, shape and clast alignment, photo same location as A. D) A section of the pebbly sandstone overlying the conglomerate, note the clast shape and roundness variation, photo same location as A. E) The upper sandstone showing concretionary layers (Lat: -40.285779, Long: 175.863647).

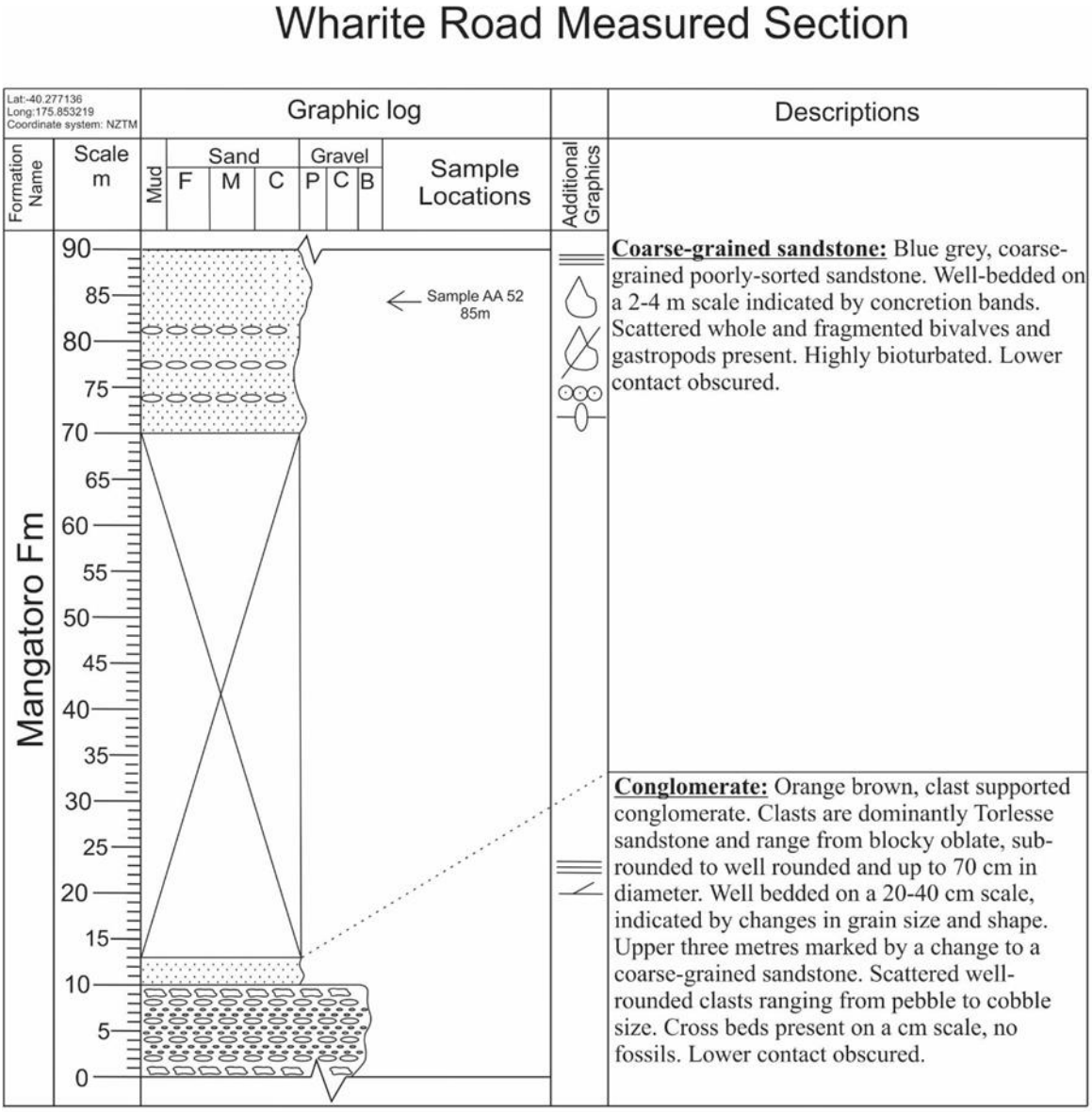

Figure 3-6: Wharite Road measured section.

3.6 Eastern Manawatu Gorge Entrance Measured section

Location: Lat: -40.335586, Long: 175.820174, Coordinate system: NZTM.

This section was measured on the eastern side of the Manawatu Gorge. The measured section made use of recent earth works related to the removal of a railway tunnel (Fig 3-7), providing unpresented exposure of the sedimentary rocks. An 80 metre measured section of sedimentary rocks that had been tilted up to 40º was measured by Dr Cliff Atkins at the time of the earthworks. This study expanded this 80 metre section by measuring the underlying Mangatoro Formation (150 metre exposure) to the Ruahine Fault, and combined the two sections to now provide a 230 metre thick section (Fig 3-9). Two formations are observed in this measured section, the Mangatoro Formation and the Kumeroa Formation. Based on

observations made when measuring the section, there appears to be no evidence that would indicate a Te Aute Formation equivalent is present. A grain size sample was taken from the Mangatoro Formation, and microfossil samples were collected from both the Mangatoro and Kumeroa formations. Both sections were measured using the Jacob's staff and Abney level method. This measured section is bounded by both the Ruahine and Mohaka faults.

Figure 3-7: Earthworks at the Eastern Manawatu Gorge Entrance measured section. Note the white annotated line indicates the location of the measured section.

The Mangatoro Formation makes up the lower 150 metres of this measured section. The formation at this location comprises massive sandy mudstone that is highly bioturbated and contains scattered shell fragments, and rare whole bivalves and gastropods. At a stratigraphic height of 65 metres, a sample was taken for grain size analysis (GS-1), as this outcrop was highly bioturbated and the grain size sample helped characterise the formation and allow for correlation. The grain size results confirmed the outcrop was Mangatoro Formation and consists of a sandy mudstone. A grain size plot can be found in Appendix Two. The upper five metres of the formation is marked by a medium-grained sandstone with abundant whole

and fragmented bivalves and gastropods. The lower contact of the formation is obscured, and truncated by the Ruahine Fault.

The Kumeroa Formation is unconformably overlying the sandy mudstone of the Mangatoro Formation. The Kumeroa Formation is much thicker at this measured section than any other location in the Manawatu Saddle. The formation consists predominantly of a pebbly shell hash limestone, with thin conglomerate and siltstone beds separating the limestones (Fig 3-8 A,B). The lower part of the Kumeroa Formation is marked by a 15 metre thick sequence of sandy conglomerates and sandstones with interbedded siltstones. Overlying this is a 25 metre thick sandy shell hash limestone. The limestone consists mostly of coarse-grained poorly-sorted sandstone, with the shell hash component made up of fragmented bivalves, gastropods and barnacle plates. Irregularly spaced beds less than 1 metre thick, consisting of sub-rounded conglomerate pebbles, are present throughout the limestone. The overlying sandy limestone is a 21 metre thick sequence of conglomerate and siltstones marked by sharp lower contacts. The conglomerates consist broadly of both clast and matrix supported blocky shaped sub-rounded Torlesse sandstone clasts. Rare clasts with whole attached barnacles are scattered throughout the conglomerate beds. The siltstones are massive with scattered shell hash. Overlying this sequence is another 20 metre thick sequence of pebbly limestone, similar to the lower sandy limestone marked by a gradational lower contact.

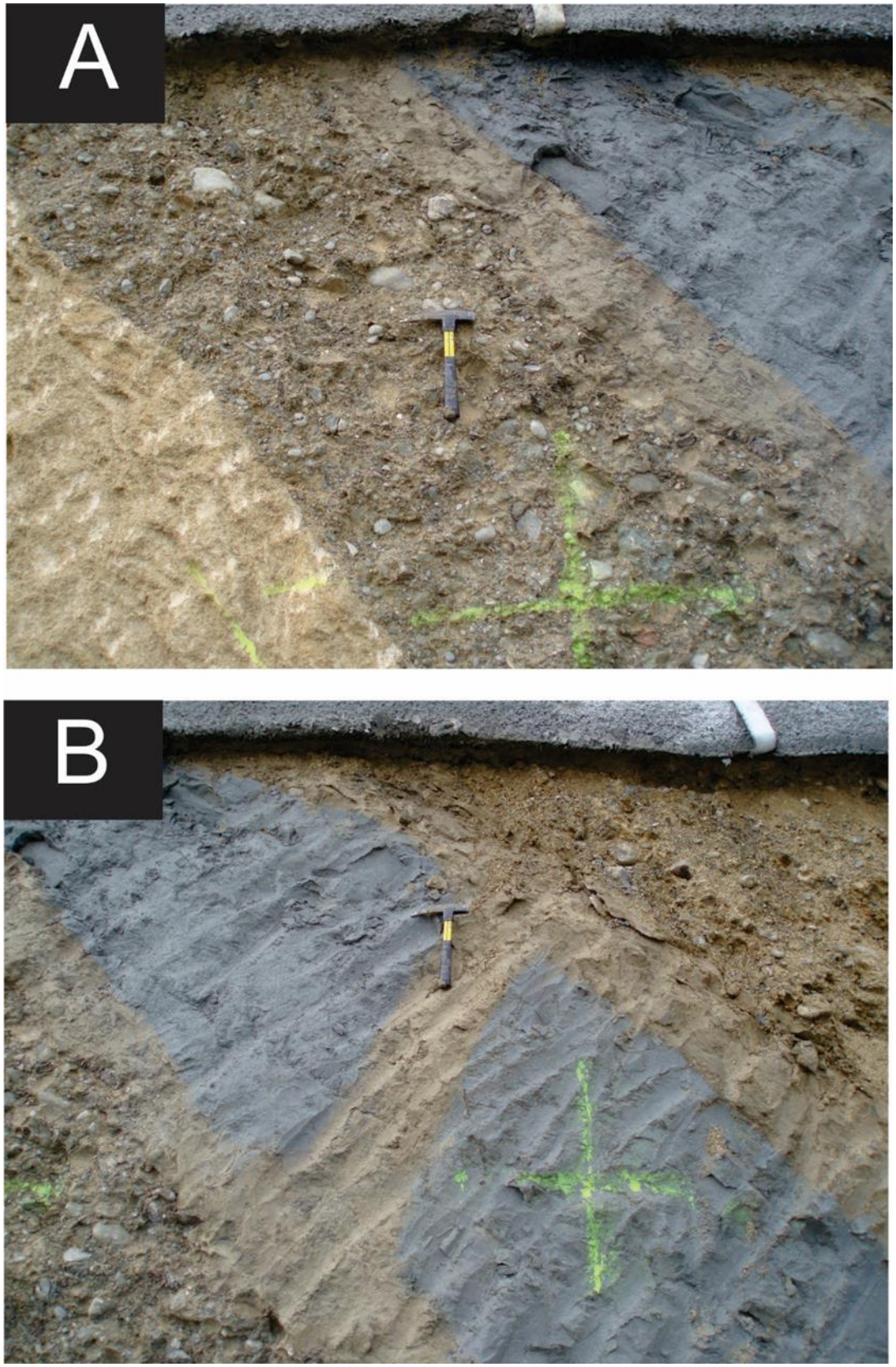

Figure 3-8: Outcrop photos of the Eastern Manawatu Gorge Entrance measured section. A) Sharp contacts between a sandy limestone, thin conglomerate and siltstone. B) Sharp contacts between a conglomerate, siltstone and sandy conglomerate.

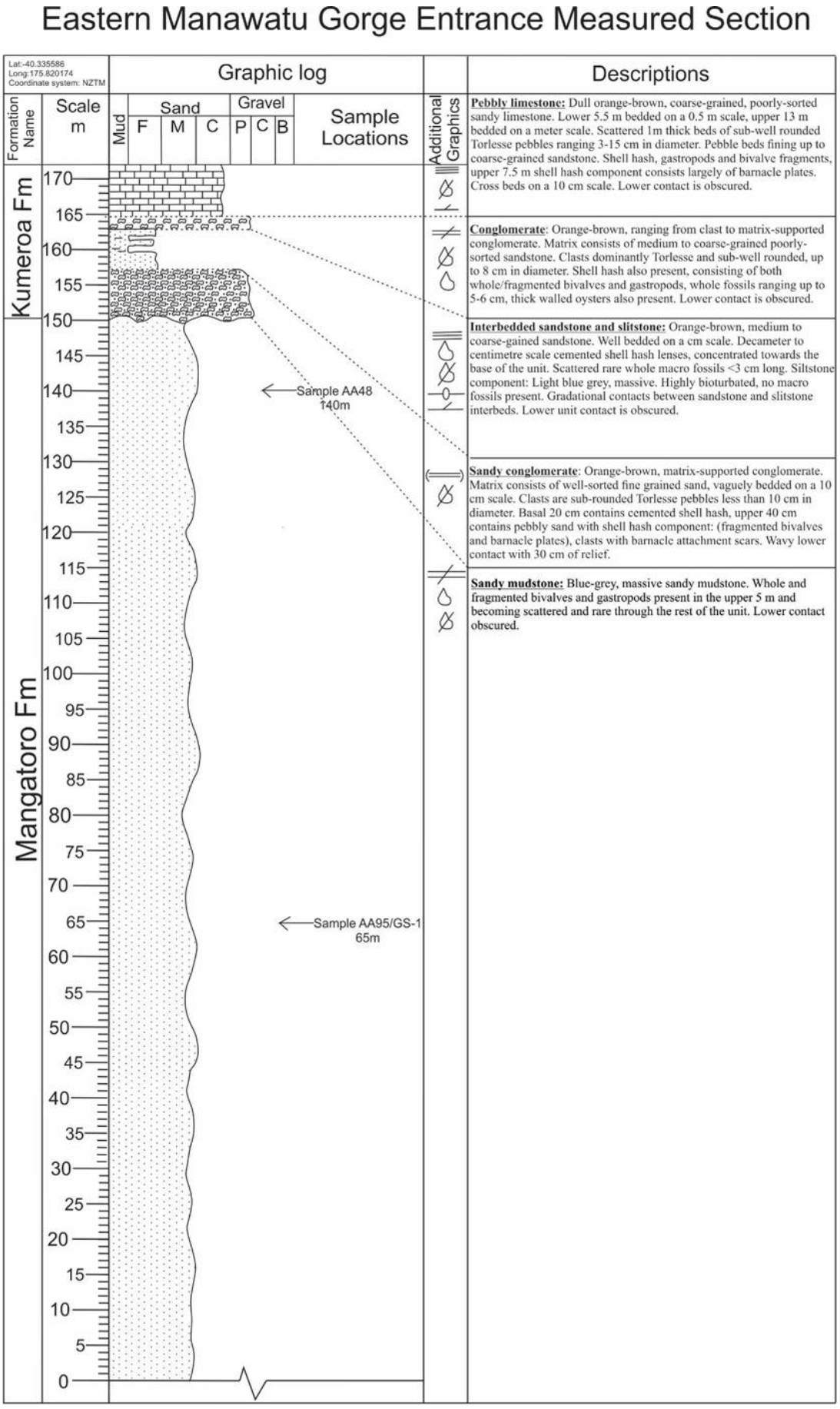

Figure 3-9: Eastern Manawatu Gorge Entrance measured section.

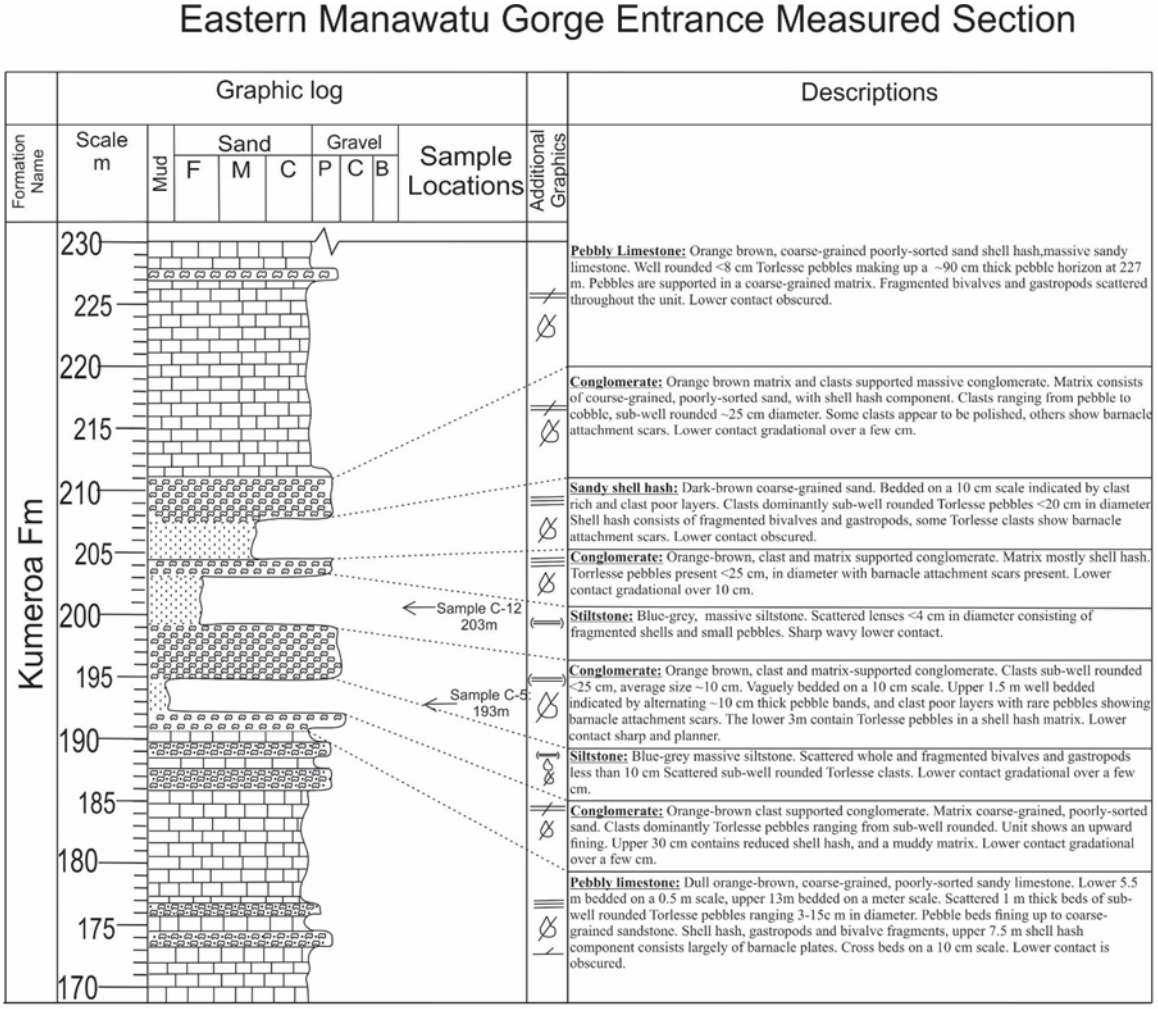

Figure 3-9 Continued.

3.7 Broadlands Stream measured section

Location: Lat: -40.27946, Long: 175.790606, Coordinate system: NZTM:

This section was measured on the western side of the Manawatu Saddle, in the Broadlands Stream, 1 km north from the Saddle Road (Fig 1-1). This section is 105 metres thick and was measured using Jacob's staff and Abney level method for the exposed section (Fig 3-11).

Two formations are observed in this section, 85 m of Te Aute Formation and 20 m of Kumeroa Formation. The lower 24 m of the exposed Te Aute Formation comprises conglomerate with coarse-grained sandstone interbeds. The basal conglomerate is characterised as well-bedded, with matrix supported blocky shaped sub-rounded clasts. The sandstone interbeds range from one to three metres. Overlying this is a three metre thick conglomerate that contains whole and fragment bivalves and gastropods. These conglomerates are overlain by an eight metre thick blue-grey siltstone, which is vaguely bedded on a metre scale, with millimetre scale scattered organic stringers and centimetre scale wood fragments, and shell hash marked by a gradational lower contact.

Overlying the siltstone is a 13 m thick conglomerate with interbedded sandstone lenses. Clasts range from clast to matrix supported, are cobble sized and mostly disk shaped. Sandstone lenses are coarse-grained and well-sorted, up to one metre thick with decimetre scale bedding. Overlaying the conglomerate is a thin five metre thick coarse-grained sandy limestone (Fig 3-10A). The limestone is well-sorted and well-bedded on a metre scale, indicated by altering barnacle plate dominated beds, high angle metre scale cross beds and abundant shell hash, marked by a gradational contact. Overlying the thin sandy limestone, 24 m thick well-bedded conglomerate marks the top of the Te Aute Formation in this section. Alternating beds of matrix to clast supported, disk shaped clasts with whole attached barnacles (Fig 3-10B) are marked by a gradational lower contact.

The base of the Kumeroa Formation is marked by a 10 m thick blue-grey siltstone, vaguely bedded on a metre scale, and marked by a gradational lower contact. The top of the Broadlands Stream measured section is marked by a 10 m thick sandy limestone. This sandstone is coarse-grained and poorly-sorted, vaguely bedded on a metre scale with irregularly spaced < 1m thick siltstone lenses, whole and fragmented macro fossils and Torlesse pebbles (Fig 3-10C). Dewatering structures are present in Fig 3-10D, and the lower contact sharp planar is highly bioturbated (Figure 3-10E).

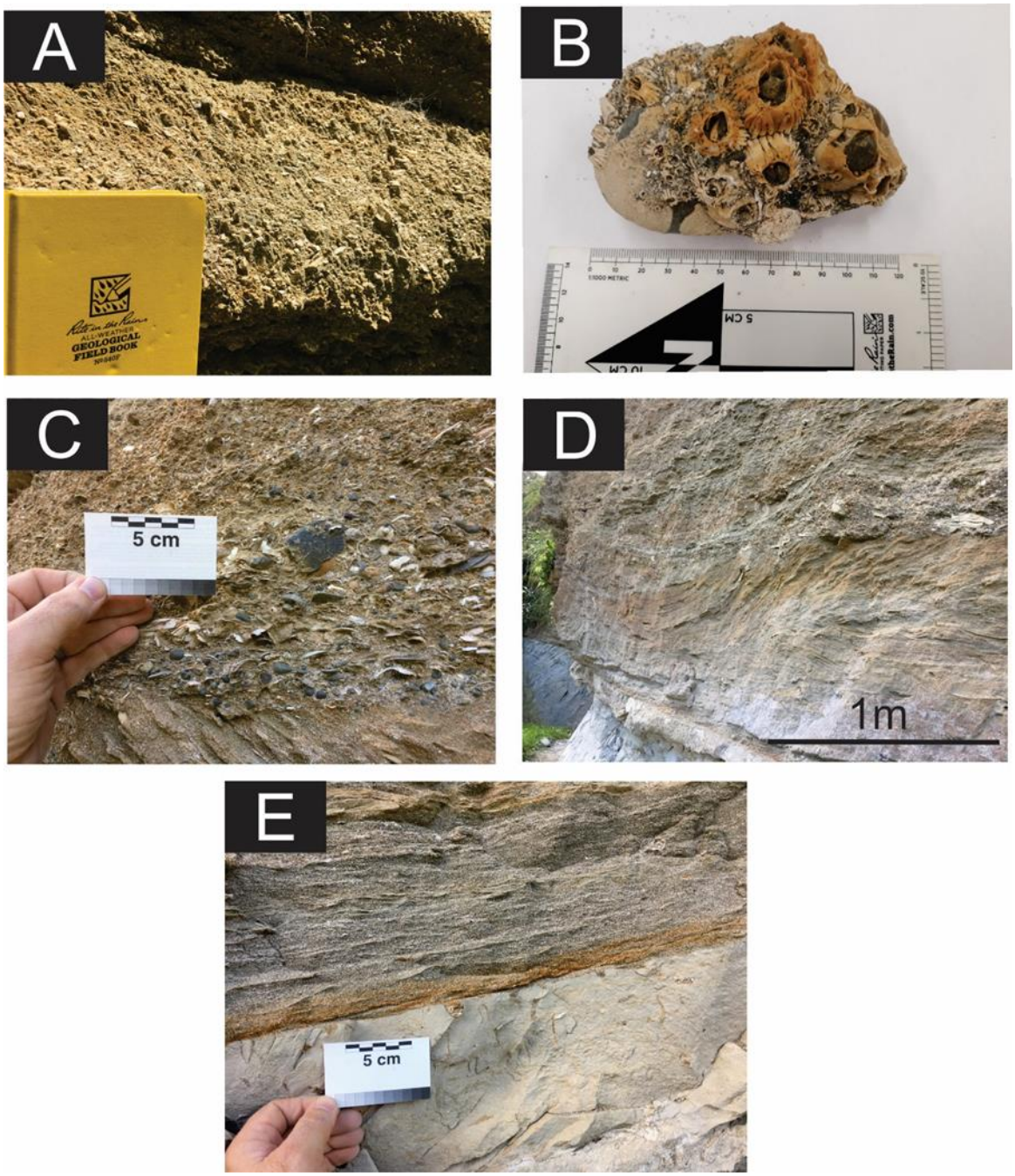

Figure 3-10: Outcrop pictures of the Broadlands Stream measured section.
A) Barnacle plate dominated bed in the thin Te Aute Formation limestone (Lat: -40.27982, Long: 175.787773). B) Clast with whole attached barnacles from a conglomerate bed in the Te Aute Formation (Long: -40.279591, Long: 175.785713). C) A shell hash bed with cm scale sub-rounded to well-rounded pebbles in the sandy limestones of the Kumeroa Formation, photo same location as B. D) Sedimentary structures within the sandy limestone from the Kumeroa Formation, photo location same as B. E) Lower contact between the Kumeroa Formation siltstone and limestone, Photo location same as B.

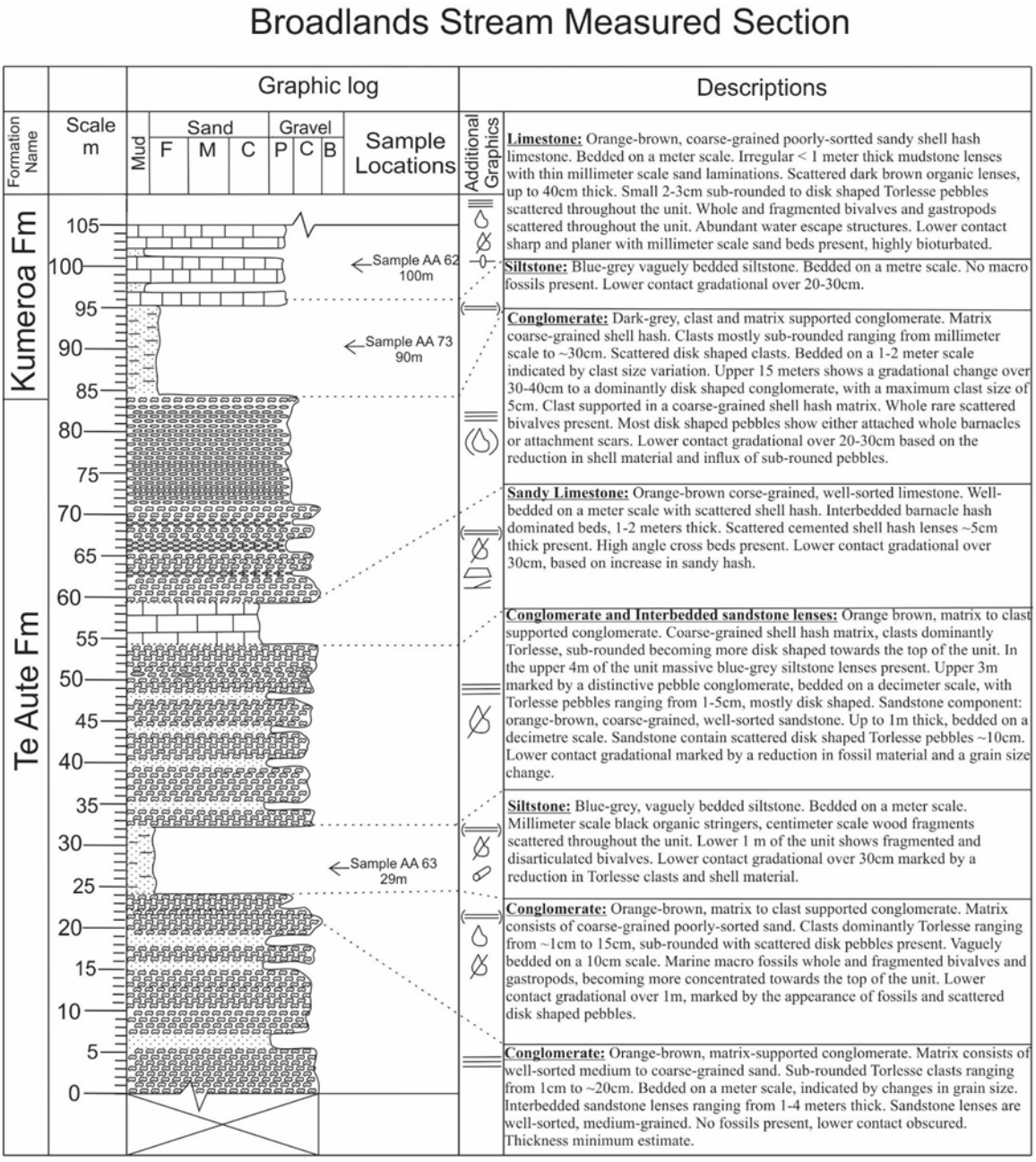

Figure 3-11: Broadlands Stream measured section.

3.8 Western Saddle Road measured section:

Location: Lat: -40.286564, Long: 175.786743, coordinate system: NZTM:

The Western Saddle Road section (Fig 3-13) was measured on the western side of the Manawatu Saddle, and is located 1 kilometre south of the Broadlands Stream measured section (Fig 1-1). The section utilised fresh outcrops related to earthworks on Saddle Road. The thickness was measured using the Jacob's staff and Abney level method. A total of 240m of section was measured and comprises two formations, the Te Aute and the Kumeroa Formations.

The Te Aute Formation makes up the lower 85m of the section and is dominated by conglomerates. This conglomerate is well-bedded, indicated by variations in grain size and clast shape. A distinctive feature of this formation is the presence of oblate to disk shaped, well-rounded clasts with attached whole barnacles, similar to those observed in the Broadlands Stream section. Large-scale cross beds are also present. The lower contact of the Te Aute Formation at this location is obscured.

Directly overlying the conglomerate is the Kumeroa Formation. The lower interval (85-115 m) of the Kumeroa Formation comprises a 30 m thick vaguely-bedded siltstone. Overlying this, the middle interval (115-128 m) is marked at the base by a 14 m thick well-bedded medium to fine-grained well-sorted sandstone. Overlying the sandstone is an 11 m thick sandy limestone (128-140 m) (Fig 3-12A), with abundant water escape structures and cross beds (Fig 3-12B), scattered whole and fragmented bivalves, gastropods and barnacle plates.

The upper section of the Western Saddle Road measured section is marked by the Mangatarata Formation (140-240 m), consisting of a 100 m thick sequence of medium to fine-grained well-sorted sandstone with thin interbedded siltstones. The sandstones contain thin decimetre mudstone laminations, whole and fragmented shells, and are highly bioturbated with convolute laminations present. The lower contact with the underlying Kumeroa Formation is gradational.

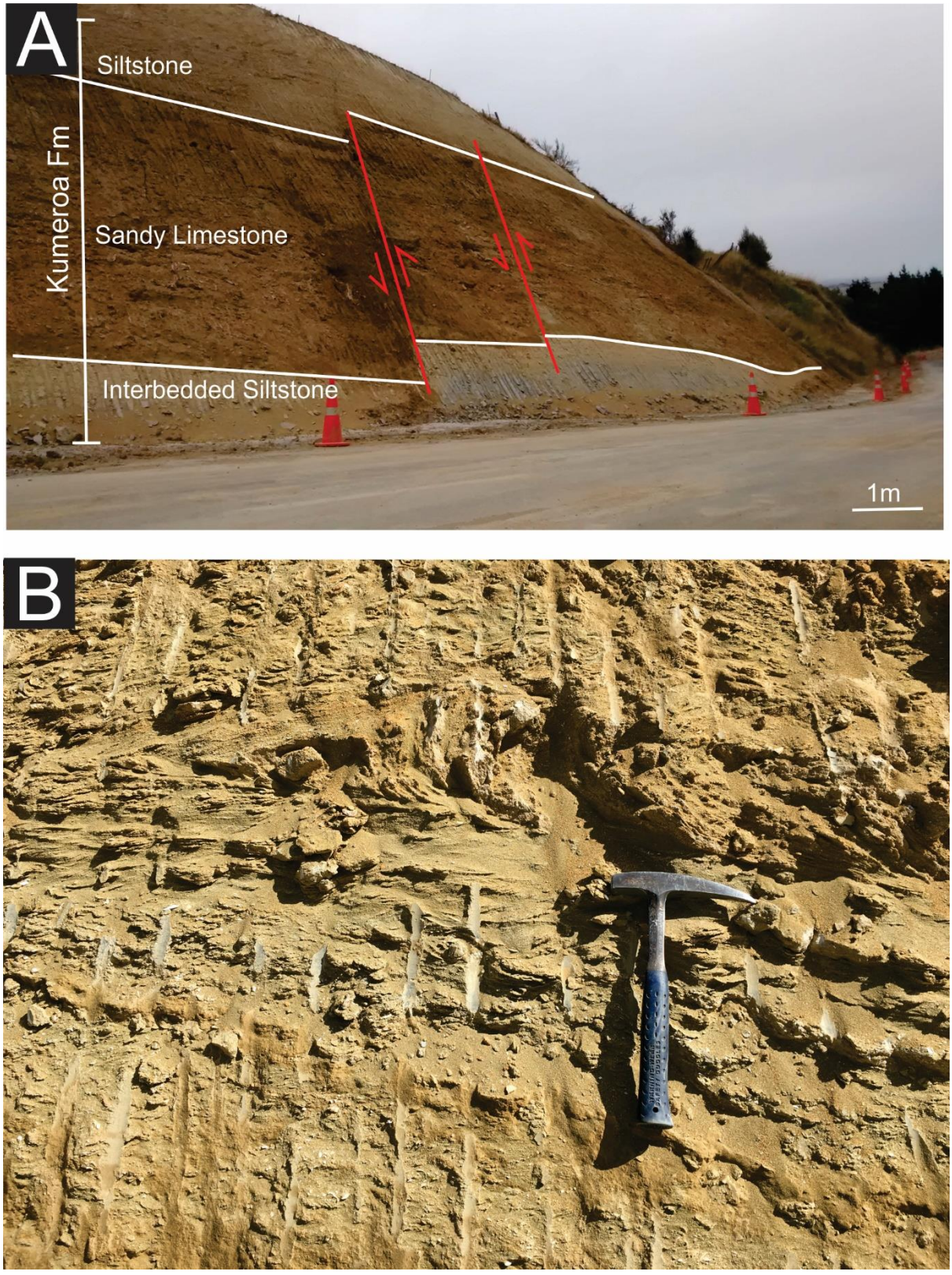

Figure 3-12: Outcrop photos of the Western Saddle Road measured section.
A) Exposure of the Kumeroa Formation showing the sandy limestone overlying siltstone bed, photo location (Lat: -40.28627, Long: 175.781679). B) Outcrop photo of the Kumeroa Formation limestone showing dewatering structures, photo location (Lat: -40.28627, Long: 175.781679).

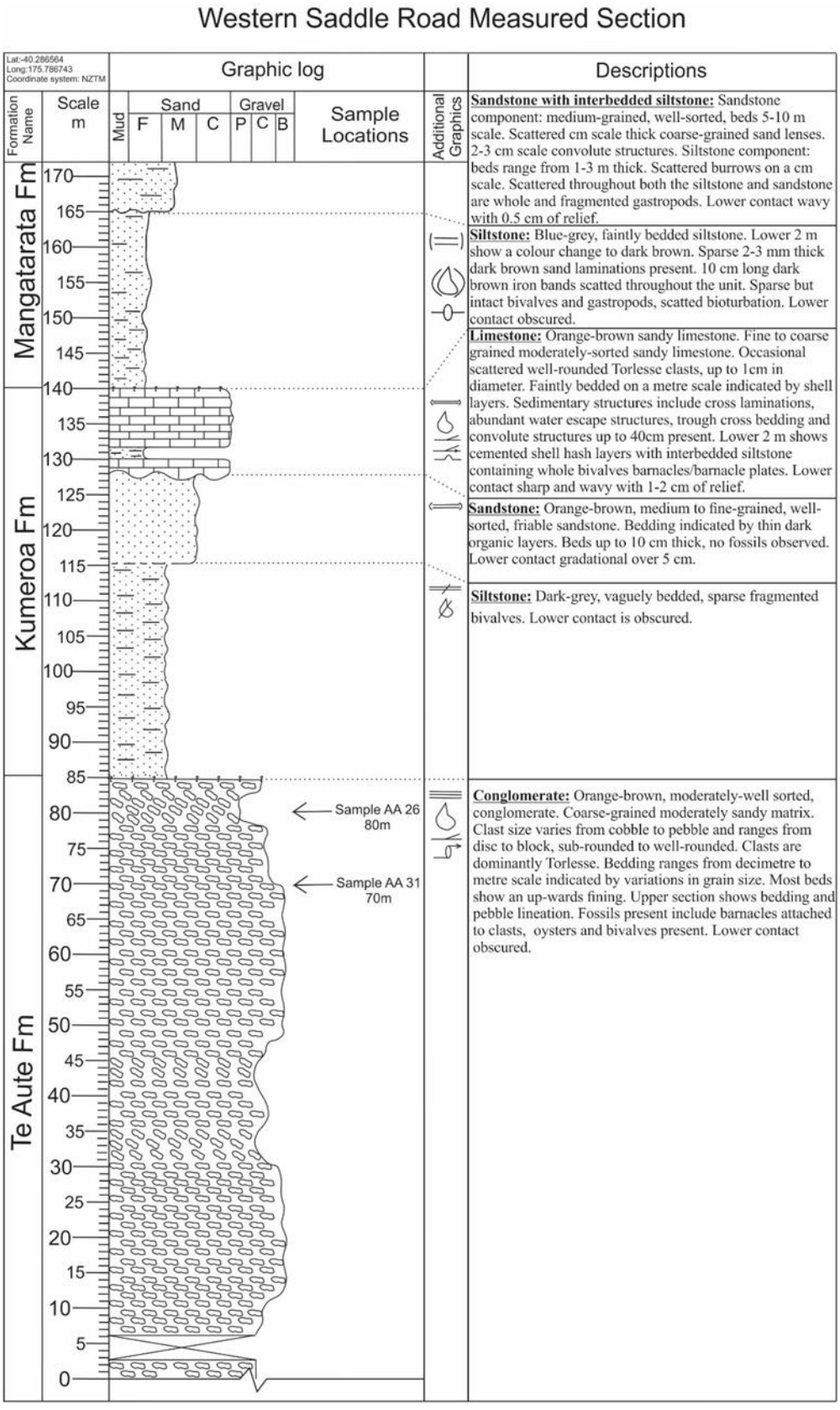

Figure 3-13: Western Saddle Road measured section.

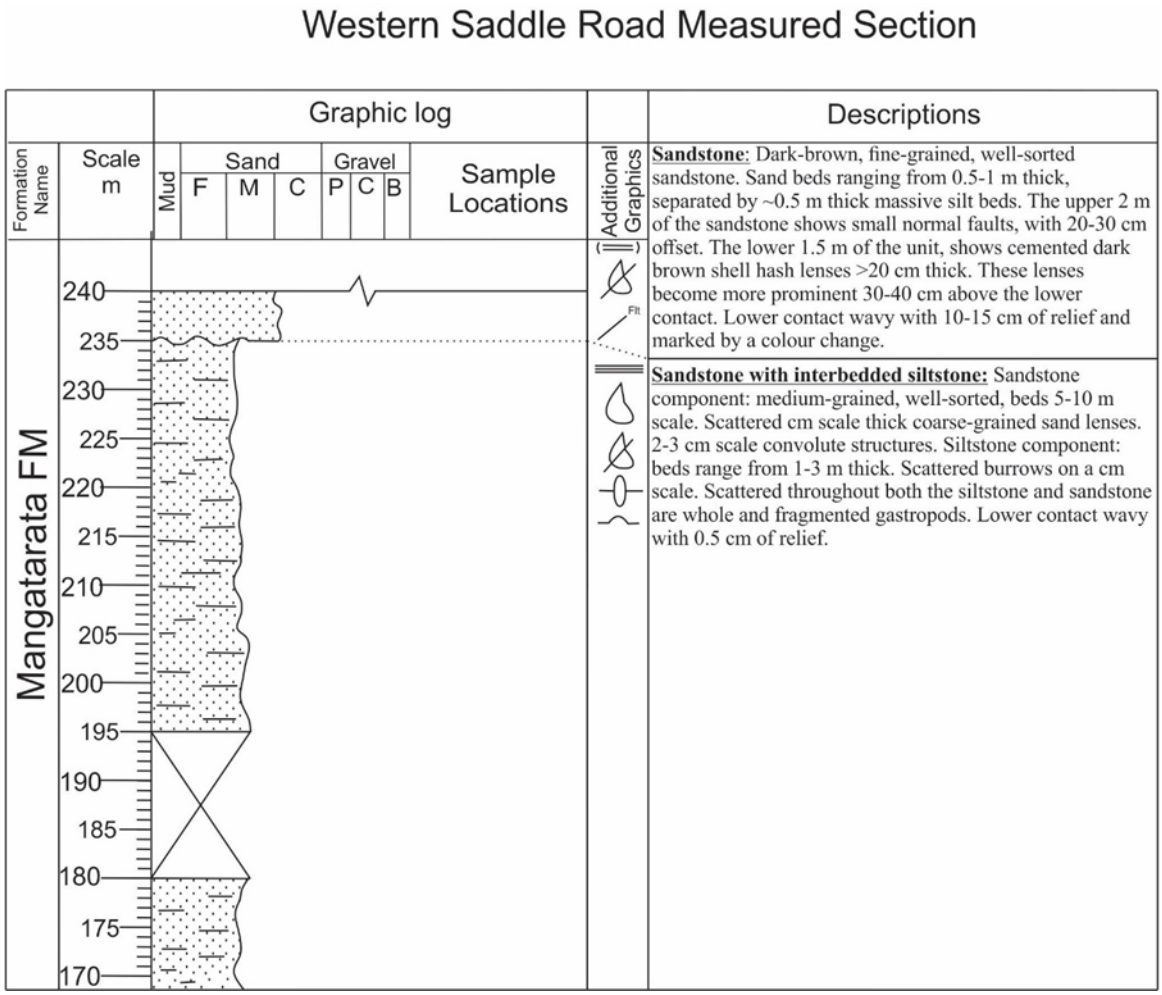

Figure 3-13 Continued

Chapter 4 Biostratigraphy

4.1 Introduction:

This chapter discusses the age ranges of each formation using biostratigraphy, and compares the ages found in this study to those proposed by past authors. When examining the age ranges of both the macro and microfossils found within each formation, it was noted that the microfossils showed very large age ranges. Based on this, the information presented in this chapter will focused on the macrofossils collected. The microfossil data is used in chapter five. The age range for the oldest formation, the Mangatoro Formation, was found to be consistent with past studies, spanning the Opoitian. The age range identified for the Te Aute Formation is unable to be as tightly constrained as in past studies. The Kumeroa Formation spans the Nukumaruan, which is similar to past studies. The resolution of the data does not allow this study to constrain the formations to early, middle or late parts of stages. Nevertheless, this study presents the most up-to-date biostratigraphy carried out on the sedimentary rocks within the Manawatu Saddle, and allows past authors' ranges to be reviewed.

4.2 Mangatoro Formation:

The Mangatoro Formation unconformably overlies the basement rock of the Manawatu Saddle. The formation contains the oldest sedimentary rocks (aside from the basement) in the field area that this study focuses on, outcrops on the eastern side of the Manawatu Saddle. Abundant, mostly well-preserved macrofossils are scattered throughout the formation, with the most diverse fauna sampled at the Eastern Manawatu Gorge Entrance measured section.

Based on four key macrofossils, the Mangatoro Formation can be constrained to Opoitian (5.33-3.70 Ma) in age (Fig. 4-1). The presence of *Struthiolaria (Callusaria) obesa* (Fig 4-2 A) constrains the upper range of the Mangatoro Formation to the Opoitian-Mangapanian boundary (3.70 Ma). *Amalda (Baryspira) mucronata, Zeacolpus vittatus* and *Clavatoma pulchra* (Fig 4-2, B,C,D) constrain the lower range of the Mangatoro Formation to the Kapitean-Opoitian boundary (5.33 Ma) (Beu *et al.*,1990, Beu, 2012). *Pelicaria canaliculata* (Fig 4-2 E) is Waipipian (3.70-3.00 Ma) restricted and was identified in the Eastern Manawatu Gorge Entrance section. However, due to the fragmentary nature of the sample, it is thought not to be in situ, and the result of post deposition reworking. The age range for the Mangatoro Formation presented in this study is consistent with the ranges presented by past authors (Lillie, 1953; Piyasin, 1966).

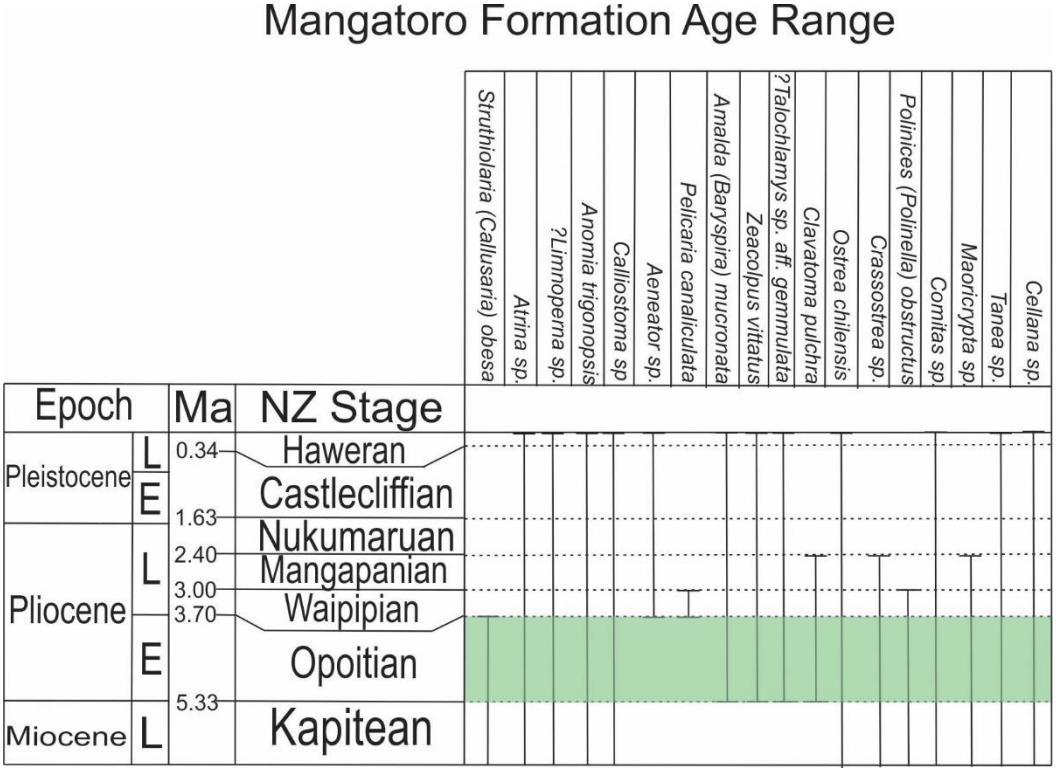

Figure 4-1: Age range chart for the Mangatoro Formation.

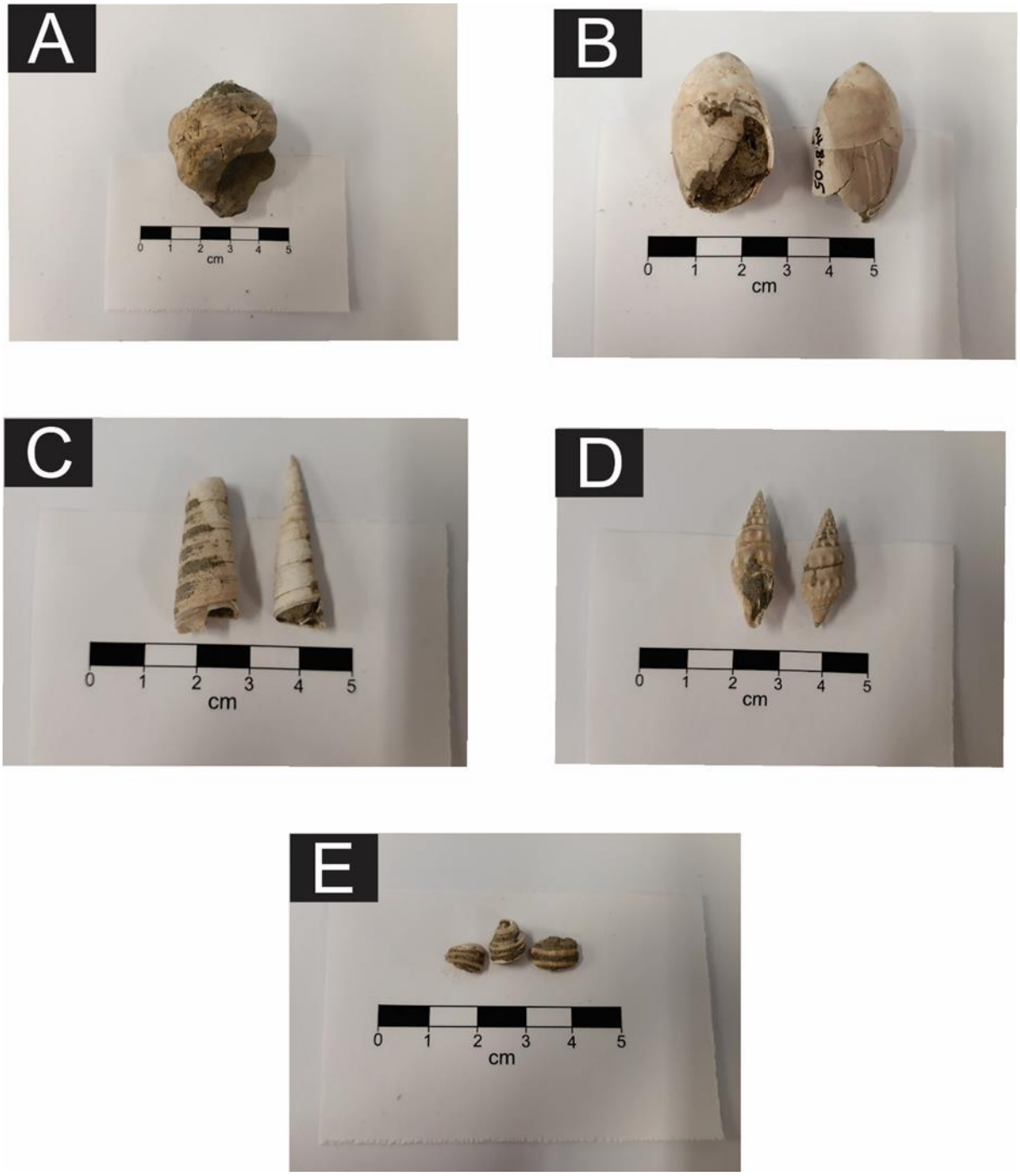

Figure 4-2: Mangatoro Formation macro fossils.
A) Struthiolaria (Callusaria) obesa. B) Amalda (Baryspira) mucronata. C) Zeacolpus vittatus. D) Clavatoma pulchra. E) Pelicaria canaliculate.

4.3 Te Aute Formation:

The Te Aute Formation overlies the Mangatoro Formation, and crops out on the western side of the Manawatu Saddle. Only a small number of the macrofossils found in this formation were able to be identified, as most were preserved as shell hash within the conglomerate. Most of the identifiable macrofossils for this formation were found exposed in the Broadlands Stream measured section.

Based on three key macrofossils, the Te Aute Formation can be constrained to range from the Opoitian (5.33 Ma) to Nukumaruan (1.63 Ma) by this study (Fig 4-3). The presence of *Neopanis zealandica* (Lillburnian to Nukumaruan, 15.1 Ma to 1.63 Ma) and *Patro sp* (Kapitean to Nukumaruan, 7.2 Ma to 1.63 Ma) has constrained the upper Te Atue Formation to being no younger than the Nukumaruan. The presence of *Stiracolopus sp* (Opoitian 5.33 Ma to recent) restrict the Te Aute Formation to Opoitian or younger (Beu *et al.,* 1990, Beu, 2012).

The Te Aute Formation overlies the Mangatoro Formation, indicating that the Te Aute Formation is younger. Unfortunately the resolution of the biostratigraphy is not high enough to constrain either formation to early, middle, or late within the Opoitian stage.

This age range differs from past authors such as Lillie (1953) and Piyasin (1966), as Lillie was able to conservatively constrain the age range of the Te Aute Formation from Waipipian (3.70 Ma) to Mangapanian (2.40 Ma) (Fig 4-4). Two macrofossils *Maoricardium spatiosum* Tongaporutuan (11.04 Ma) to Mangapanian (3.00 Ma) and *Spinomelon Sp* Duntroonian (27.3 Ma) to Mangapanian (3.00 Ma), have allowed the base of the Te Aute Formation to be constrained to the Waipipian. *Phialopecten triphooki* has allowed the upper range for the Te Aute Formation to be constrained to Mangapanian. The range based on Lillie's (1953) collections is conservative as the preservation of the macrofossils is not noted, meaning we are unsure if any fossils may be reworked. However, this study adopts the age range based on Lillie's (1953) work, as this allows the age range of the Te Aute Formation to be better constrained.

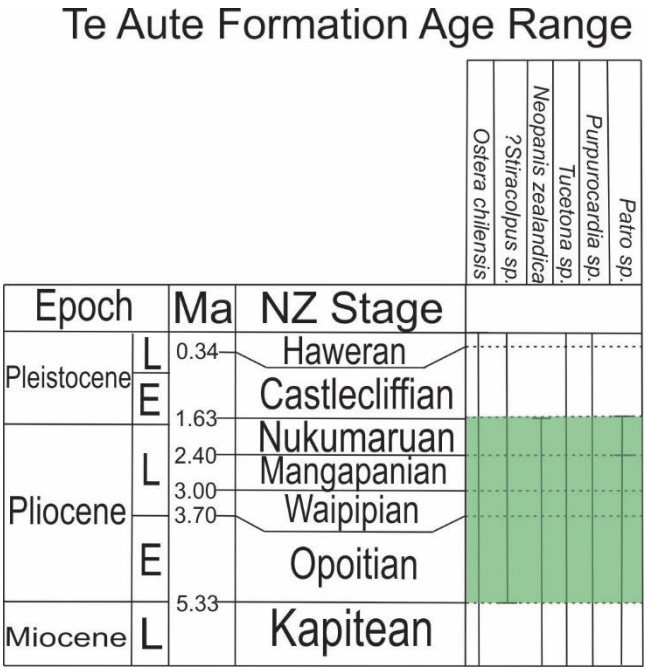

Figure 4-3: Age range chart for the Te Aute Formation. Using macrofossils from the Broadlands Stream measured section.

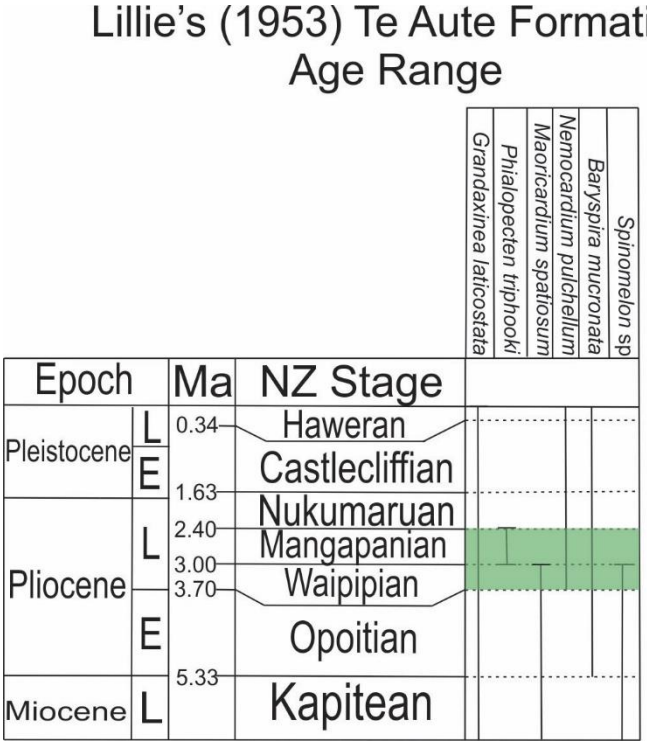

Figure 4-4: Lillie (1953) Te Aute Formation age range based on key macrofossils.

4.4 Kumeroa Formation:

The Kumeroa Formation stratigraphically overlies the Te Aute Formation, and outcrops on both the western and eastern sides of the Manawatu Saddle. The isolated eastern outcrops are dominated by pebbly shell hash limestone and contain limited intact and identifiable macrofossils. The western outcrops show a similar shell hash character. Outcrops of the Kumeroa Formation in the Broadlands Stream measured section, however, show a mixture of shell hash and a moderate number of intact macrofossils that were identifiable.

The Kumeroa Formation ranges from the Mangapanian to Nukumaruan (Fig 4-5). Based on the presence of *Pleuromeris (hectori?)* (Mangapanian 3.00 Ma to upper Nukumaruan) the formation is constrained to the lower Mangapanian boundary. The presence of *Patro sp* and *Pleuromeris (hectori?)* has constrained the narrowest lower age range of the Kumeroa Formation to the base of the Nukumaruan.

The age range for the Kumeroa Formation found by this study is not as well constrained as past studies such as Lillie (1953) and Piyasin (1966). Both these authors quote the Kumeroa Formation to be Nukumaruan in age. Based on their tighter constraint of the formation this study will adopt their age range.

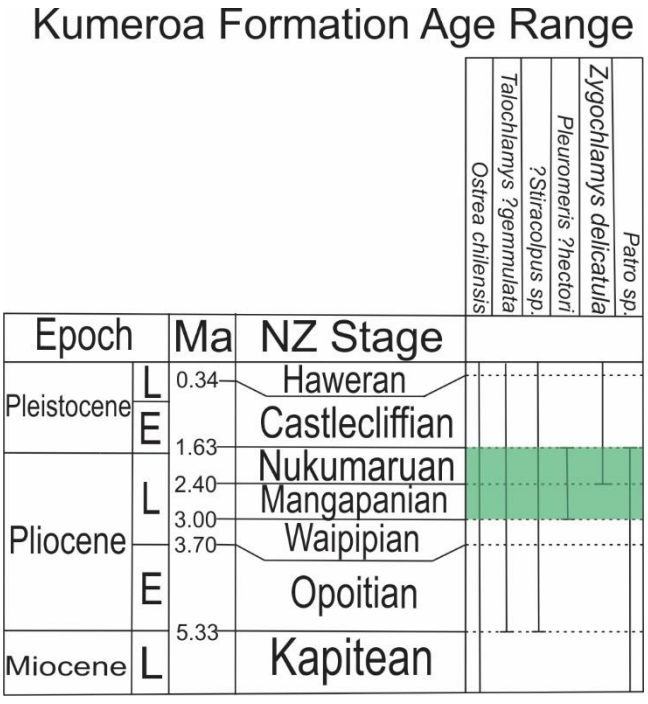

Figure 4-5: Age range chart for the Kumeroa Formation.

4.5 Mangatarata Formation:

The Mangatarata Formation was not sampled, as the age of this formation is widely accepted by past authors, such as Lillie (1953) and Piyasin (1966) and, more recently Rees (2015), as Castlecliffian (1.63 Ma to 0.34 Ma), based the presence of tephra layers such as the Rewa (1.20 ± 0.14 Ma) and Potaka (1.05 ± 0.05 Ma) tephras (Pilans *et al.*, 2005; Rees, 2015).

4.6 Summary:

This study has constrained the age of the Mangatoro Formation to be similar to that proposed by Lillie (1953) and Piyasin (1966). The age range of the Te Aute Formation was unable to be well constrained based on the biostratigraphic data obtained in this study. As a result the age range identified by Lillie (1953), ranging from Waipipian to Mangapanian, will be used in this study. The age range of the Kumeroa Formation identified by this study is similar to past studies, constrained to the Nukumaruan. The Mangatarata Formation was not sampled, as the age of this formation is widely agreed by past authors to be Castlecliffian.

Chapter 5 Lithofacies

5.1 Introduction:

This chapter presents a lithofacies scheme for the sedimentary rocks deposited across Manawatu Saddle. A lithofacies scheme provides an objective way to characterise similar sedimentary rock units throughout a field area. Based primarily on their lithological characteristics, such as grain size, composition, sorting, clast shape and sedimentary structures, it allows the depositional environment for each facies to be interpreted. The incorporation of both macro and microfossil faunal assemblages, where available, allows a more detailed depositional environment to be interpreted. To enhance our understanding of depositional environments and changes that have occurred over time, lithofacies association such as those applied by Naish and Kamp (1997) and Bland (2006) are used. This requires examining each bed in association with the ones above and below, and comparing the lithofacies successions that occur. Succession patterns can be recognised and translated into systematic changes in depositional environments, further enhancing our understanding of the development of each formation.

The zones used to define water depth and energy regimes recognised in this study are presented in Fig 5-1. These zones include the shoreface, which is subdivided into three sub-divisions: the upper, middle and lower shoreface. These divisions show decreasing grain size, sorting and energy with increasing water depth. Following the shoreface is the shelf, which shows the lowest energy regime. This study has identified twelve separate lithofacies that each fit within these zones: two limestone lithofacies, two mudstone lithofacies, four sandstone lithofacies and four conglomerate lithofacies. A summary of each lithofacies is found in Table 2. Key characteristics are described and interpreted in part one of this chapter. In part two, the lithofacies associations and successions for each measured section are presented and briefly discussed.

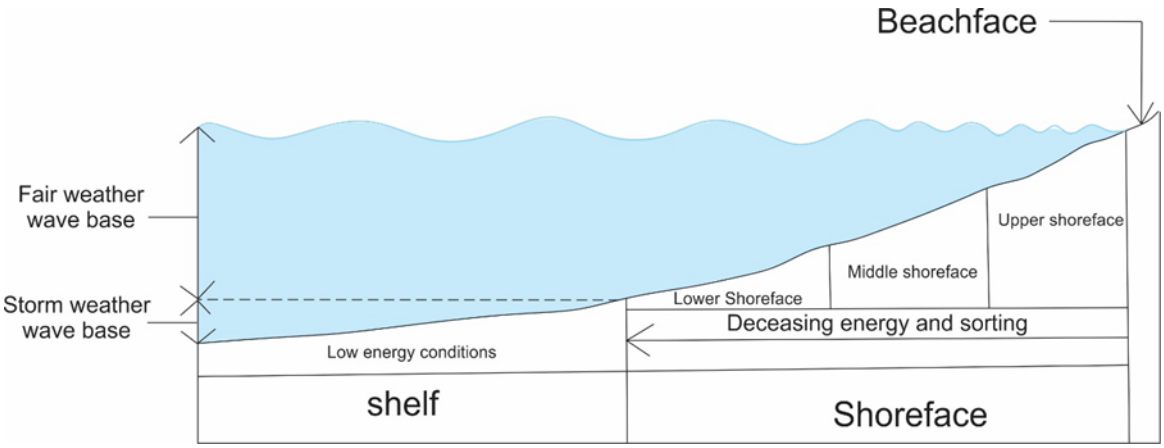

Figure 5-1: Continental shelf subdivisions used in this study.
Figure adapted from Walker and James (1992).

5.2 Part One: Lithofacies and depositional environments:

Table 2: Lithofacies and summary lithological descriptions.
Lithofacies M1 S1-S4 adapted from Naish &Kamp (1997), Lithofacies L1,C1-C3 adapted from Bland (2006).

Lithofacies		Description	Inferred depositional environment	Typical faunal assemblage
Limestone Lithofacies Group:				
L1	Pebbly shell hash limestone	Coarse-grained, moderately-sorted, well to moderately bedded, cross bedded, irregularly spaced 1 metre thick conglomerate beds, shell hash present.	Upper shoreface zone with a high fluvial input	Shell hash dominated
L2	Sandy limestone	Fine to coarse-grained, moderately to poorly-sorted well-bedded, convolute laminations, high angle cross beds, decimetre thick silstone lenses, whole and fragmented fossils, scattered bioturbation.	Upper to middle shoreface zone	*Patro sp, Zygochlamys delicatula, Pleuromeris ?hectori, ?Stiracolpus sp, Talochlamys ?gemmulata, Ostrea chilensis*
Mudstone Lithofacies Group:				
M1	Blue grey siltstone	Vaguely-bedded, scattered millimeter scale organic stringers, centimeter scale wood fragments, bioturbation and shell hash.	Lower shoreface	*Notorotalia depressa, Elphidium advenum f. limbatum Nonionoellina fleminigi, Oolina melo, Rosalina bradyi, Quinqeloculina incisa, Zeaflorilus parri, Elphidium novozealandicum, Bolivina subspinescens, Legena striata, Notoralia depressa, Anomalinoides subonionoides, Globigerina falconensis, Evuigrina delicatula, Oolina borealis, Lagenosolenia confossa, Haynesina depressula.*
M2	Sandy mudstone	Fine-grained, faintly bedded, thin irregularly spaced sandstone lenses, scattered thin organic layers, highly bioturbated, whole and fragmented macro fossils.	Shelf zone	Macro fossils: *Atrina sp, Struthiolaria (Calluscris) obesa Limnoperna sp, Anomia trigonopsis, Glycymeris (glycymeris) shrimptoni Crassostrea sp, Ostrea chilensis, Clavatoma pulchra Talochlamys ?gemmulata, Zeacolpus vittatus, Amalda (Baryspra) mucronata* . Micro fossils: *Rosalina bradyi, Oolina melo, Langena spicata, Bolivinita plipzea, Euvgrina pliozea, Anomalinoides sphericus, Notoroalia finlayi.*
Sandstone Lithofacies Group:				
S1	Coarse-grained sandstone	Coarse-grained, poorly-sorted, moderately to poorly-bedded, contains a variety of clast shape and size ranging from pebble to cobble and sub-rounded to blocky shaped, scattered shell hash, moderate bioturbation.	Upper shoreface	Shell hash dominated
S2	Medium-grained sandstone with coarse-grained sandstone interbeds	Medium to fine-grained, moderately-sorted, well-bedded moderately bioturbated. Coarse-grained sandstone poorly-sorted, whole/fragmented macrofossils, moderately bioturbated.	Middle shoreface	Scattered whole macrofossils not in an identifiable sate
S3	Medium to fine-grained, well-sorted Sandstone	Medium to fine-grained, well-sorted, moderately to well-bedded, friable, scattered thin organic layers, shell hash lenses.	Beachface	Scattered shell hash
S4	Sandstone with interbedded siltstone	Sandstone is medium-grained, well-sorted, convolute laminations, flaser bedding. Decimetre scale thin horizontal siltstone laminations present. Highly bioturbated, scattered fragmented macrofossils.	Tidal flat environment	shell hash

Lithofacies		Description	Inferred depositional environment	Typical faunal assemblage
Conglomerate Lithofacies Group:				
C1	Non-fossiliferous conglomerate	Coarse-grained, pebble to cobble sized clasts, blocky shaped clasts, matrix to clast supported, moderately-sorted, well-bedded. Coarse-grained sandstone lenses. Scattered organic fragments. No fossils.	Terrestrial fluvial environment	No fossils present
C2	Disk shaped conglomerate	Coarse-grained, pebble to cobble sized clasts, dominated by disc shaped clasts, matrix to clast supported, moderately-sorted, interbedded coarse-grained well-sorted sandstone lenses, scattered fragmented macrofossils.	Beachface to gravel bar	Fragmented macro fossils
C3	Barnacle rich conglomerate	Coarse-grained, pebble to cobble sized clasts, dominantly disc shaped clasts, matrix to clast supported, well to moderately sorted, well-bedded indicated by attached barnacles and clasts with attachment scars, interbedded with beds showing no barnacles, mixture of shell hash and whole macrofossils.	Barnacle dominated gravel bar	*Cellana sp, Purpurocardia sp, Tucetona sp, Neopanis zealandica, Ostrea chilensis. Zygochlamys delicatula, Polinices sp, Dosinia sp, Limnoperna sp, Talochlamys gemmulata, Aulacomys sp.*
C4	Pebble to boulder conglomerate	Coarse-grained, pebble to boulder sized clasts, matrix to clast supported, well to poorly-sorted, well-bedded, cross-bedded, some locations show beds dominated by disc shaped clasts, shell hash and whole macrofossils.	High energy gravel shoreface	*Crassostrea ingens*

5.2.1 Limestone Lithofacies:

There are two limestone lithofacies identified in this study, with limestone lithofacies L_1: Pebbly shell hash limestone, the thickest but most restricted. This facies is observed at the eastern Manawatu Gorge entrance. Lithofacies L_1 shows a higher concentration of Torlesse pebbles and shell hash, when compared to the much thinner limestone lithofacies L_2: Sandy limestone. The sandy limestone lithofacies shows more extensive outcrops on only the western margin of the Manawatu Saddle and a much higher portion of whole macrofossils.

Lithofacies L1: Pebbly shell hash limestone:

Lithology: Dull orange-brown, coarse-grained, moderately-sorted sandy limestone. Well to moderately bedded on a 0.5-1 metre scale, with irregularly spaced approximately one metre thick conglomerate beds. These beds consist of sub-rounded, blocky shaped matrix supported clasts (Fig 5-2 A); some clasts show barnacle attachment scars. There is abundant shell hash material throughout the lithofacies; a moderate percentage of the shell hash consists of fragmented barnacle plates.

Interpretation: This lithofacies is inferred to have been deposited within the upper shoreface zone with a high fluvial input. The moderately to coarse-grained, poorly-sorted sandy limestone gross lithology is characteristic of a lithofacies formed in a high energy

environment. The consistent reworking by currents and fluvial input has led to the development of this mixed carbonate facies, i.e. the mixture of shell hash, coarse-grained sandstone and Torlesse clasts (Kamp *et al*., 1988). The presence of sub-rounded Torlesse clasts indicates a fluvial influence; similar lithofacies have been observed by Caron *et al*. (2004a) where Torlesse clasts are attributed to the influence of discharging streams and tidal channels.

Lithofacies L2: Sandy limestone:

Lithology: Orange-brown, fine to coarse-grained, moderately to poorly-sorted sandy limestone. Well-bedded on a one to two metre scale indicated by poorly-sorted shell hash beds. Rare scattered sub-rounded Torlesse pebbles, high angle cross beds and convolute laminations present throughout the lithofacies (Fig 5-2 B). Interbedded decimetre irregularly spaced blue-grey vaguely bedded siltstone lenses (Fig 5-2 C). Whole and fragmented macrofossils present.

Macrofossils: *Patro sp, Zygochlamys delicatula, Pleuromeris ?hectori, ?Stiracolpus sp, Talochlamys ?gemmulata, Ostrea chilensis.*

Interpretation: The inferred depositional environment for this lithofacies is situated within the middle to upper shoreface zone, as the moderately-sorted characteristic of the sandstone indicates a moderate to high energy regime. The high angle cross beds indicate influence by strong currents. Similar structures within sandy limestones, showing broadly the same lithological characteristics, were observed by Caron *et al*. (2004b) and interpreted to represent a setting showing strong tidal currents. The macrofossil assemblage also supports this interpretation. The macrofauna, *Patro sp, Zygochlamys delicatula, Pleuromeris? hectori?, Stiracolpus sp, Talochlamys ?gemmulata, Ostrea chilensis,* indicate an environmental preference of moderate to high energy conditions in shallow water (Beu & Maxwell, 1990; Beu & Raine, 2009).

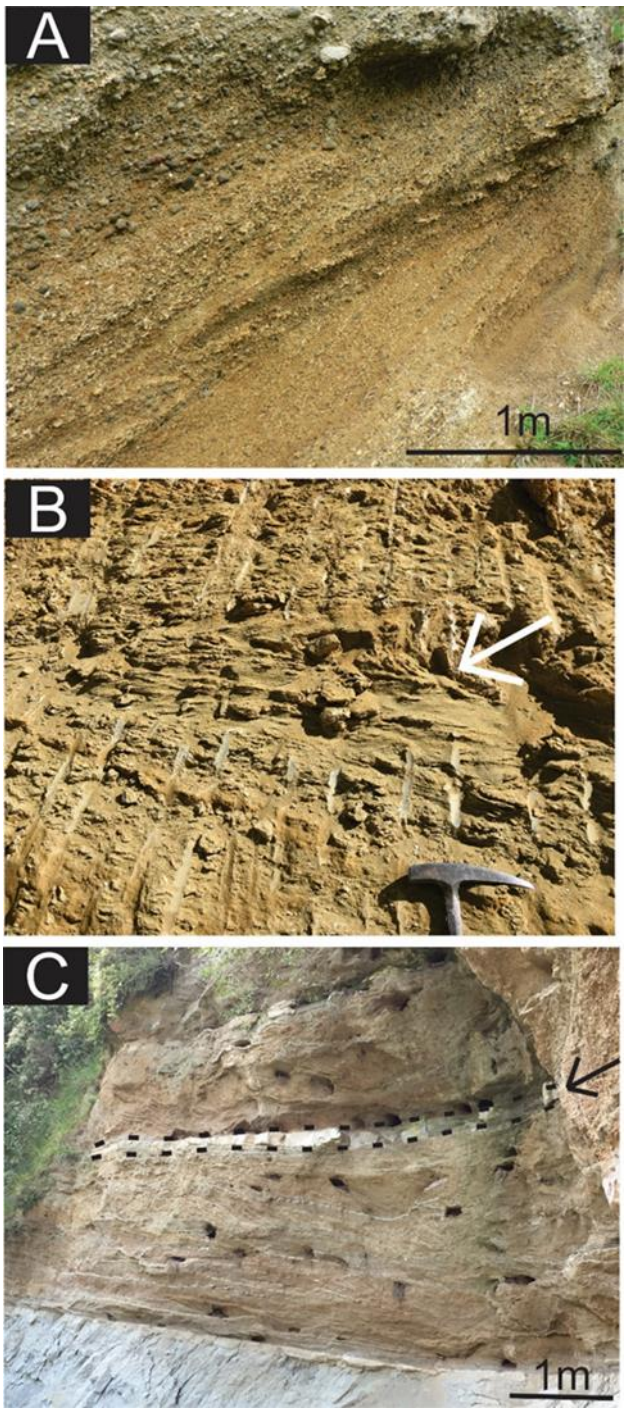

Figure 5-2: Limestone lithofacies.
A) Pebbly limestone with shell hash characteristic of lithofacies L1, photo location (Lat: -40.332773, Long: 175.830345). B) Dewatering structure characteristic of lithofacies L2 with the bedding orientation dipping roughly west, photo location (Lat: -40.28627, Long: 175.781679). C) Outcrop photo of thin interbedded siltstone of lithofacies (L2, photo location, (Lat: -40.279558, Long: 175.785155).

5.2.2 Mudstone Lithofacies:

Two deep water mudstone lithofacies have been identified in this study. Siltstone lithofacies M_1: Blue-grey siltstone is found to be of variable thickness and is only observed to outcrop on the western side of the Manawatu Saddle. Lithofacies M_2: Sandy mudstone is the thickest lithofacies observed in this study and only outcrops on the eastern side of the Manawatu Saddle. Both lithofacies show well preserved microfossil assemblages, which are key to interpreting the depositional setting.

Mudstone Lithofacies M1: Blue-grey siltstone:

Lithology: Blue-grey, vaguely-bedded siltstone (Fig 5-3 A). Scattered black thin millimetre scale organic stringers, centimetre scale wood fragments. Moderately bioturbated, scattered shell hash and abundant microfossils.

Microfossils: *Notorotalia depressa, Elphidium advenum f. limbatum, Nonionoellina fleminigi, Oolina melo, Rosalina bradyi, Quinqeloculina incisa, Zeaflorilus parri, Elphidium novozealandicum, Bolivina subspinescens, Legena striata, Notoralia depressa, Anomalinoides subonionoides, Globigerina falconensis, Evuigrina delicatula, Oolina borealis, Lagenosolenia confossa, Haynesina depressula.*

Interpretation: This lithofacies represents sedimentary rocks deposited within the lower shoreface zone, as the siltstone lithology indicates a lower energy setting when compared to the courser gained sandstone and conglomerate facies. The lower shoreface zones are characterised as a setting where fine to very fine-grained sediments are deposited; for example, Bland (2006) interpreted similar siltstone lithofacies as lower shoreface deposits. The presence of thin organic matter can be attributed to terrestrial material washed out and settling out of suspension in deeper, calm water.

The microfossil assemblage confirms this water depth estimate. Microfossils, such as *Notorotalia depressa, Haynesina depressula, Elphidium advenum f. limbatum, Nonionoellina fleminig, Rosalina bradyi* and *Quinqeloculina incisa*, indicate depth ranges up to 50-100 m that fit within the lower shoreface zone and calm low energy environment (Hayward *et al.*, 1997, 1996; Hayward, 2010).

Mudstone Lithofacies M2: Sandy mudstone:

Lithology: Blue-grey sandy mudstone (Fig 5-3 B). Vaguely-bedded on a centimetre scale, irregularly spaced thin (less than one metre thick) sub-rounded Torlesse pebble beds. Scattered thin organic matter layers. Upper intervals of this lithofacies show a moderate amount of whole macrofossils. Well preserved microfossils throughout the lithofacies.

Macrofossils: *Atrina sp, Struthiolaria (Calluscris) obesa, Limnoperna sp, Anomia trigonopsis, Glycymeris (glycymeris) shrimptoni, Crassostrea sp, Ostrea chilensis, Clavatoma pulchra, Talochlamys ?gemmulata, Zeacolpus vittatus, Amalda (Baryspra) mucronata.*

Microfossils: *Rosalina bradyi, Oolina melo, Langena spicata, Bolivinita plipzea, Euvgrina pliozea, Anomalinoides sphericus, Notoroalia finlayi.*

Interpretation: This lithofacies is representative of sedimentary rocks deposited in the shelf zone. The sandy mudstone lithology is characteristic of this low energy environment. The scattered pebble beds are interpreted as material washed from shallower zones by storm events, similar to those observed by Bland (2006). This lithofacies shows scattered macrofossils that indicate a shelfal depth, with the exception of *Atrina sp, Limnoperna sp* and *Glycymeris (glycymeris) shrimptoni*, which prefer high energy rocky substrate environments. These macrofossils have likely been reworked to be incorporated into the observed assemblage. The bulk macrofossils present inhabit shallow calm soft bottom substrate settings (Beu and Maxwell, 1990; Beu and Raine, 2009). Therefore, with the exception of *Rosalina bradyi* and *Bolivinita plipzea* that indicate relatively shallower water (Hayward, 2010), the microfossils present indicate a shelf zone.

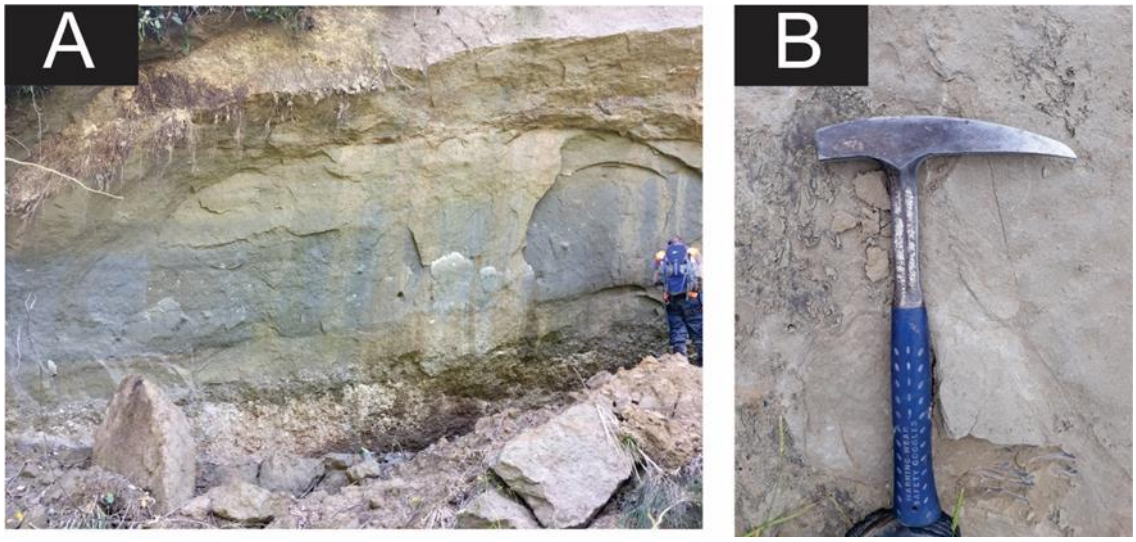

Figure 5-3: Mudstone lithofacies outcrop photos.
A) Lithofacies M1: Blue-grey siltstone, photo location (Lat: -40.280246, Long: 175.796142). B) Lithofacies M2: sandy mudstone, photo location (Lat: -40.299134, Long: 175.829916).

5.2.3 Sandstone Lithofacies:

Four sandstone lithofacies have been identified in this study. They show a range of outcrop appearances, fossil contents and thicknesses, resulting in several interpreted depositional conditions. These lithofacies are: S_1:Coarse-grained sandstone, S_2: Medium-grained sandstone with coarse-grained sandstone interbeds, S_3: Medium to fine-grained, well-sorted sandstone and S_4: Sandstone with interbedded siltstone. The sandstone lithofacies outcrop on both the eastern and western sides of the Manawatu Saddle.

Sandstone Lithofacies S1: Coarse-grained sandstone:

Lithology: Rusty brown, coarse-grained sandstone. Moderately to poorly-bedded, indicated by grain size changes. Scattered sub-rounded and blocky shaped Torlesse clasts ranging from pebble to cobble, with scattered shell hash (Fig 5-4 A).

Interpretation: This lithofacies is interpreted to represent a sandstone deposited in the upper shoreface zone, based on the grain size and the presence of scattered Torlesse clasts ranging in size from cobble to pebble, which indicates a high energy regime (Bland, 2006). Given the size of the clasts (pebble to cobble), it is likely that the clasts have been transported by shallow water currents, i.e. longshore drift processes from a fluvial source.

Sandstone Lithofacies S2: Medium-grained sandstone with coarse-grained sandstone interbeds:

Lithology: Light grey, medium to fine-grained, moderately-sorted sandstone with coarse-grained sandstone interbeds (Fig 5-4 B). Well-bedded on a metre scale, moderately bioturbated and contain scattered shell hash. Coarse-sandstone interbeds: poorly-sorted, well-bedded on a 2-4m scale. Scattered concretions and cemented shell hash, moderately bioturbated, whole and fragmented macrofossils present.

Interpretation: This lithofacies represents sedimentary rocks deposited in the middle shoreface zone, indicated primarily by the dominant grain size. The coarse-grained sandstone interbeds are interpreted as material washed out to the middle shoreface zone by periodic storm events. Naish *et al*. (2005) and Bland (2006) described lithofacies with similar characteristics, and attributed the coarse-grained interbeds to transport flows from storm events. These storm events were likely periodic in nature and allowed the bioturbation of each bed inbetween events. Unfortunately the microfossils from this lithofacies are poorly preserved and showed a very small yield when sampled. As a result they did not provide any additional water depth or environmental indicators.

Sandstone Lithofacies S3: Medium to fine-grained, well-sorted sandstone:

Lithology: Orange-brown, medium to fine-grained, well-sorted friable sandstone (Fig 5-4 C). Well-bedded on an approximately one metre scale with thin organic layers and decimetre scale siltstone laminations. Scattered shell hash lenses.

Interpretation: This sandstone lithofacies represents material deposited in the beachface zone. Similar fine-grained, well-sorted lithofacies were observed by Naish *et al*. (2005), and interpreted to represent a beachface zone. These environments are influenced by marginal marine processes, such as wave swash and backwash, which sort the sediment leading to the well-sorted, parallel bedded (on a decimetre scale) cross laminated sandstone.

Sandstone Lithofacies S4: Sandstone with interbedded siltstone:

Lithology: Dull-brown, medium-grained, well-sorted sandstone with decimetre scale interbedded siltstone. Sandstone: well-bedded on a centimetre scale. Abundant convolute and flaser bedding, along with occasional dish and pillar structures (Fig 5-4 D), and rare scattered shell hash.

Interpretation: This lithofacies is interpreted to represent a tidal flat/estuarine environment, as the combination of well-sorted, medium-grained sandstone with interbedded siltstone indicates an environment with fluctuating hydraulic regimes (Naish *et al*., 2005).

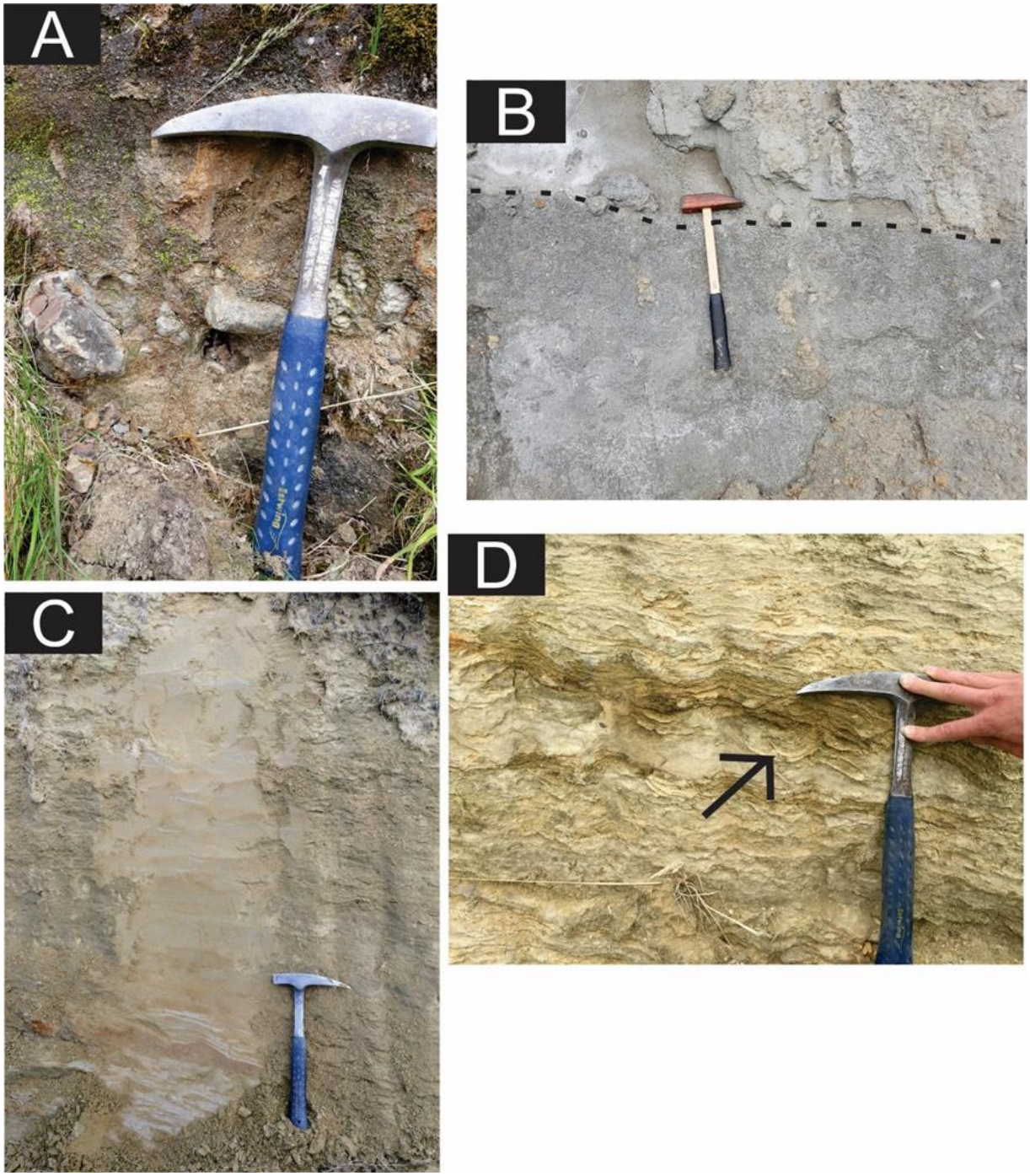

Figure 5-4: Sandstone lithofacies outcrop photos.
A) Coarse-grained sandstone with scattered Torlesse clasts, characteristic of sandstone lithofacies S1, photo location (Lat: -40.300378, Long: 175.835066). B) Sandstone lithofacies S2, the darker coloured sandstone is a coarse-grained sandstone interbed, photo location (Lat: -40.298741, Long: 175.830903). C) Fine-grained well-sorted sandstone lithofacies S3, photo location (Lat: -40.284567, Long: 175.776358). D) Dish and pillar structures marked by the arrow, in sandstone lithofacies S4, photo location (Lat: -40.28532, Long: 175.777559).

5.2.4 Conglomerate Lithofacies:

Four conglomerate lithofacies have been identified in this study. They are well exposed on the western Manawatu Saddle, and are all dominated by Torlesse sandstone clasts. The lithofacies are as follows: Lithofacies C_1: Non-fossiliferous conglomerate, Lithofacies C_2: Disc shaped conglomerate, Lithofacies C_3: Barnacle rich conglomerate and lithofacies C_4: Pebble to bolder conglomerate.

Conglomerate Lithofacies C1: Non-fossiliferous conglomerate:

Lithology: Orange-brown, moderately-sorted, matrix to clast supported conglomerate. Matrix consists of well-sorted, medium to coarse-grained sandstone. Torlesse clasts are sub-rounded and blocky in shape, pebble to cobble size. The conglomerate is well-bedded on a metre scale, indicated by changes in clast size and shape. Coarse-grained, well-sorted interbedded sandstone lenses (Fig 5-5A), ranging from 1-4m thick and containing scattered organic fragments. No macro or microfossils present.

Interpretation: This conglomerate lithofacies has been interpreted to represent a terrestrial river environment. Clast shape, roundness and size is consistent with a high energy turbulent fluvial environment. Thin coarse-grained sandstone to represent overbank deposits.

Conglomerate Lithofacies C2: Disc shaped conglomerate:

Lithology: Orange-brown, matrix to clast supported conglomerate. Matrix consists of coarse-grained moderately-sorted shell hash sandstone lenses. Well-bedded indicated by clasts showing continuous horizontal stratification (Fig 5-5B). Torlesse clasts range from disc to sub-round and from pebble to cobble sized. Disc shaped pebble Torlesse clasts dominate the lithofacies. Sandstone lenses consist of coarse-grained, well-sorted friable sandstone.

Interpretation: Based on the dominance of disc shaped clasts, this lithofacies is interpreted to represent a gravel beach deposit, as disc shaped clasts are characteristic of gravel bar/shoreface deposits (Browne & Naish, 2003). The coarse-grained shell hash sandstone interbeds are interpreted as sandy zones within the gravel beach system, as these coastal facies vary laterally.

Conglomerate Lithofacies C3: Barnacle rich conglomerate:

Lithology: Dark-grey clast to matrix supported conglomerate. Well bedded on a less than one metre scale, indicated by changes in clast size, alternating barnacle content and variable imbrication. Torlesse sandstone clasts are dominantly disc shaped, and pebble to cobble size. A distinctive feature of this lithofacies is the presence of whole attached barnacles and barnacle attachment scars (Fig 5-5 D). The sandy shell hash matrix consists of an estimated 60% barnacle plate fragments. Both whole and fragmented macrofossils are present.

Macrofossils: *Cellana sp, Purpurocardia sp, Tucetona sp, Neopanis zealandica, Ostrea chilensis.*

Interpretation: This lithofacies is interpreted to represent an offshore gravel fan/bar, deposited in the middle to upper shoreface zone. The deposit was likely subjected to high tidal/wave currents, as a high flow of nutrients delivered by currents and water with limited suspended sediment is required to promote barnacle growth (Kamp *et al*., 1988). Both the barnacles and the macro fossil assemblage present indicate a shallow water high energy regime with a rocky substrate (Beu & Maxwell, 1990). The presence of bedding indicated by changes in clast size is characteristic of a gravel fan/bar.

Conglomerate lithofacies C4: Pebble to boulder conglomerate:

Lithology: Orange-brown, clast supported conglomerate. Well-bedded on a 20-40 cm scale, indicated by changes in clast size and shape (Fig 5-5 C). Clasts range from blocky to disc-shaped, and pebble to bolder in size. Scattered rare thick-walled macrofossils present.

Macrofossils: Predominantly *Crassostrea ingens.*

Interpretation: This lithofacies has been interpreted to represent a high energy gravel shoreface consisting of Torlesse basement. The presence of thick walled macrofossils known to dominate shorefaces and the variety of grain size and shape indicate a high energy environment (Bland, 2006).

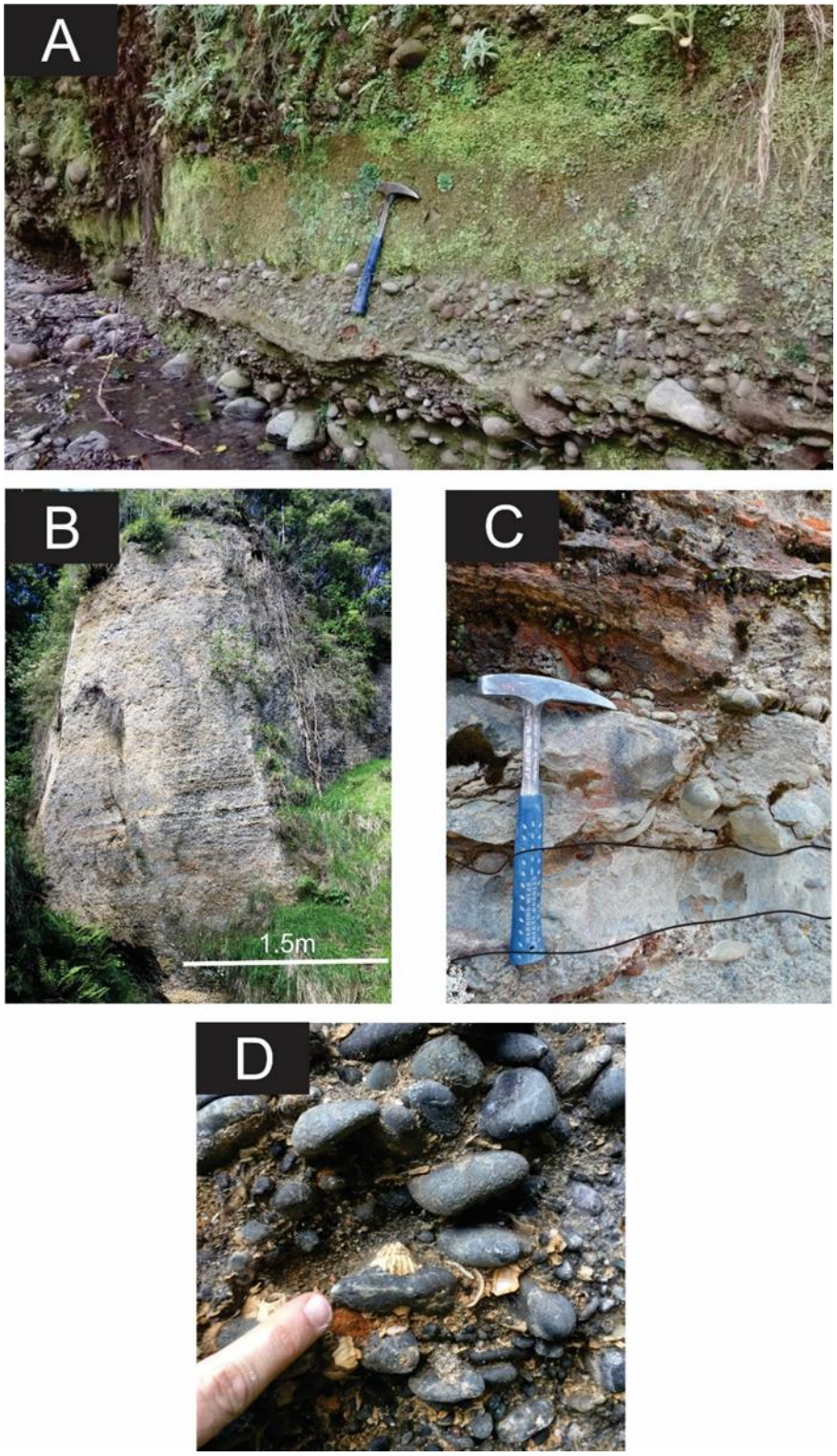

Figure 5-5: Conglomerate lithofacies outcrop photos.
A) Non-fossiliferous conglomerate lithofacies: C1, photo location (Lat: -40.280541, Long: 175.797429). B) Disk shaped conglomerate lithofacies C2, photo location (Lat: -40.279689, Long: 175.78949). C) Boulder to pebble lithofacies C4, photo location (Lat: -40.276612, Long: 175.852575). D) Barnacle rich conglomerate lithofacies: C3, photo location, (Lat: -40.279755, Long: 175.787172).

5.3 Summary:

The lithofacies identified in this study describe a complex shallow marine and coastal environment. Fig 5-6 shows a cartoon representation of where each lithofacies is situated in relation to the continental shelf divisions used in this study, and also demonstrates the significant lateral variation within the coastal environment. This model allows the facies association and vertical successions of lithofacies in each measured section to be interpreted to infer how the depositional environments and water depths have changed over time within the Manawatu Strait.

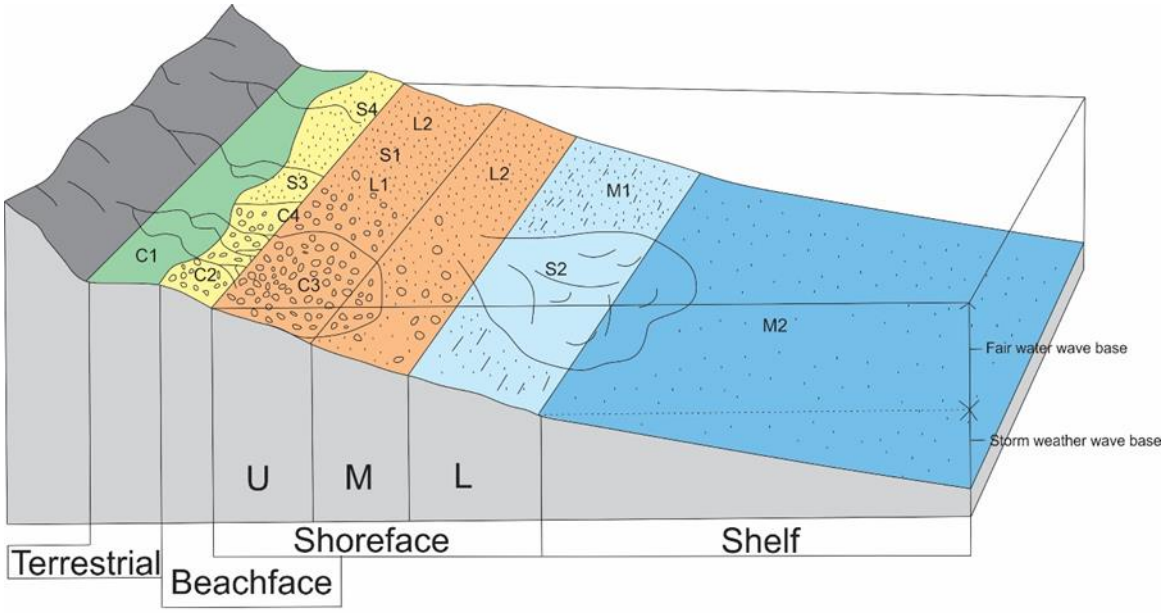

Lithofacies Key

L1: Pebbly shell hash limestone.	M2: Sandy mudstone.	S3: Medium to fine-grained well-sorted sandstone	C2: Disk shaped conglomerate.
L2: Sandy limestone.	S1: Coarse-grained sandstone	S4: Sandstone with interbedded siltstone.	C3: Barnacle rich conglomerate
M1: Blue-grey siltstone.	S2: Medium-grained sandstone with coarse-grained sandstone interbeds.	C1: Non-fossiliferous conglomerate	C4: Pebble to boulder conglomerate.

Figure 5-6: Lithofacies depositional model.

5.4 Part two: Lithofacies associations and succession:

5.4.1 Introduction:

Each lithofacies is considered in association with related facies as indicated in Figure 5.6. Each lithostragraphic unit identified in the measured section is assigned a lithofacies code, allowing the vertical succession of facies to be interpreted. An inferred water depth curve is presented for each measured section, based on the association with the lithofacies above and below each individual unit. Based on the lithofacies identified for each measured section and the interpreted water depth of deposition, a brief summary of the changes occurring in each formation at each measured section is presented. The mechanism and timing of each major environmental change is discussed in detail in Chapter Six.

5.4.2 Ballantrae Farm measured section:

The Ballantrae Farm measured section shows the Mangatoro Formation containing four separate lithofacies (Fig 5-7). The lower-most conglomerate unit (facies C_4) unconformably overlies the Torlesse basement and shows a beachface to upper shoreface water depth deepening to an upper shoreface water depth (unit two, facies S_1). Unit three (facies M_2) shows lithofacies consist with shelfal water depths. The nature of this transgression from upper shoreface to shelf is unknown due to poor section exposure. Overlying unit three is unit four, showing a transition from shelf water depths to lower shoreface depths (facies S_2).

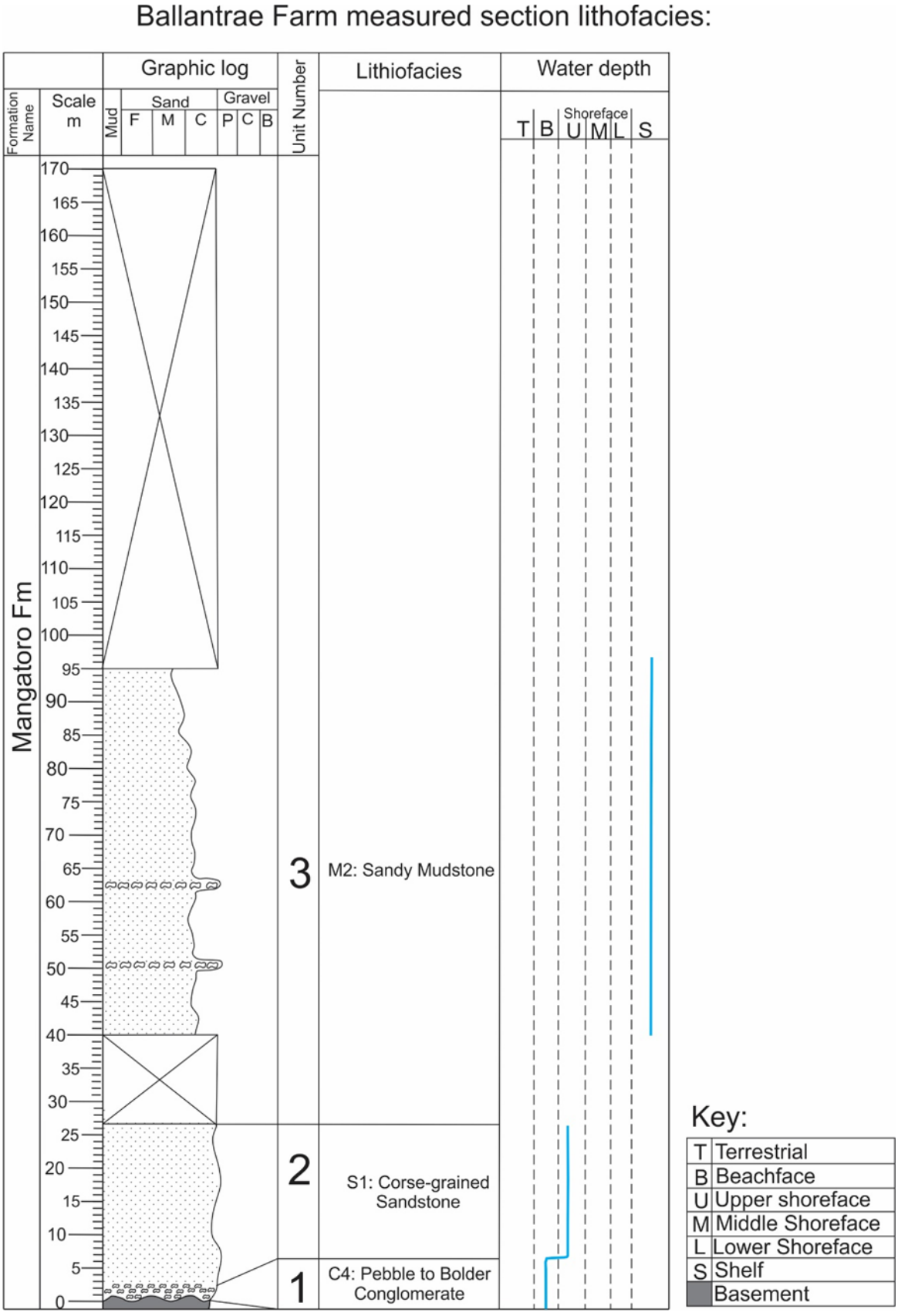

Figure 5-7: Lithofacies and water depth curve for the Ballantrae Farm measured section.

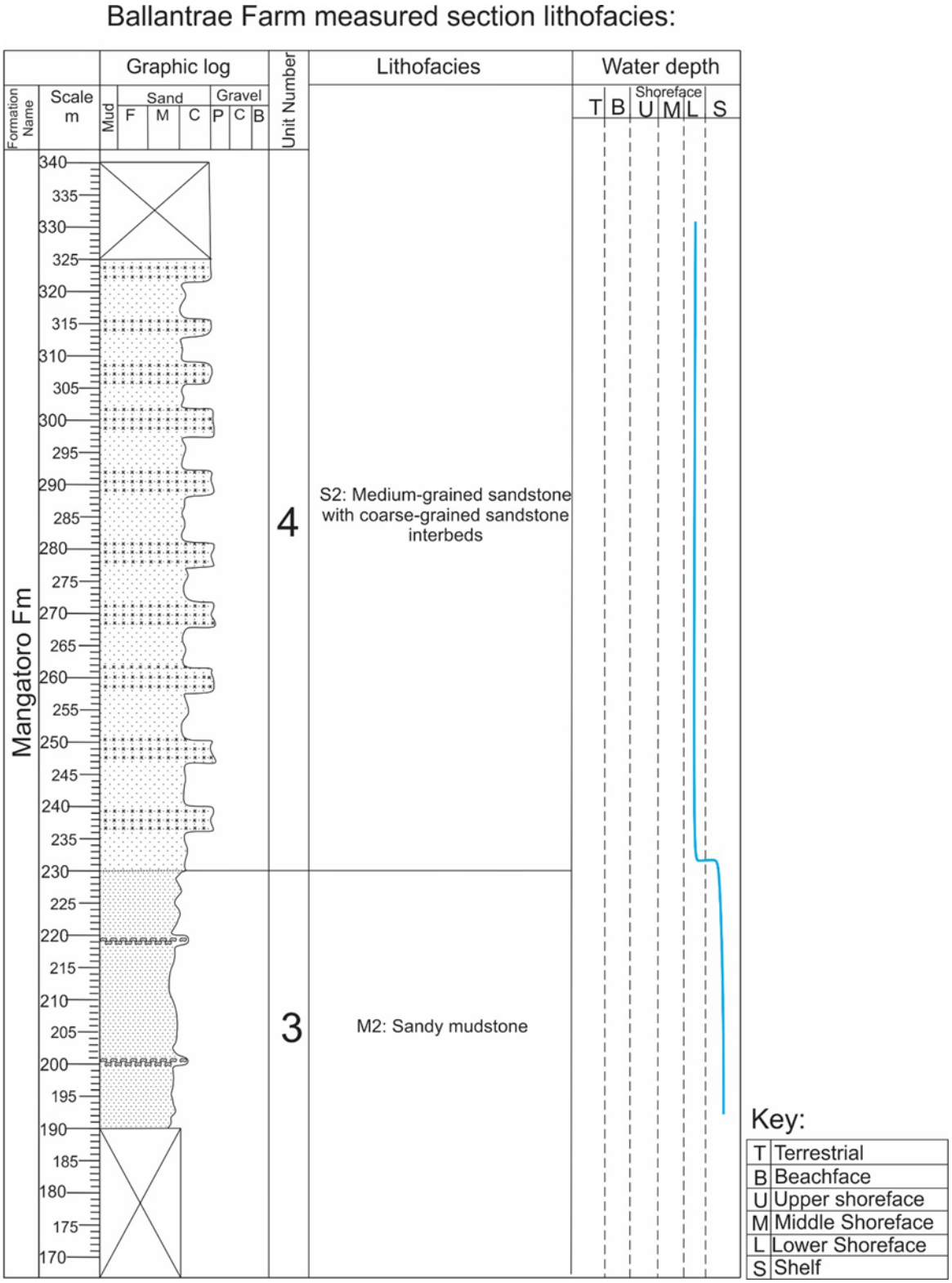

Figure 5-7 Continued.

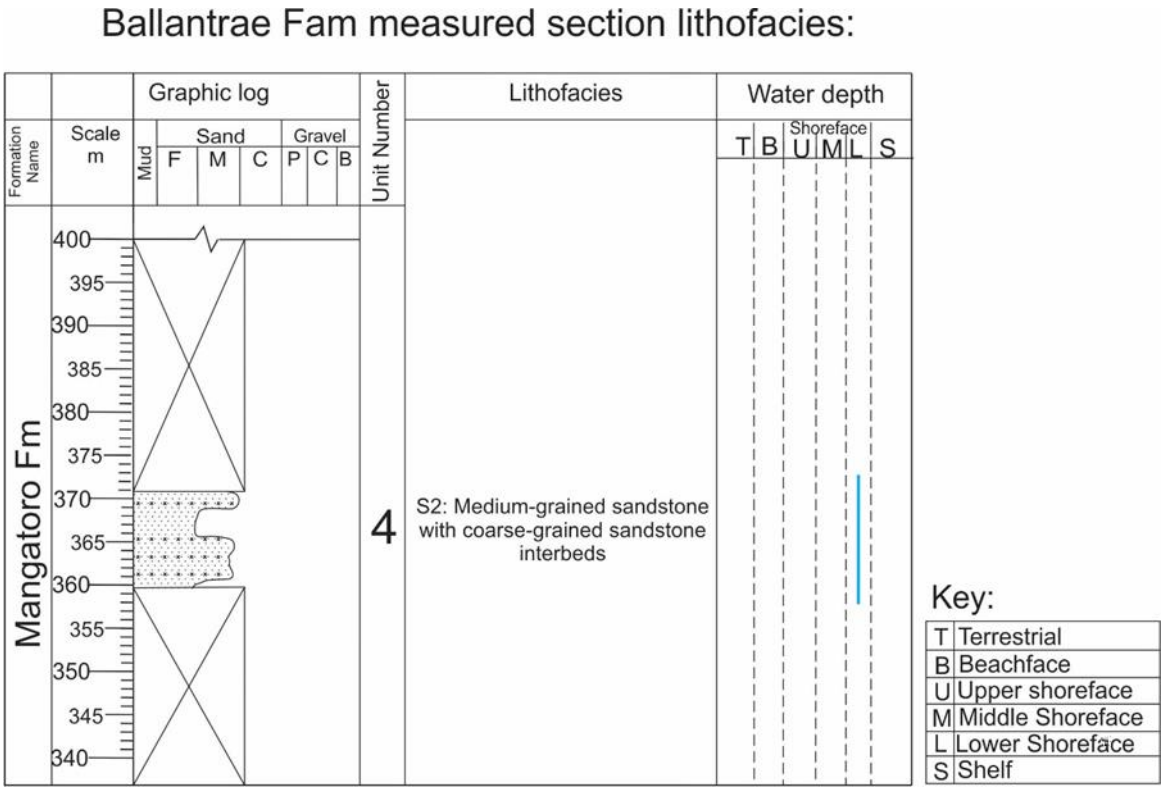

Figure 5-7 Continued.

5.4.3 Wharite Road measured section:

This section shows the Mangatoro Formation unconformably overlying the basement (Fig 5-8). The lithofacies indicate an uppershore face zone from the basal conglomerate (facies C_4). The top of the section is marked by a muddy sandstone (facies M_2) interpreted to indicate shelfal water depths. The transition between these two lithofacies is unclear, due to poor exposure.

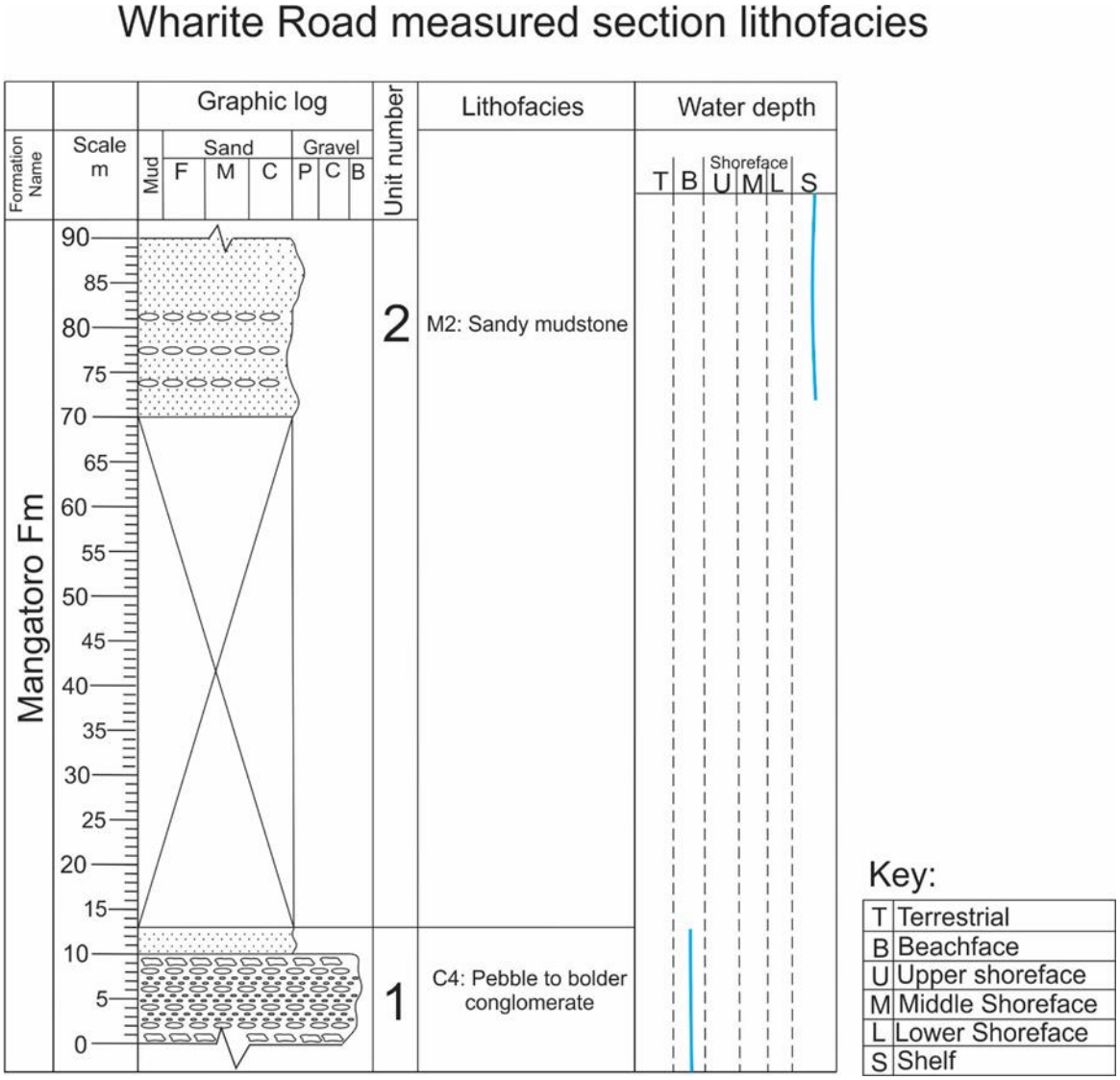

Figure 5-8: Lithofacies and water depth curve Wharite Road measured section.

5.4.4 Eastern Manawatu Gorge Entrance measured section:

This measured section shows the Kumeroa Formation unconformably overlying the Mangatoro Formation (Fig 5-9). The Mangatoro Formation present in this measured section is interpreted as a shelf lithofacies (unit one, facies M_2). The Kumeroa Formation shows a dramatic change to shallow water depths, with units two to five showing environments indicating an upper shoreface environment. Units six to nine show water depth fluctuations between upper shoreface to lower shoreface. The uppermost units, ten to twelve, show changes of lower to upper shoreface.

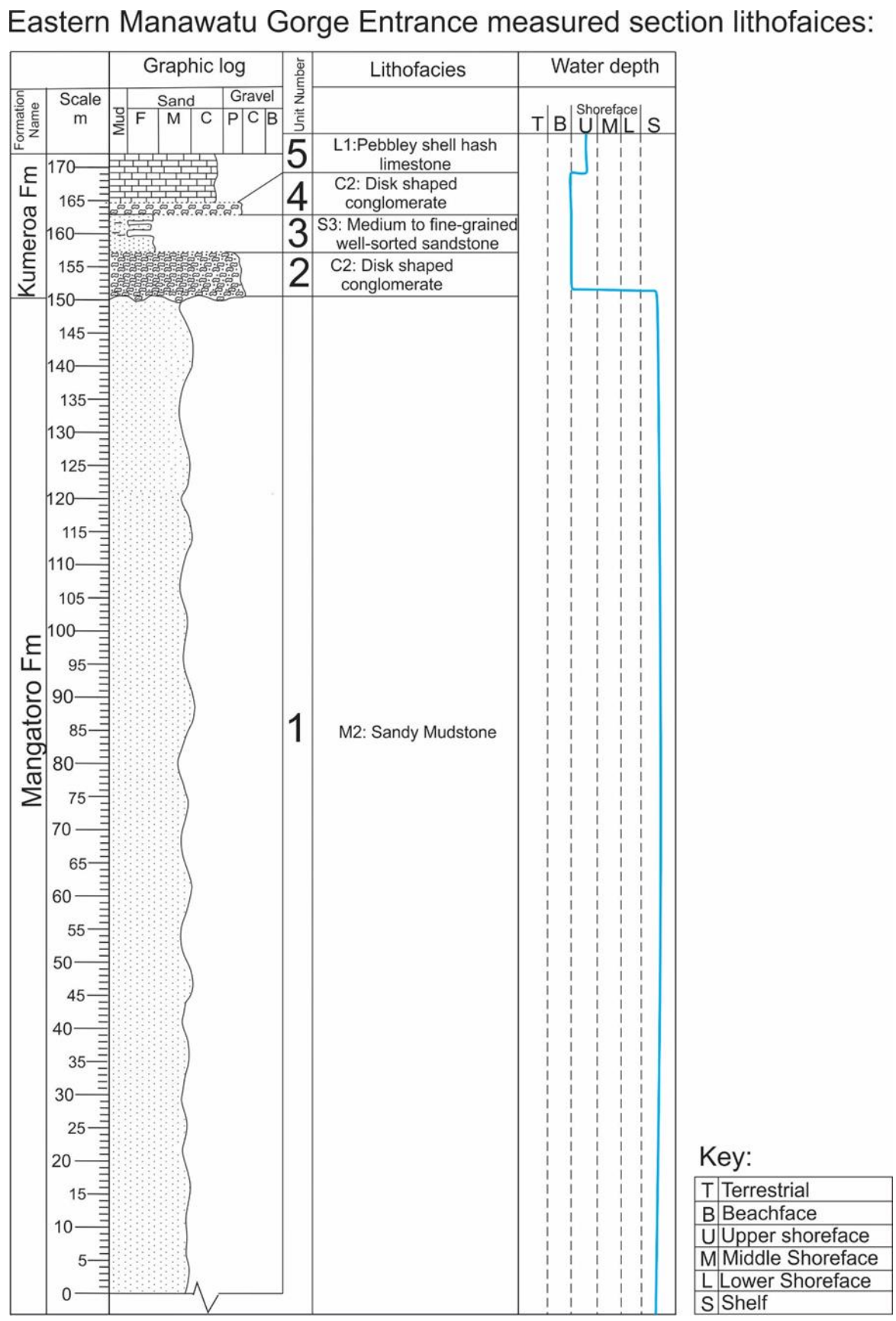

Figure 5-9: Lithofacies and water depth curve for the Eastern Manawatu Gorge Entrance measured section.

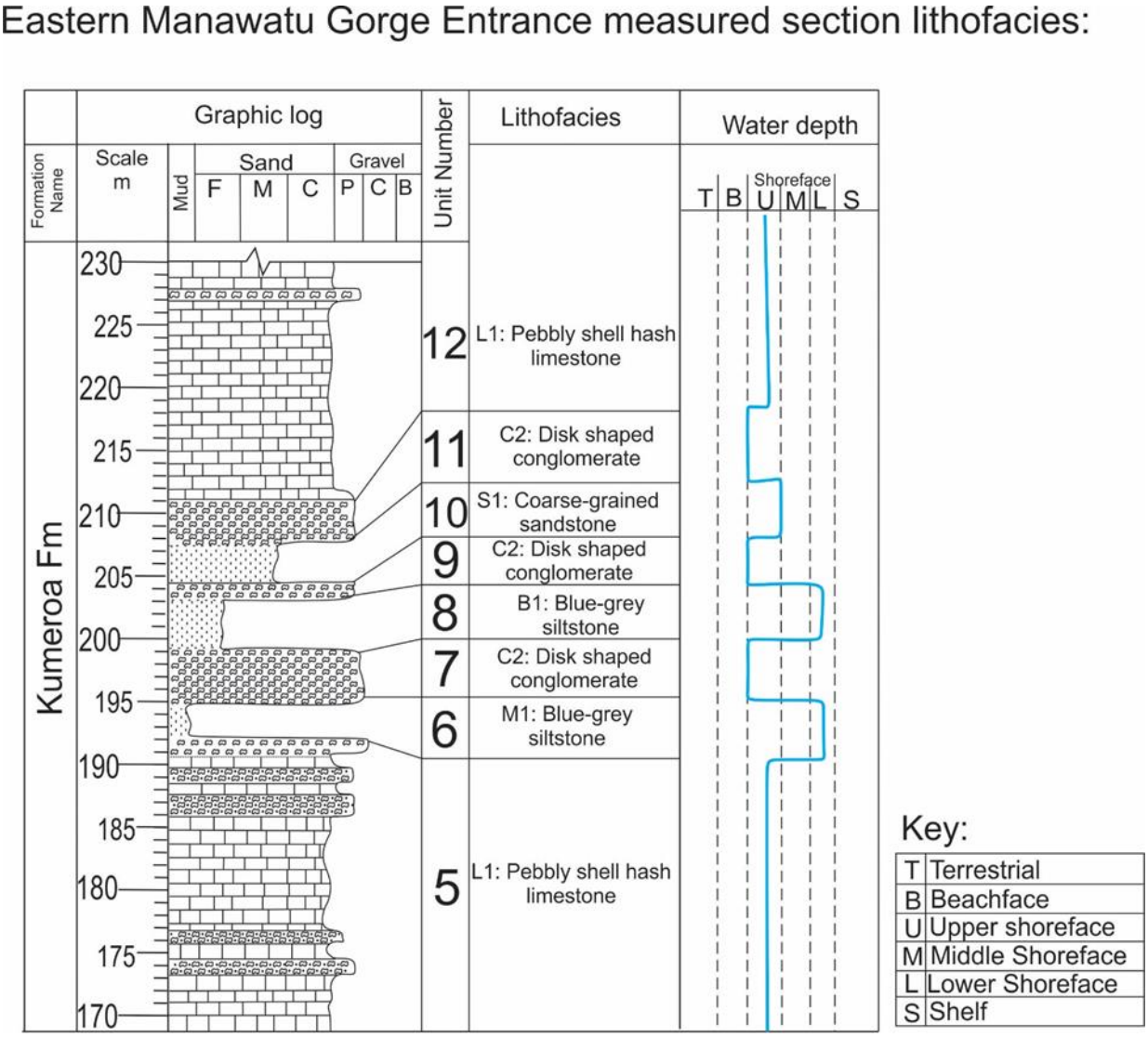

Figure 5-9: Counited.

5.4.5 Western Saddle Road measured section:

The Western Saddle Road measured section shows the following three formations: Te Aute, Kumeroa and Mangatarata formations (Fig 5-10). The Te Aute Formation makes up the base of the measured section, and shows conglomerates (facies C_2 and C_3) ranging in depth from upper shoreface to beachface. An unconformable contact separates the underlying Te Aute Formation from the overlying Kumeroa Formation. The bottom unit of the Kumeroa Formation, unit four, is interpreted as a lower shoreface environment (facies M_1). The contact between unit four and five is unobserved; however, there is significant change in water depth, with unit five (facies S_3) interpreted as a beachface lithofacies. The upper unit of the Kumeroa Formation (facies L_2) shows an upper shoreface water depth. Overlying the Kumeroa Formation (facies S_4) is the tidal flat facies of the Mangatarata Formation. The

measured section is capped by unit eight (facies S_3), interpreted to represent a beachface environment.

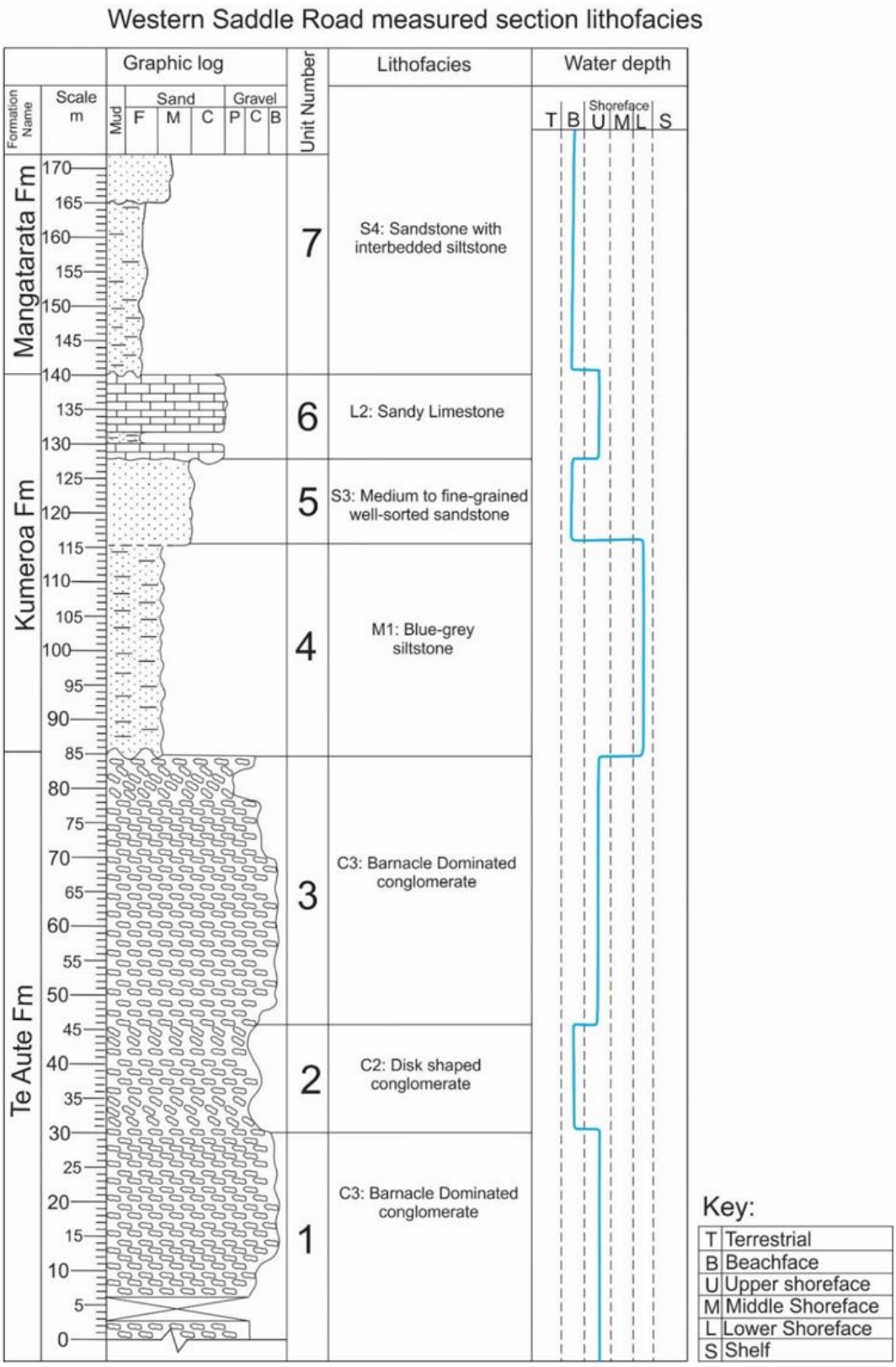

Figure 5-10: Lithofacies and water depth curve for the Western Manawatu Saddle Road measured section.

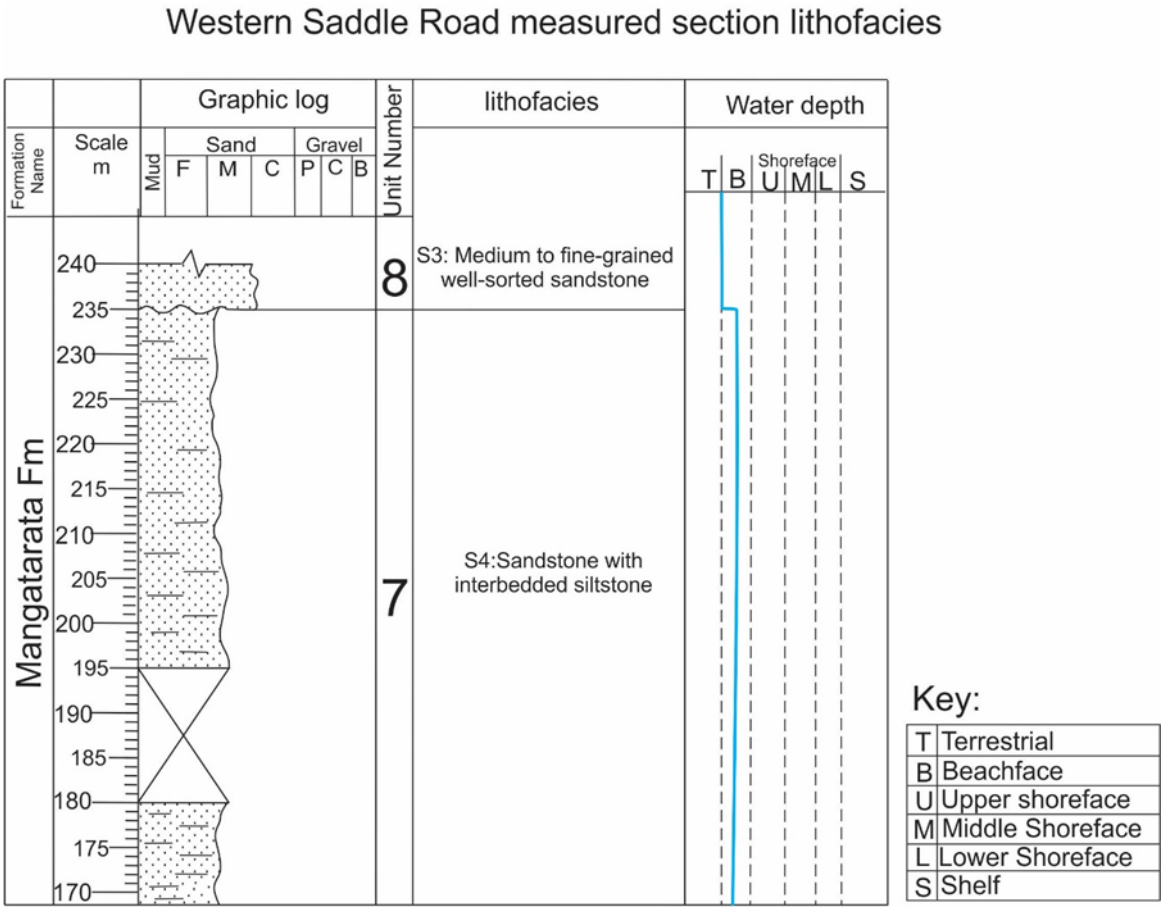

Figure 5-10: Continued.

5.4.6 Broadlands Stream measured section:

The Broadlands Stream measured section show the Te Aute Formation unconformably overlying the Kumeroa Formation (Fig 5-11). The base of the Te Aute Formation is marked by unit one, a terrestrial deposit (facies C_1). Overlying is unit two (facies C_2), representing a beachface environment. Unconformably overlying is unit three (facies M_1), showing a deepening to a lower shoreface environment. Unit four sharply overlies unit three, and consists of facies C_2, interpreted to represent an upper shoreface environment. Overlying is unit five showing facies L_2, interpreted to represent an upper shoreface environment. Unit six marks the upper section of the Te Aute Formation and consists of facies $C_{3,}$ also interpreted as representing an upper shoreface environment The base of the Kumeroa Formation is marked by unit seven (facies M_1) interpreted as a lower shoreface deposit. The top of the section is marked by unit eight (facies L_2) indicating shallowing to an upper shoreface depth.

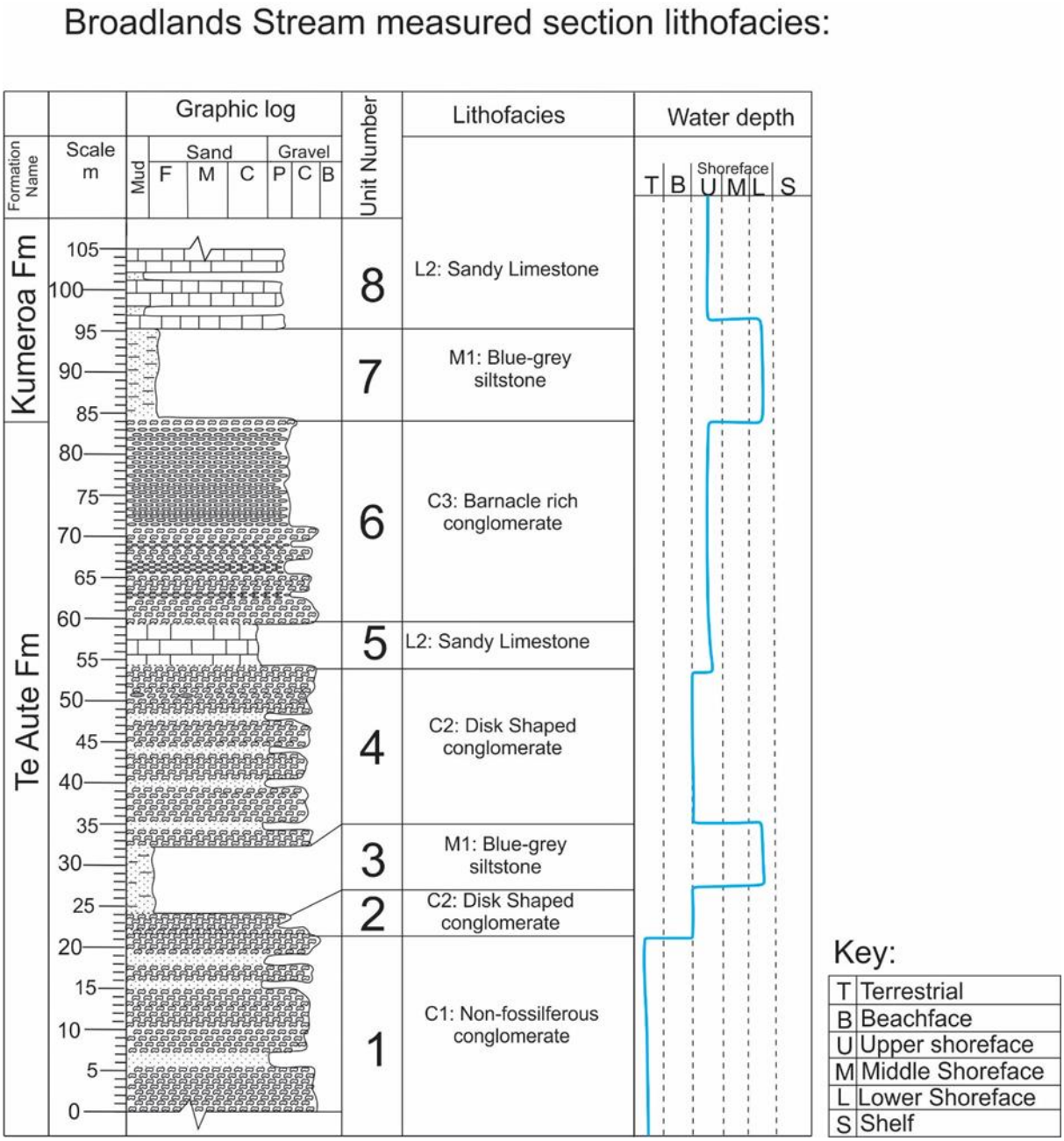

Figure 5-11: Lithofacies and water depth curve for the Broadlands Stream measured section.

5.5 Summary:

The above lithofacies associations and successions highlight the complex changes among terrestrial, shallow and deep marine depositional settings recorded by the Manawatu Strait sedimentary rocks. Overall the Mangatoro Formation shows an abrupt transition from beachface to shelf water depths, then a gradual change to lower shoreface depths. The Te Aute Formation unconformably overlies the Mangatoro Formation, and is marked by a terrestrial lithofacies at the base. The majority of the Te Aute Formation is interpreted to range in depth from upper shoreface to beachface. Unconformably overlying the Te Aute

Formation is the Kumeroa Formation, which shows repeated water depth changes ranging from upper to lower shoreface. The youngest formation observed in the Manawatu Saddle is the Mangatarata Formation, which shows lithofacies ranging from a beachface to tidal flat setting.

Chapter 6 Geological history and discussion

6.1 Introduction:

This chapter discusses the geological history of the Manawatu Strait from its formation in the Opoitian, to final emergence in the Castlecliffian resulting from rapid uplift of the axial ranges (Beu *et al*., 1981; King, 2000; Lee & Begg, 2002). Each sedimentary rock formation is discussed in terms of key events and timing. Summary schematic diagrams are presented showing how the water depth and depositional environments of the Manawatu Strait have changed over time. This chapter also highlights the complex interaction between tectonic uplift and eustatic sea-level change experienced by the Manawatu Strait, and shows how each process dictates the depositional environments present. The relationship between the Manawatu Strait and the adjacent Wanganui Basin and Ruataniwha Strait are briefly explored. Comparisons are also made with the northern Kuripapango Strait that formed in similar conditions to the Manawatu Strait during the Late Miocene to Pliocene (Kingma, 1971; Browne, 2004; Bland *et al.,* 2008; Trewick & Bland, 2012).

6.2 Geological history and discussion:

Mangatoro Formation: Opoitian (5.33-3.70 Ma):

The basement rocks of the Manawatu Saddle show an undulating surface, and crop out at locations throughout the eastern side of the Manawatu Saddle, see (Fig 1-5). These undulations are thought to have acted as localised highs and are likely small islands, providing a local source of sediment until they were submerged during the drowning of the strait. Similar highs have been observed by Kamp *et al*. (1988) in the Ruataniwha Strait, albeit on much larger scale than those present during the initial flooding of the saddle. Unconformably overlying the basement are the sedimentary rocks deposited within the Manawatu Strait. The oldest post-basement sedimentary rocks within the Manawatu Saddle are part of the Mangatoro Formation, cropping out on the eastern side of the Manawatu Saddle. Based on the macro and microfossils collected during this study, the age range for the Mangatoro Formation is constrained to the Opoitian Stage. This age range is consistent with that suggested by past authors (Lillie, 1953; Piyasin, 1966). Kingma (1971), Harmsen (1985), Lee and Begg (2002) and Browne (2004) have mapped the Mangatoro Formation in adjacent basins, and suggest a similar age for the formation.

The base of the Mangatoro Formation is marked by a thin widespread pebble to boulder conglomerate, which unconformably overlies the basement. This thin conglomerate is interpreted to represent a rocky shoreface (lithofacies C_4) that formed during the initial flooding and subsidence of the Manawatu Saddle. A thin ~20 metre-thick coarse-grained sandstone overlies the basal conglomerate (lithofacies S_1) and indicates a lower shoreface high-energy environment. Overlying the coarse-grained sandstone is a thick sandy mudstone (lithofacies M_2); the nature of the contact between these two units is unknown due to the patchy outcrop exposure on the Eastern Manawatu Saddle. The sandy mudstone has been interpreted to represent deposition at shelf depths, based on the microfossil assemblages present (see chapter five, lithofacies M_2). Although the contact between the lower shoreface sands and shelf sandy mudstone of the Mangatoro Formation was not observed, it is thought the transition from lower shoreface to shelf depth was a rapid transition related to the subsidence and flooding of the Manawatu Saddle during the early formation of the Manawatu Strait.

At the time the shelf sediments were deposited, the Manawatu Strait was likely at its most extensive, as this is the only time in the strait's history that shelf facies are recorded. This indicates that the Opoitian not only marks the formation of the Manawatu Strait but also the time when the strait reached maximum transgression. Fig 6-1 presents a schematic 3D diagram looking west through the Manawatu Strait, showing the paleogeography of the strait at the point of maximum transgression. Note that these figures do not show the southern margin of the Manawatu Strait, as this study was unable to place any constraints on the width of the strait due to limited exposure on the southern Manawatu Saddle/Gorge region. The figure also shows how there is limited terrestrial exposure and a narrow coarse-grained shoreline, in comparison to the deep water facies present at this time. The upper to middle shoreface zones are also thought to be relatively restricted due to the expansion of the shelf zone.

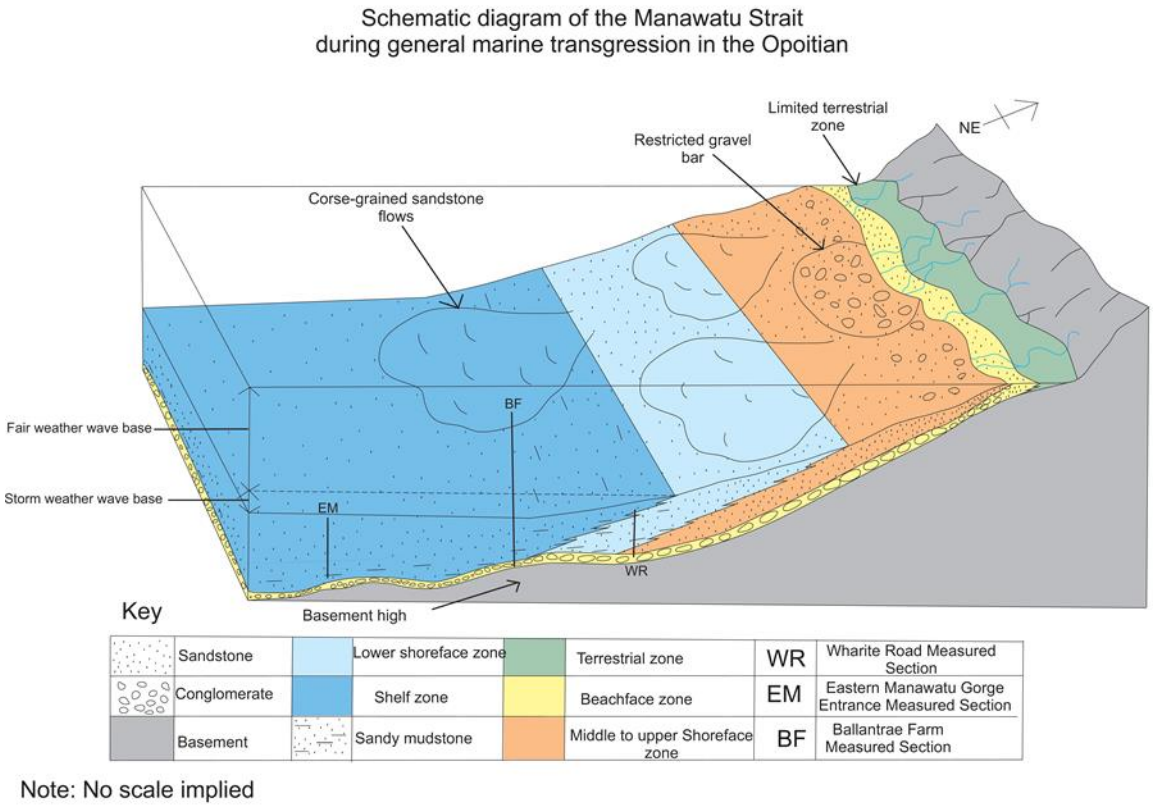

Figure 6-1: Schematic diagram of the Manawatu Strait during the Opoitian.
Peak marine transgression is reached showing water reaches shelf depth. This period is characterised by limited and narrow terrestrial, beach face, and middle to upper shoreface zones, and extensive shelf facies.

The Manawatu Strait was not the only location in the proto-North Island to experience major marine transgression during the Opoitian. The adjacent East Coast basins show evidence of a major marine transgression event during the Opoitian. The Mangatoro equivalent, the Opoitian aged Matemateaonga Formation of the West Coast basins, also shows evidence of marine transgression (Kamp *et al.*, 2004). Furthermore, extensive Mangatoro Formation outcrops in the proto-Ruataniwha Strait throughout the East Coast basins to the east of the Manawatu Strait also provide evidence for a similar transgression event (Lillie, 1953; Beu, 1995; Bland 2006). The Kuripapango Strait to the north of the Manawatu Strait contains the Mangatoro Formation, interpreted to represent the sediments deposited at shelf depths during the Opoitian (Browne, 1981, 2004).

The cause of the major transgression occurring during the Opoitian in the west coast basins has been suggested by Kamp *et al*. (2004) and Nicol (2011) to be the result of the so-called 'Tangahoe pull down' event, in which mantle instabilities caused faulting within the basins and subsidence. This in turn resulted in the marine transgression and flooding of the King

Country Basin area ~5 Ma ago (Kamp *et al*., 2004; Nicol, 2011). The timing of this instability and marine flooding coincides with the broad time range of the oldest sedimentary rock formation deposited above the basement in the Manawatu Strait. It is therefore proposed that the 'Tangahoe pull down' event was a possible mechanism for the formation of the Manawatu Strait.

The upper Mangatoro Formation in the Manawatu Saddle shows a change in lithofacies to a fine-grained sandstone with coarse-grained interbeds (lithofacies S_3). This lithofacies has been interpreted to have been deposited in a lower shoreface setting, and marks the point where transgression ends and regression begins in the Manawatu Strait.

Te Aute Formation: Waipipian (3.70 Ma) - Mangapanian (2.40 Ma):

The Te Aute Formation represents sedimentary rocks deposited in the Manawatu Strait between the Waipipian to Mangapanian stages. The biostratigraphy presented by Lillie (1953) indicates that the Te Aute Formation ranges from the Waipipian to Mangapanian (Chapter four). The Te Aute Formation crops out on the western side of the Manawatu Saddle and consists of conglomerate lithofacies, ranging from terrestrial to lower shoreface high-energy depositional settings, based on the lithofacies interpretations as non-fossiliferous, disc-shaped, barnacle-rich and pebble- to boulder-dominated conglomerates (see Chapter Five).

The Te Aute Formation lies unconformably over the Mangatoro Formation and is marked at its base by a terrestrial conglomerate (lithofacies C_1). The presence of this terrestrial conglomerate indicates a significant shift in the depositional environment in the Manawatu Strait, indicating a period of rapid uplift resulting from sea level fall. The associated erosion and non-deposition, due to the change in environment, likely removed the underlying marine facies we would reasonably expect to be associated with a shift from shelf to terrestrial environments. Overlying the terrestrial conglomerates are beachface to shallow-water upper shoreface conglomerates (see Chapter Five, lithofacies successions and associations). The uppermost conglomerate of the Te Aute Formation consists of a barnacle-rich facies interpreted to have been deposited as a shallow-water marine gravel bar. Based on the abundance of barnacles within this lithofacies, it suggests the Manawatu Strait was influenced by strong currents. Work by Beu *et al*. (1980), Kamp *et al*. (1988), Beu (1995) and Bland (2006) in the adjacent Ruataniwha Strait shows that barnacles appear more commonly

in shallow-water high-energy facies. The currents supply nutrients and reduce suspended sediment, in turn promoting barnacle growth (Beu *et al.*, 1980). The strong currents within the Manawatu Strait were likely driven by tidal forces. As the strait's location lies between the active Ruataniwha Strait (east coast) and developing Wanganui Basin, it can be inferred that there was a similar tidal regime to the modern day Cook Strait (K. Bland personal communications July 12th 2017). In the modern Cook Strait area, high-tide at one end of the strait generally corresponds to low-tide at the other side, inducing strong tidal flows.

The dominance of conglomerates within the Te Aute Formation throughout the Manawatu Strait indicates that the Waipipian to Mangapanian was a time period where the Manawatu Strait was restricted and experiencing a phase of regression. The water depths present within the strait during the Waipipian to Mangapanian were much shallower than conditions during the Opoitian deposition of the Mangatoro Formation. Fig 6-2 shows a schematic 3D diagram of the Manawatu Strait during this phase of regression. The figure shows how the strait was dominated by terrestrial and lower shoreface environments, with a high volume of fluvial material sourced from the uplift of the developing North Island axial ranges north and south of the strait.

Carter (1972), Browne (1978), Beu *et al.* (1981) and Beu (1995) suggest that the Ruahine and Tararua Ranges experienced rapid uplift during the Waipipian to Nukumaruan. The sediments observed by these authors show lithofacies with a high percentage of terrigenous material likely sourced from uplifting fault blocks, therefore suggesting significant uplift and erosion of the adjacent ranges occurred to provide a sediment source for these facies. Browne (2004) notes the absence of any Waipipian-aged sediments within the Kuripapango Strait; Bland (2006) and Bland *et al*. (2008) also note the absence of Waipipian-aged sediments in sections of the east coast basin. The Te Aute Formation recorded in this study could not be constrained tightly in terms of its age range, so it is possible that the Te Aute Formation within the Manawatu Strait follows similar trends to adjacent basins i.e. the absence of any Waipipian-aged sediments. These two examples are cited as further evidence for uplift occurring during the Waipipian in this part of North Island, with resulting unconformities associated with the extension and dextral faulting occurring throughout the East Coast Basin.

The terrestrial to shallow-water facies observed in the Manawatu Saddle align in both age and general depositional environments with the timing of uplift for the axial ranges, as inferred by Beu *et al*. (1980) and Beu (1995). The uplifting ranges are cited as an abundant source of

terrestrial material, giving rise to the conglomerate facies. Similar facies were observed by Browne (2004) during the early formation of the Kuripapango Strait and attributed to the interaction between developing ranges and the resulting sediment transport and deposition as bars. Changes in the tectonic regime of proto-New Zealand were not the only processes driving environmental change during the Waipipian to Mangapanian time. Eustatic sea-level fluctuations were also occurring (Beu *et al*. 1980; Beu & Edwards, 1984; Beu, 1995; Naish *et al*., 2005; Bland, 2006). These changes likely had an influence on conditions within the Manawatu Strait. However, the basin was uplifting, and accommodation space was therefore reduced, meaning any eustatic sea-level signals were likely overprinted by tectonic signals. The changes in sea level within the Manawatu Strait do not correlate with adjacent basins in terms of their frequency or magnitude (the higher resolution timing of events is uncertain due to the course resolution biostratigraphy). The reduced magnitude of events could be due to the reduced accommodation space for sediment accumulation, due to the tectonic uplift of the strait. There is a very likely chance that the Manawatu Strait was affected by eustatic sea level change; however, based on the tectonic conditions and poor fossil preservation, the eustatic sea level signal was overprinted by a tectonic signal.

Kumeroa Formation: Nukumaruan (2.40-1.63 Ma):

The Kumeroa Formation unconformably overlies the Te Aute Formation within the Manawatu Saddle, and crops out on both the western and eastern margins of the Manawatu Saddle. The Kumeroa Formation is the only formation to show an alternating sequence of sandy/pebbly limestone and siltstones. Outcrops on the eastern Manawatu Saddle, at the Eastern Manawatu Gorge Entrance measured section, show a higher resolution of these alternating sequences than the western outcrops, likely due to the fact this exposure is thicker. The lower section of the Kumeroa Formation on the Eastern Manawatu Saddle shows a series of beachface sandstones and conglomerates, which transition into an upper shoreface pebbly limestone. Overlying the pebbly limestone is a series alternating of siltstones and conglomerates, indicating changes from the lower shoreface (represented by the siltstones) to a beach-face setting (represented by the conglomerates). This sequence is followed by an alternation between a coarse-grained sandstone and disc-shaped conglomerate, indicating a relatively smaller fluctuation in water depth or energy, with changes ranging from upper

shoreface to beachface. The section is capped by another pebbly limestone representing an upper shoreface setting.

The outcrops of the Kumeroa Formation on the western Manawatu Saddle show limited exposure when compared to the outcrops on the western Manawatu Saddle. Outcrops on the Western Saddle Road and the Broadlands Stream measured sections show alternations between sandy limestones, representing deposition within the upper shoreface zone, and siltstones from lower shoreface depths. The Eastern Manawatu Saddle is affected by major faults such as the Ruahine and Mohaka faults, which, when combined with the undulating basement topography, possibly led to higher accommodation space for the development of this higher-resolution.

Another key feature to take into account is the difference in limestone characteristics between the eastern and western limestones, in that the eastern limestones show a higher basement-derived ("greywacke") pebble content that indicates close proximity to fluvial sources. Fig 6-2 shows a schematic diagram of how the paleogeography of the Manawatu Strait may have looked throughout the Waipipian to Nukumaruan time period, where upper shoreface deposits dominated the Manawatu Strait.

A possible mechanism for the transition from the Te Aute Formation conglomerate to the limestones and thin siltstones of the Kumeroa Formation is that, at two million years ago, the rotation and uplift associated with the development of the Hikurangi margin to the east of New Zealand is interpreted as having temporally slowed (Walcott, 1989; King, 2000). Such an interpretation is supported by the relatively little uplift that occurred in the central and southern parts of the North Islands axial ranges during the mid to late Nukumaruan (Beu *et al*., 1981; King, 2000). The variety of Nukumaruan-aged lithofacies suggests that sea level within the Manawatu Strait was influenced by relatively rapid changes in eustatic sea level, as opposed to tectonic processes, throughout the Nukumaruan.

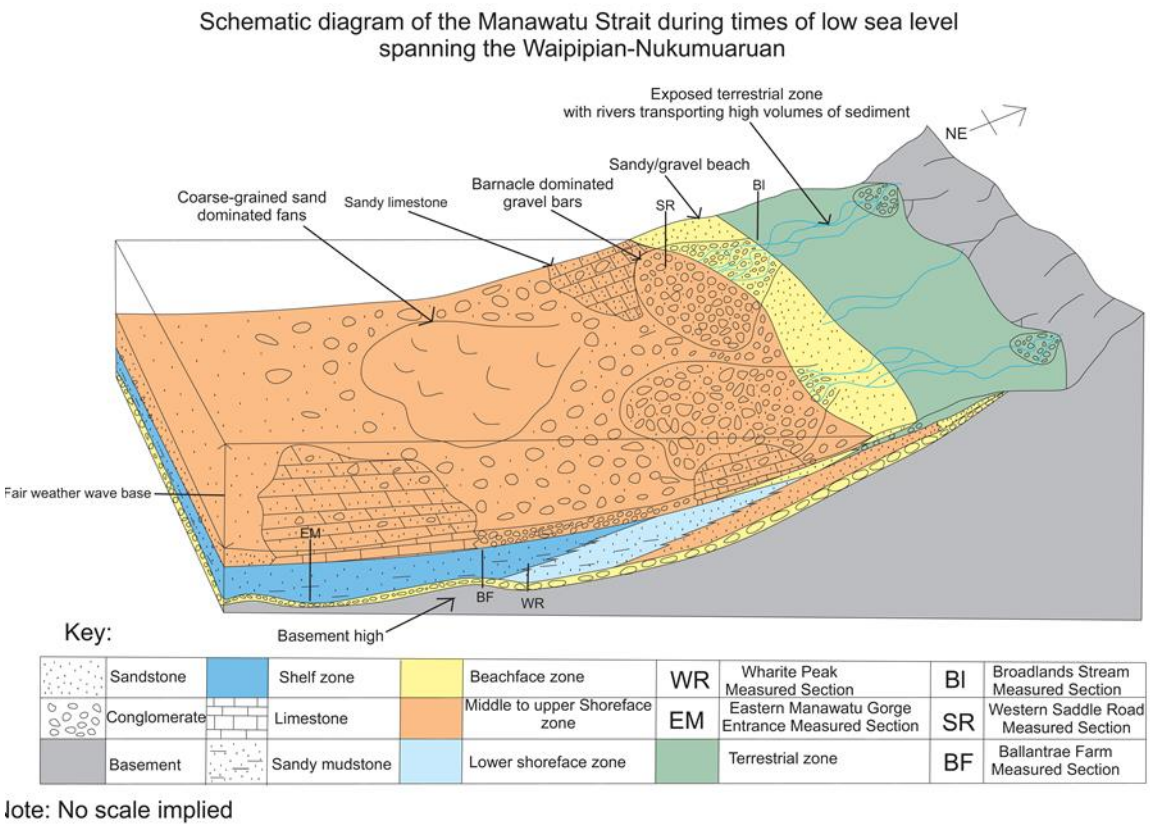

Figure 6-2: Schematic diagram of the Manawatu Strait during the Waipipian to Nukumnaruan. Note the extended terrestrial zone and upper to middle shoreface zones. Gravel bars and beaches dominated this time, along with sandy limestones showing high-angle cross-beds indicating strong sea-floor current influences.

Adjacent basins such as the Wanganui and East Coast recorded a much higher-resolution record of Nukumaruan-aged eustatic sea-level change when compared to the Manawatu Saddle (Beu & Edwards, 1984; Haywick *et al.*, 1992; Beu, 1995; Naish *et al.*, 2005; Naish & Wilson, 2009). For example, the Ruataniwha Strait shows a variety of alternating lithofacies ranging from non-marine conglomerates through shallow-water limestones to deep-water mudstones that, when stacked, show cyclothems related to eustatic sea-level change (e.g., Beu, 1983; Beu & Edwards, 1984; Haywick *et al*., 1992; Caron *et al*., 2004b). The same is also seen in the Wanganui Basin where accommodation space kept pace with sediment deposition, to preserve a high resolution record of sea level change (e.g. Naish *et al*., 1996; Naish *et al*., 2005). The reduced accommodation space in the Manawatu Strait meaning no truly deep water facies could be deposited, combined with strong currents washing key fauna through the strait (resulting in limited macro and microfossils being preserved), is likely responsible for the reduced record of sea level cycles.

Mangatarata Formation: Castlecliffian (1.63-0.34 Ma):

Overlying the Kumeroa Formation is the Castlecliffian-aged Mangatarata Formation, which consists of decimetre-thick interbedded sandstones and siltstones, showing sedimentary structures characteristic of a marginal-marine tidal flat environment (see Chapter Five for more information). The change in lithofacies, from upper shoreface Kumeroa Formation limestones to the tidal-flat sandstone and siltstones of the Mangatarata Formation, shows evidence for further shallowing, regression, and the final emergence of the Manawatu Strait. The Mangatarata Formation shows sea level at its lowest recorded point within the Manawatu Strait, which is interpreted as showing the strait closure. The Mangatarata Formation is mapped in this study as a thin formation on the western margin of the Manawatu Saddle extending into the adjacent Pohangina region, but the formation is also mapped throughout the Woodville region east of the Manawatu Saddle (Piyasin, 1966; Neef, 1967; Lee & Begg, 2002), suggesting that the centre of the Manawatu Strait had uplift by this time and the margins of the strait contained marginal-marine environments.

Fig 6-3 shows a schematic diagram of how environments of the emerging Manawatu Strait may have looked. The age of deposition of the Mangatarata Formation is constrained to the Castlecliffian Stage on the basis of tephra beds such as the Rewa (1.20 ± 0.14 Ma) and Potaka tephras (1.05 ± 0.05 Ma) identified within the formation cropping out on the western margin of the Manawatu Saddle (Pillans *et al*., 2005; Rees 2015).

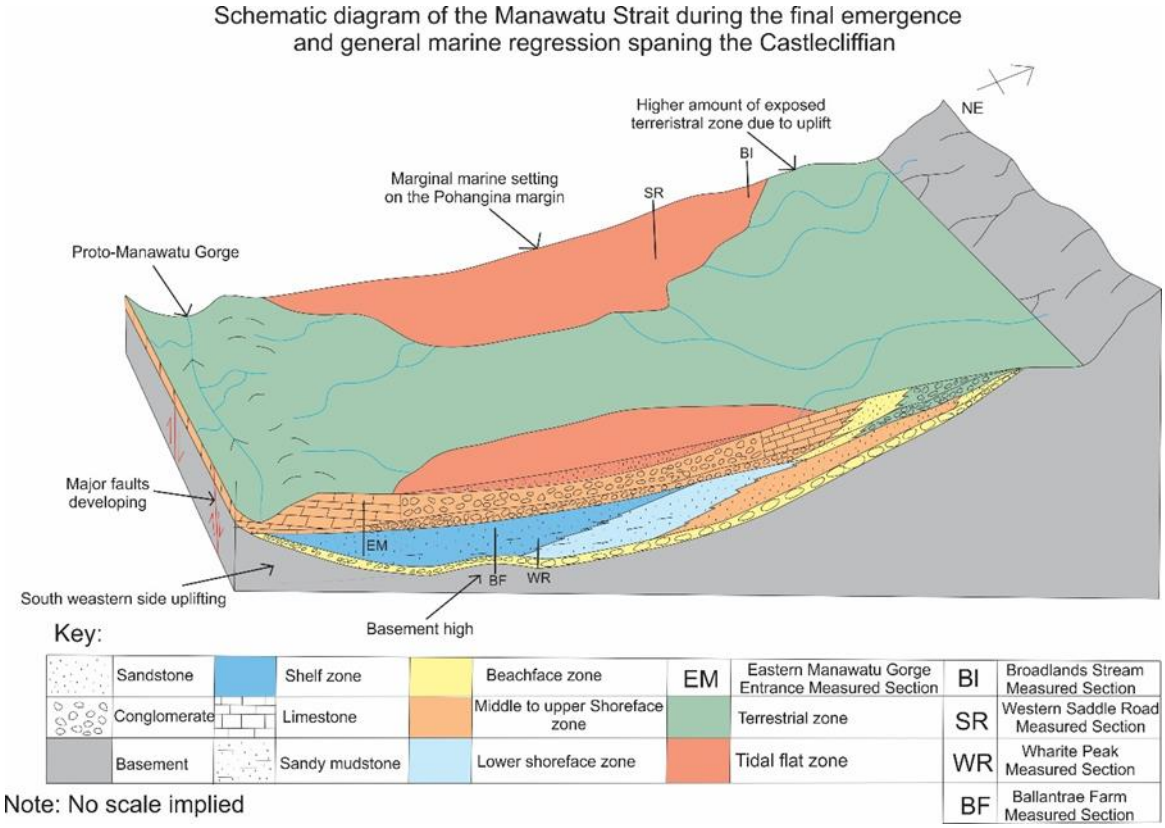

Figure 6-3: Schematic diagram of the emerging Manawatu Strait during the Castlecliffian. Both the western and eastern margins of the Manawatu Strait are dominated by tidal-flat environments, as the centre of the Manawatu Strait uplifts. Major faults such as the Mohaka and Ruahine faults are likely to have been active during this final phase of uplift (e.g. Lee & Begg 2002; Trewick & Bland 2012, and references therein). The proto-Manawatu Gorge and river also began to carve its antecedent path through the uplifting south-west Manawatu Strait.

The emergence of the Manawatu Strait is attributed to the rapid uplift of the axial ranges in the Castlecliffian (Beu *et al*., 1981; King, 2000). The uplift of the Manawatu Strait meant that, for the first time the East Coast Basin and Wanganui Basin became geographically isolated from one another by land, the only passageway for water between the two being the marine opening at Cook Strait, to the south of the basins, from ~0.5 Ma (Lewis *et al*., 1994).

The Manawatu Strait was not the only seaway to emerge during the Castlecliffian. As the Ruataniwha Strait emerged, due to movement on the Mount Bruce fault block in the early Nukumaruan, a series of lakes formed to the east of the Manawatu Strait (Piyasin, 1966; Neef, 1967; Lee & Begg, 2002). The formation and drainage of these lakes and estuarine environments on the eastern margin of the Ruataniwha Strait likely had an impact on the development of the proto-Manawatu River. As the lakes and associated environments drained and shifted, the shape and path of the proto-Manawatu River changed with them. The

Manawatu Strait was beginning to drain by the Castlecliffian. So, it is therefore possible that the proto-Manawatu River was deflected towards the Tararua Ranges due to a combination of the changing environments and uplift the ranges and associated fault blocks (Beanland, 1995). Once the river had established a flow path, it was able to maintain the flow direction during the uplift of the ranges to form the Manawatu Gorge we see today.

Chapter 7 Conclusions

7.1 Summary:

This study set out to investigate the sedimentary rocks of the Manawatu Saddle and reconstruct the Pliocene-Pleistocene formation, uplift and emergence history of the Manawatu Strait, and to understand how this feature fits within the wider context of the development of the lower North Island of New Zealand. In order to achieve this, a stratigraphic approach was taken, where five key sections were measured to take advantage of the recent fresh outcrop exposure. These sections have allowed the development of a composite record spanning from the oldest sedimentary rocks representing the initial formation of the strait, through to the youngest sedimentary rocks marking the final emergence and closure of the strait. Bio-stratigraphic techniques were applied to provide constraints to each recognised formation, and incorporated along with stratigraphic techniques to clarify the formation boundaries defined by past authors. A lithofacies scheme was created to interpret the depositional environments though time in the Manawatu Strait. The results from this study have allowed key events and time intervals to be constrained within the Manawatu Strait development and uplift. The paleogeography of the Manawatu Strait at these time intervals are presented as schematic 3D diagrams. The key events have been considered in the wider context of the development of the East Coast and West Coast basins.

7.2 Key findings:

The key findings highlighted by this study are as follows:

- New measured sections have allowed the most comprehensive documentation of the Manawatu Saddle geology to date. As a result, a lithofacies scheme has been applied, providing a detailed insight into the changing depositional environments within the Manawatu Strait.

- Field observations and biostratigraphy in this study largely confirm the original formation boundaries and biostratigraphy proposed by Lillie (1953).

- The Manawatu Strait first developed during the Opoitian (5.33-3.70 Ma). This is based on the unconformable relationship between Opoitian aged Mangatoro Formation and the basement, and has been attributed to the Tangahoe pull down event.

- The Opoitian also marks the time interval where the Manawatu Strait was at its deepest and likely widest, as shelf depth lithofacies are recorded. The actual width is unknown due to erosion of the Pliocene-Pleistocene Sedimentary rocks on the Southern side of the Manawatu Saddle.

- Uplift of the axial ranges occurred from the Waipipian (3.70 Ma) to the Nukumaruan (1.63 Ma). The uplift of the ranges is indicated by the deposition of terrestrial and shallow marine Te Aute Formation conglomerates unconformably overlaying the Mangatoro Formation. These conglomerates mark the point when the sea way was at its most restricted.

- During the Nukumaruan, the Kumeroa Formation limestones and siltstones were deposited in a high energy current swept shallow marine environment. The alternating facies characters indicate the Manawatu Strait recorded some sea level change signals, although determining eustatic change versus tectonic influence was not possible due to the resolution of the biostratigraphy.

- The final emergence and closure of the Manawatu Strait occurred in the Castlecliffian (1.63-0.34 Ma), marked by the presence of the marginal marine lithofacies of the Mangatarata Formation. The final emergence of the Manawatu Strait also marks the final separation of the East Coast (Ruataniwha Strait) and basins.

7.3 Suggested future work:

The findings of this study have highlighted aspects for further research to enhance and constrain the geological history of the Manawatu Strait:

- A higher resolution approach to the biostratigraphy to provide more constraints to the ages of formations, to allow higher resolution paleogeographic maps to be produced.

- A higher resolution approach to reconstructing Nukumaruan-aged eustatic sea level changes within the Manawatu Strait.

- More detailed field mapping of the limited Pliocene-Pleistocene exposure on the Tararua Range southern margin of the Manawatu Strait to constrain the geometry of the Manawatu Strait.

- Investigations into the offset and timing of major faulting within the Manawatu Saddle, to constrain the timing of uplift.

Reference List:

Anderton, P. W. (1981). Structure and evolution of the south Wanganui Basin, New Zealand. New Zealand Journal of Geology and Geophysics, 24(1), 39-63.

Beanland, S. (1995). The North Island Dextral Fault Belt, Hikurangi Subduction Margin, New Zealand. (Unpublished PhD thesis in Geology), Victoria University of Wellington.

Beu, A., & Edwards, A. (1984). New Zealand Pleistocene and late Pliocene glacio-eustatic cycles. Palaeogeography, Palaeoclimatology, Palaeoecology, 46(1-3), 119-142.

Beu, A., Browne, G., & Grant-Taylor, T. (1981). New Chlamys delicatula localities in the central North Island and uplift of the Ruahine Range. New Zealand Journal of Geology and Geophysics, 24(1), 127-132.

Beu, A., Hornibrook, N. de B., & Grant-Taylor, T. L. (1980). The Te Aute Limestone Facies: Poverty Bay to Northern Wairarapa: New Zealand Geological Survey, Department of Scientific and Industrial Research.

Beu, A. G. (1995). Pliocene limestones and their scallops: lithostratigraphy, pectinid biostratigraphy, and paleogeography of eastern North Island late Neogene limestone: Institute of Geological & Nuclear Sciences Monograph 10, No 68. Lower Hutt Institute of Geological & Nuclear Sciences.

Beu, A. G., Maxwell, P. A., & Brazier, R. C. (1990). Cenozoic mollusca of New Zealand. New Zealand Geological Survey Palaeontological Bulletin, 58, 1–518.

Beu, A. (1990). Molluscan generic diversity of New Zealand Neogene stages: extinction and biostratigraphic events. Palaeogeography, Palaeoclimatology, Palaeoecology, 77(3), 279-288.

Beu, A. G., & Raine, J. (2009). Revised descriptions of New Zealand cenozoic mollusca from Beu and Maxwell (1990). GNS Science Miscellaneous Series, 27.

Beu (2012): Marine mollusca of the last 2 million years in New Zealand. Part 5. Summary. Journal of the Royal Society of New Zealand, 42:1, 1-47, DOI: 10.1080/03026758.2011.559727.

Bland, K. J. (2006). Analysis of the central Hawke's Bay sector of the late Neogene forearc basin, Hikurangi margin, New Zealand. (Unpublished PhD thesis), Waikato University, Hamilton New Zealand.

Bland, K. J., Kamp, P. J., & Nelson, C. S. (2008). Late Miocene–Early Pleistocene paleogeography of the onshore central Hawke's Bay sector of the forearc basin, eastern North Island, New Zealand, and some implications for hydrocarbon prospectivity. 2008 Petroleum Conference Proceedings.

Browne, G. H. (1978). Wanganui strata of the Mangaohane Plateau, northern Ruahine Range, Taihape. Tane, 24, 199-210.

Browne, G. (1981). The geology of the Kuripapango-Blowhard District, W. Hawkes Bay. (Masters of Science in Geology, with Honours), University of Auckland.

Browne, G. H., & Naish, T. R. (2003). Facies development and sequence architecture of a late Quaternary fluvial-marine transition, Canterbury Plains and shelf, New Zealand: implications for forced regressive deposits. Sedimentary Geology, 158(1), 57-86.

Browne, G. H. (2004). Late Neogene sedimentation adjacent to the tectonically evolving North Island axial ranges: Insights from Kuripapango, western Hawke's Bay. New Zealand Journal of Geology and Geophysics, 47(4), 663-674.

Caron, V., Nelson, C. S., & Kamp, P. J. (2004a). Contrasting carbonate depositional systems for Pliocene cool-water limestones cropping out in central Hawke's Bay, New Zealand. New Zealand Journal of Geology and Geophysics, 47(4), 697-717.

Caron, V., Nelson, C. S., & Kamp, P. J. (2004b). Transgressive surfaces of erosion as sequence boundary markers in cool-water shelf carbonates. Sedimentary Geology, 164(3), 179-189.

Carter, R. (1972). Wanganui strata of Komako District, Pohangina Valley, Ruahine Range, Manawatu. Journal of the Royal Society of New Zealand, 2(3), 293-324.

Cole, J., & Lewis, K. (1981). Evolution of the Taupo-Hikurangi subduction system. Tectonophysics, 72(1-2), 1-21.

Grammer, T. R. (1971). The Geology of the Eastern Saddle Road area, Manawatu, North Island, New Zealand (BSc Hons), University of Otago, Dunedin.

Harmsen, F. (1985). Lithostratigraphy of Pliocene strata, central and southern Hawke's Bay, New Zealand. New Zealand Journal of Geology and Geophysics, 28(3), 413-433.

Hayward, B. W., Grenfell, H., Cairns, G., & Smith, A. (1996). Environmental controls on benthic foraminiferal and thecamoebian associations in a New Zealand tidal inlet. Journal of Foraminiferal Research, 26(2), 150-171.

Hayward, B. W., Grenfell, H., & Reid, C. (1997). Foraminiferal associations in Wanganui Bight and Queen Charlotte Sound, New Zealand. New Zealand Journal of Marine and Freshwater Research, 31(3), 337-365.

Hayward, B. W. (2010). Recent New Zealand deep-water benthic foraminifera: Taxonomy, ecologic distribution, biogeography and use in paleoenvironmental assessment: GNS Science.

Haywick, D. W., Carter, R. M., & Henderson, R. A. (1992). Sedimentology of 40 000 year Milankovitch-controlled cyclothems from central Hawke's Bay, New Zealand. Sedimentology, 39(4), 675-696.

Jackson, J., van Dissen, R., & Berryman, K. (1998). Tilting of active folds and faults in the Manawatu region, New Zealand: evidence from surface drainage patterns. New Zealand Journal of Geology and Geophysics, 41(4), 377-385.

Kamp, P. J., Harmsen, F. J., Nelson, C. S., & Boyle, S. F. (1988). Barnacle-dominated limestone with giant cross-beds in a non-tropical, tide-swept, Pliocene forearc seaway, Hawke's Bay, New Zealand. Sedimentary Geology, 60(1), 173-195.

Kamp, P. J., Vonk, A. J., Bland, K. J., Hansen, R. J., Hendy, A. J., McIntyre, A. P., Ngatai, M., Cartwright, S., Haytin, S & Nelson, C. S. (2004). Neogene stratigraphic architecture and tectonic evolution of Wanganui, King Country, and eastern Taranaki Basins, New Zealand. New Zealand Journal of Geology and Geophysics, 47(4), 625-644.

King, P. R. (2000). Tectonic reconstructions of New Zealand: 40 Ma to the present. New Zealand Journal of Geology and Geophysics, 43(4), 611-638.

Kingma, J. T. (1971). Geology of Te Aute Subdivision: New Zealand Dept. of Scientific and Industrial Research.

Langridge, R., Berryman, K., & Van Dissen, R. (2005). Defining the geometric segmentation and Holocene slip rate of the Wellington Fault, New Zealand: the Pahiatua section. New Zealand Journal of Geology and Geophysics, 48(4), 591-607.

Lee, J. M., Begg, J., & Forsyth, P. (2002). Geology of the Wairarapa area: Institute of Geological & Nuclear Sciences 1:2500 000 geological map 11. 1 sheet +66pg. Lower Hutt, New Zealand. Institute of geological & Nuclear Sciences Limited.

Lewis, K. B., Carter, L., & Davey, F. J. (1994). The opening of Cook Strait: interglacial tidal scour and aligning basins at a subduction to transform plate edge. Marine Geology, 116(3), 293-312.

Lillie, A. R. (1953). The geology of the Dannevirke Subdivision: (No. 46). RE Owen. New Zealand Geological Survey.

Mortimer.N., Rattenbury. M., King. P., Bland. K., Barrell, D., Bache. F., Begg. J., Campbell, H., Cox. S., Crampton. J., Edbrooke, S., Forsyth. P., Johnston, R., Lee. J., Leonard, G., Raine, J., Skinner, D., Timm, C., Townsend, D., Tulloch, A., Turnbull, I., & Turnbull, R. (2014). High-level stratigraphic scheme for New Zealand rocks. New Zealand Journal of Geology and Geophysics 57(4): 402-419.

Naish, T., Kamp, P. J., Alloway, B. V., Pillans, B., Wilson, G. S., & Westgate, J. A. (1996). Integrated tephrochronology and magnetostratigraphy for cyclothemic marine strata, Wanganui Basin: implications for the Pliocene-Pleistocene boundary in New Zealand. Quaternary International, 34, 29-48.

Naish, T., & Kamp, P. J. (1997). Sequence stratigraphy of sixth-order (41 ky) Pliocene–Pleistocene cyclothems, Wanganui basin, New Zealand: a case for the regressive systems tract. Geological Society of America Bulletin, 109(8), 978-999.

Naish, T. R., Abbott. S., Alloway, V., Beu. A., Carter. R., Edwards. A., Journeaux, T., Kamp, K., Pillans, B., Saul, G., & Woolf, K. (1998). Astronomical calibration of a southern hemisphere Plio-Pleistocene reference section, Wanganui Basin, New Zealand. Quaternary Science Reviews, 17(8), 695-710.

Naish, T. R., Field, B. D., Zhu, H., Melhuish, A., Carter, R. M., Abbott, S. T., Edwards, S., Alloway, B., Wilson, G., Niessen, F., Barker, A., Browne, G., & Maslen, G. (2005). Integrated outcrop, drill core, borehole and seismic stratigraphic architecture of a cyclothemic, shallow-marine depositional system, Wanganui Basin, New Zealand. Journal of the Royal Society of New Zealand, 35(1-2), 91-122.

Naish, T. R., & Wilson, G. S. (2009). Constraints on the amplitude of Mid-Pliocene (3.6–2.4 Ma) eustatic sea-level fluctuations from the New Zealand shallow-marine sediment record. Philosophical Transactions of the Royal Society of London A: Mathematical, Physical and Engineering Sciences, 367(1886), 169-187.

Neef, C. (1967). The geology of Eketahuna (N.Z.M.S. 1. N.153). (Unpublished Ph.D thesis in Geology), Victoria University of Wellington.

Nelson, C. S., Winefield, P. R., Hood, S. D., Caron, V., Pallentin, A., & Kamp, P. J. (2003). Pliocene Te Aute limestones, New Zealand: expanding concepts for cool-water shelf carbonates. New Zealand Journal of Geology and Geophysics, 46(3), 407-424.

Nicol, A. (2011). Landscape history of the Marlborough Sounds, New Zealand. New Zealand Journal of Geology and Geophysics, 54(2), 195-208.

Pillans, B., Alloway, B., Naish, T., Westgate, J., Abbott, S., & Palmer, A. (2005). Silicic tephras in Pleistocene shallow-marine sediments of Wanganui Basin, New Zealand. Journal of the Royal Society of New Zealand, 35(1-2), 43-90.

Piyasin, S. (1966). Plio-Pleistocene geology of the Woodville area. (Unpublished MSc thesis), Victoria University of Wellington.

Pulford, A., & Stern, T. (2004). Pliocene exhumation and landscape evolution of central North Island, New Zealand: the role of the upper mantle. Journal of Geophysical Research: Earth Surface, 109(F1).

Rees, C. (2015). The Geology of the Lower Pohangina Valley, Manawatu, New Zealand. Unpublished MSs thesis), Massey University.

Rich, C. C. (1959). Late Cenozoic geology of the Lower Manawatu Valley, New Zealand (Doctor of Philosophy Geology), Harvard University.

Sutherland, R. (1999). Basement geology and tectonic development of the greater New Zealand region: an interpretation from regional magnetic data. Tectonophysics, 308(3), 341-362.

Trewick, S., & Bland, K. (2011). Fire and slice: palaeogeography for biogeography at New Zealand's North Island/South Island juncture. Journal of the Royal Society of New Zealand, 42(3), 153-183.

Walcott, R. I. (1989). The Paleogene plate boundary through New Zealand. Geological Society of New Zealand Miscellaneous Publication 43: 99.

Walker, R. G., & James, N. P. (1992). Facies models: response to sea level change. Geological Association of Canada, 2nd ed.

Appendix One: Sample locations and fossil contents:

Table 3: Sample locations and notes.

Sample Number	Sample Location	Coordinates	Stratigraphic Formation	Date Collected
C-5	Siltstone bed at a stratigraphic height of 193m at the Eastern Manawatu Gorge Entrance Measured Section.	.-40.336044. 175.820003	Kumerora Fm	2014 by Cliff Akins
C-12	Siltstone bed at a stratigraphic height of 205m at the Eastern Manawatu Gorge Entrance Measured Section.	.-40.335586. 175.820175	Kumerora Fm	2014 by Cliff Akins
AA 26	Conglomerate at a stratigraphic height of 80 m at the Western Saddle Road Measured Section.	.-40.28856. 175.79462	Te Atue Fm	15/06/2016
AA31	Conglomerate at a stratigraphic height of 70 m at the Western Saddle Road Measured Section.	.-40.28819. 175.79568	Te Atue Fm	15/06/2016
AA48	Sandy mudstone at a stratigraphic height of 140m at the Eastern Manawatu Gorge Entrance Section.	.-40.35710.0 175.81980	Mangatoro Fm	16/06/2016
AA52	Sandy mudstone at a stratigraphic height of 85 m at Wharite Road Measured Section	.-40.284795. 175.861598	Mangatoro Fm	16/06/2016
AA62	Sandy limestone at a stratigraphic height of 100m at the Broadlands Stream Measured Section.	.-40.27969. 175.785933	Kumerora Fm	25/08/2016
AA63	Siltstone bed at a stratigraphic height of 29 m at the Broadlands Stream Measured Section.	.-40.27978. 175.788495	Te Atue Fm	25/08/2016
AA73	Siltstone bed at a stratigraphic height of 90 m at the Broadlands Stream Measured Section.	.-40.279752. 175.785495	Kumerora Fm	25/08/2016
AA80	Sandy mudstone stratigraphic height uncertain due to interaction with faults at Ballantrae Farm Measured Section.	.-40.29672. 175.842505	Mangatoro Fm	19/01/2017
AA81	Sandy mudstone stratigraphic height uncertain due to interaction with faults at Ballantrae Farm Measured Section.	.-40.295534. 175.842416	Mangatoro Fm	19/01/2017
AA91	Medium-grained sandstone with coarse-grained sandstone interbeds at a stratigraphic height of 360m at the Ballantrae Farm Measured Section	.-40.301964. 175.82455	Mangatoro Fm	19/01/2017
AA95/GS-1	Sandy mudstone at a stratigraphic height of 65m at the Eastern Manawatu Gorge Entrance Measured Section.	.-40.335484. 175.820067	Mangatoro Fm	19/01/2017

C-5: Microfossils:

Cibasises s.p.

Zeaflorilus parri

Notoroalia finlayi

Oolina borealis

C-12: Microfossils:

Cibicides s.p.

Anomalinoides subinonionoides

Zeaflorilus parri

Elphidium novozealandicum

Bolivina subspinescens

Lagena striata

Oolina melo

Notorotalia depressa

AA-26: Macrofossils:

Anomia Sp

?Cellana Sp

?Sigapatella Sp

AA-31: Macrofossils:

Patro Sp

AA-48: Macrofossils:

Polinices (Polinella) obstructus

Pelicaria acuminate

Brachiopoda indent

Zeacuminia murdochi

Austrofuss pagoda

Aeneator Sp

Ostrea chilensis

?Cellana Sp

Clavatoma pulchar

Maoricrypta Sp

Zeacolpus vittutus

Amalda (baryspim) muronata

Crassostrea ingens

AA-52: Macrofossils:

Veneride indent ?Eumariac

Struthioloria (Callusaria) obesa

AA-63: Microfossils:

Notoroalia depressa

Zeaflorius parri

Anomalinoides subonionoides

Globigerina falconensis

Cibicides s.p

Evuigerina delicatula

Oolina borealis

Lagenosolenia confossa

Haynesina depressula

AA-73: Microfossils:

Notorotalia depressa

Elphidium advenum f. limbatum

Nonionoellina fleminigi

Oolina melo

Rosalina bradyi

Quninqueloculina suborbicularis

Quinqeloculina incisa

AA-80/81: Macrofossils:

Glycymeris (Glycymeris) shrimptoni

Amydalum striatum

Lamprodomina neozelanica

Ostria chelliensus

Trachycardium (ovicardium) rossi

AA-91: Macrofossils:

Glycymeris (Glycymeris) shrimptoni

Amalda (Baryspira) Oraria

Aeneator (Aeneator) elegans

Polinices (polinic

Appendix Two: Grain size data from sample AA-95/GS-1:

Table 4: Grain size results.
Grain size distribution for the sample GS-1 taken at 65 metres stratigraphic height. The distribution indicates a poorly sorted sandy mud. Key statistical points for run one: mean-60.87, medium-127.65 and standard deviation-56.62. Run two: mean-64.99, medium-45.50 and standard deviation-60.00. Run three: mean 62.46, medium-41.84 and standard deviation-56.87.

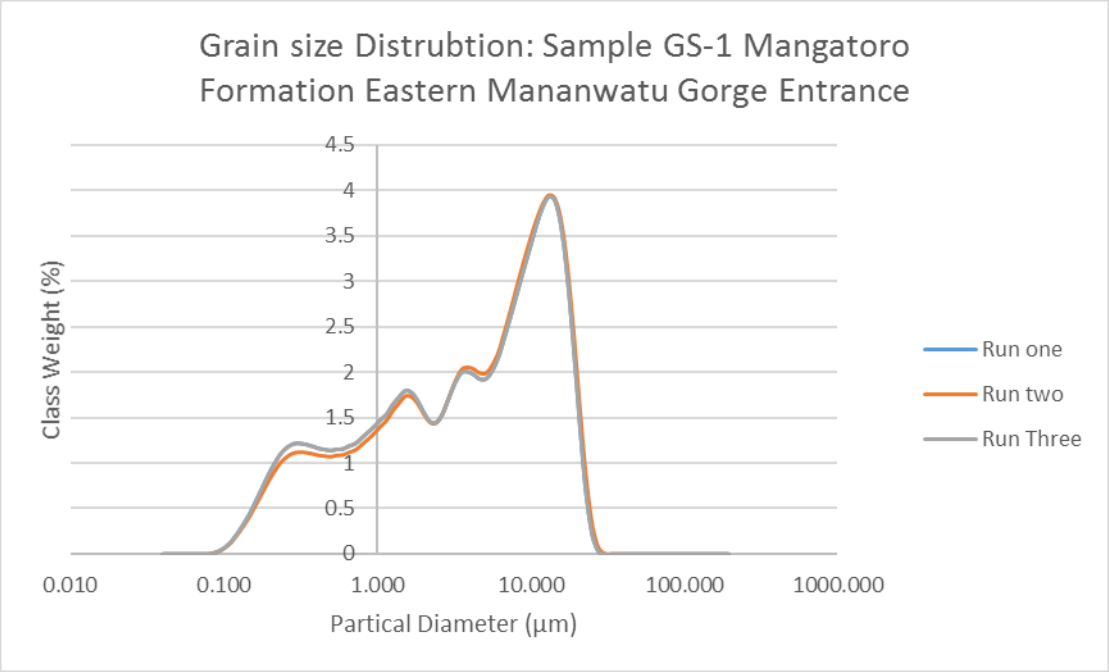

Raw Data:

Run one: 15/03/2017		Run Two: 15/03/2017		Run Three: 15/03/2017	
Channel Diameter (Lower)	Diff.	Channel Diameter (Lower)	Diff.	Channel Diameter (Lower)	Diff.
um	Volume	um	Volume	um	Volume
	%		%		%
0.375124	0	0.375124	0	0.375124	0
0.411798	0	0.411798	0	0.411798	0
0.452057	0	0.452057	0	0.452057	0
0.496252	0	0.496252	0	0.496252	0
0.544768	0	0.544768	0	0.544768	0
0.598027	7.01E-05	0.598027	0	0.598027	0
0.656493	0.00121467	0.656493	8.93E-05	0.656493	0.000104529
0.720675	0.00744094	0.720675	0.00146303	0.720675	0.00161885

0.791132	0.0240668	0.791132	0.0094540 5	0.791132	0.0101751
0.868477	0.053096	0.868477	0.0312123	0.868477	0.0328136
0.953383	0.0959003	0.953383	0.0721461	0.953383	0.0752564
1.04659	0.154133	1.04659	0.130731	1.04659	0.136425
1.14891	0.233628	1.14891	0.209431	1.14891	0.220294
1.26123	0.332379	1.26123	0.306224	1.26123	0.324746
1.38454	0.449799	1.38454	0.419912	1.38454	0.449019
1.5199	0.578581	1.5199	0.54389	1.5199	0.585334
1.66849	0.712793	1.66849	0.671268	1.66849	0.727114
1.83161	0.847806	1.83161	0.797945	1.83161	0.868581
2.01068	0.970369	2.01068	0.911342	2.01068	0.995903
2.20725	1.07477	2.20725	1.00847	2.20725	1.10356
2.42304	1.14177	2.42304	1.07308	2.42304	1.17277
2.65993	1.1803	2.65993	1.11309	2.65993	1.21245
2.91998	1.18545	2.91998	1.12441	2.91998	1.21796
3.20545	1.17603	3.20545	1.12057	3.20545	1.20781
3.51883	1.15651	3.51883	1.10745	3.51883	1.18716
3.86284	1.13444	3.86284	1.08903	3.86284	1.16339
4.24049	1.1241	4.24049	1.08216	4.24049	1.15161
4.65506	1.11347	4.65506	1.07397	4.65506	1.13979
5.11017	1.12779	5.11017	1.08877	5.11017	1.15317
5.60976	1.13186	5.60976	1.09355	5.60976	1.15672
6.1582	1.16536	6.1582	1.12258	6.1582	1.18903
6.76025	1.19416	6.76025	1.14805	6.76025	1.21666
7.42117	1.25615	7.42117	1.20356	7.42117	1.27675
8.14669	1.31925	8.14669	1.26477	8.14669	1.33871
8.94315	1.38219	8.94315	1.32869	8.94315	1.40071
9.81748	1.45965	9.81748	1.40619	9.81748	1.47568
10.7773	1.5279	10.7773	1.4732	10.7773	1.53815
11.8309	1.64575	11.8309	1.57966	11.8309	1.6446
12.9876	1.74114	12.9876	1.66396	12.9876	1.72583
14.2573	1.82348	14.2573	1.73943	14.2573	1.79536
15.6512	1.81084	15.6512	1.73353	15.6512	1.77747
17.1813	1.71312	17.1813	1.65753	17.1813	1.68429
18.861	1.57337	18.861	1.54231	18.861	1.55533
20.705	1.46422	20.705	1.45231	20.705	1.45549

22.7292	1.4553	22.7292	1.44884	22.7292	1.44849
24.9513	1.56225	24.9513	1.54726	24.9513	1.54536
27.3906	1.75089	27.3906	1.72182	27.3906	1.7143
30.0685	1.94102	30.0685	1.89911	30.0685	1.88023
33.0081	2.07474	33.0081	2.0305	33.0081	1.99376
36.2352	2.09641	36.2352	2.05969	36.2352	2.00539
39.7777	2.06515	39.7777	2.03938	39.7777	1.97283
43.6665	2.01193	43.6665	1.99406	43.6665	1.92312
47.9356	2.01645	47.9356	1.99686	47.9356	1.92814
52.622	2.11195	52.622	2.08124	52.622	2.01661
57.7666	2.2803	57.7666	2.23241	57.7666	2.16952
63.4141	2.5266	63.4141	2.46175	63.4141	2.39463
69.6138	2.7782	69.6138	2.70502	69.6138	2.6279
76.4196	3.03594	76.4196	2.96545	76.4196	2.87688
83.8907	3.2714	83.8907	3.21496	83.8907	3.11985
92.0923	3.48607	92.0923	3.44818	92.0923	3.35769
101.096	3.69466	101.096	3.66942	101.096	3.59822
110.979	3.85549	110.979	3.84393	110.979	3.79818
121.829	3.93815	121.829	3.95132	121.829	3.92537
133.74	3.84442	133.74	3.9222	133.74	3.8913
146.815	3.49228	146.815	3.69104	146.815	3.62133
161.168	2.86602	161.168	3.20714	161.168	3.08039
176.925	2.03376	176.925	2.49248	176.925	2.31297
194.222	1.14734	194.222	1.6639	194.222	1.46263
213.21	0.461346	213.21	0.885892	213.21	0.701313
234.054	0.105961	234.054	0.341545	234.054	0.226388
256.936	0.0114091	256.936	0.0797867	256.936	0.0370644
282.056	0.000184017	282.056	0.00917223	282.056	0.00231349
309.631	0	309.631	0.000255364	309.631	0
339.902	0	339.902	0	339.902	0
373.132	0	373.132	0	373.132	0
409.611	0	409.611	0	409.611	0
449.657	0	449.657	0	449.657	0
493.617	0	493.617	0	493.617	0
541.876	0	541.876	0	541.876	0
594.852	0	594.852	0	594.852	0
653.008	0	653.008	0	653.008	0
716.849	0	716.849	0	716.849	0
786.932	0	786.932	0	786.932	0
863.866	0	863.866	0	863.866	0

948.322	0	948.322	0	948.322	0
1041.03	0	1041.03	0	1041.03	0
1142.81	0	1142.81	0	1142.81	0
1254.54	0	1254.54	0	1254.54	0
1377.19	0	1377.19	0	1377.19	0
1511.83	0	1511.83	0	1511.83	0
1659.63	0	1659.63	0	1659.63	0
1821.88	0	1821.88	0	1821.88	0
2000		2000		2000	